PREDICTING STABLE CRYSTAL STRUCTURES AND THEIR ELECTRONIC PROPERTIES OF Si-RICH SILICON CARBIDE BY FIRST PRINCIPLE CALCULATION

by

NOURA DAWAS ALKHALDI

Presented to the Faculty of the Graduate School of

The University of Texas at Arlington in Partial Fulfillment

of the Requirements

for the degree of

MASTER OF SCIENCE IN PHYSICS

THE UNIVERSITY OF TEXAS AT ARLINGTON

MAY 2017

Acknowledgements

I would like to thank my supervisor Dr. Huda of the physics department at University of Texas at Arlington. You are an example of excellence as an advisor and a role model for your students. Thank you so much for guiding and supporting me in through my master study. You always are encouraging me to read in my field and increase my knowledge. Thank you for pushing me a lot to do the best. My advisor has opened his door and has allowed me to ask any questions related to my research and my writing, and he has steered me in the right direction. I want to thank my thesis committee members Dr. Weiss, and Dr. Zhang for their discussion, and feedback which are invaluable. I would like to thank my fellow graduate students for willing to help me. I would like thank University of Hafr Albatin for giving me the opportunity to complete my study in USA, and the thank should reach Saudi Arabian Cultural Mission for being the financial supporter of my research. I should express my profound gratitude to my family who are giving me unfailing support. I want to thank my father for being supportive. This accomplishment would not be possible without your support. I want to thank my mother who is not alive, but she is definitely alive in my heart. Although it has been years since you passed away, I still take your lessons with me every day. I would like to thank my sister Hanof and my brother Fahad. You are examples of great supporters who help me when I feel I can't do it. I would like to thank my sister Sara, my brothers Mefleh and Mohammad for encouraging me to do my best.

April 12, 2017

Abstract

PREDICTING STABLE CRYSTAL STRUCTURES AND THEIR ELECTRONIC PROPERTIES OF Si-RICH SILICON CARBIDE BY FIRST PRINCIPLE CALCULATION

Noura Dawas Alkhladi, MS

The University of Texas at Arlington, 2017

Supervising Professor: Muhammad N. Huda

Silicon carbide has become an attractive semiconductor material with its high stability. It has been used in variety of fundamental aspects and applications such as photovoltaic solar cells due to its unique properties, for instances high thermal conductivity and low density. Investigating thermodynamically stable non-stoichiometric silicon carbide structures can be useful as they can be used in applications without requiring a pure grade of silicon or pure grade of silicon carbide materials. Density functional theory (DFT) calculations were used to examine the stability of various structures of silicon carbide such as 2H-SiC, 4H-SiC, 6H-SiC, wurtzite structure, FeSi structure, and diamond structure of SiC. We investigated different configurations of silicon and carbon atoms in these silicon carbide structures to obtain suitable silicon rich silicon carbide materials with tailored band gap. We have studied the electronic structures of these structures. We have replaced the carbon atoms by silicon atoms to lower the band gap of the

silicon carbide. Total energies of these structures, as well as the formation enthalpies of silicon incorporations have been calculated by density functional theory.

Table of Contents

List of Illustrations

List of Tables

Chapter 1

Introduction

1.1 Silicon Carbide

Silicon carbide is a semiconductor material [1] which has equal number of silicon and carbon in its formula unit. The silicon and the carbon atoms bond with each other in which each silicon atom bonds covalently to four neighboring carbon atoms and form as tetrahedron. Due to the difference of electronegativity of Si and C atoms, Si and C bonds are partly ionic as well. This complex nature of bonding is responsible for more than 200 poly-types of silicon carbide, and the most common poly-types are 3C-SiC ($\beta - SiC$) and the hexagonal polytypes 2H, 4H [2], and 6H ($\alpha - SiC$). The cubic polytype 3C-SiC is considered as the most stable structure comparing to the hexagonal polytypes.

Silicon carbide has great properties which make it attractive material to be use in applications in extreme environment. These interesting properties include high strength, high hardness [3,4] , and Low thermal expansion [5], and it has been used in high temperature applications because of its high thermal conductivity [6] which is 3.6 W/cm K for 3C-SiC, and 4.9 W/cm K for 4H-SiC and 6H-SiC [7,8]. Tables 1-1 and 1-2 show the physical and chemical properties of 3C-SiC, 2H-SiC, 4H-SiC, and 6H-SiC.

Table 1-1 The space group and the lattice parameters of 3C-SiC, 2H-SiC, 4H-SiC, and 6H-SiC

Structure	3C-SiC ($\beta - SiC$)	2H ($\alpha - SiC$)	4H ($\alpha - SiC$)	6H ($\alpha - SiC$)
Space group	F43m	$P6_3mc$	$P6_3mc$	$P6_3mc$
Lattice constants a,b (A°)	4.358 - 4.359	3.0753 - 3.081	3.070 - 3.081	3.073 - 3.081
Lattice constant c (A°)	4.358 - 4.359	5.048	10.08	15.109 - 15.12

Table 1-2 The densities, band gaps, thermal conductivities of 3C-SiC, 2H-SiC, 4H-SiC, and 6H-SiC

Structure	3C-SiC ($\beta - SiC$)	2H ($\alpha - SiC$)	4H ($\alpha - SiC$)	6H ($\alpha - SiC$)
Density (g/cm^3)	3.219	3.21	3.215	3.212
Band gap (eV)	2.39	3.33	3.26	3.0
Thermal conductivity (W/cm K)	3.6	-	4.9	4.9

SiC can be formed as powders, fibers, whiskers, coatings, and single crystals. The methods to produce SiC depend on the product form and its application. For example, SiC powders can be produced by using the method

which called spark plasma-assisted carbothermal reduction (SPCR) where quartz sand, carbon, and phenolic resin at low temperature are used [9] or by using Acheson method where green petroleum coke mix with sand, and then heated up to 2500°C using two large graphite electrodes or it can be produced by mixing fine powders of silica and carbon at lower temperatures for short time. The most available SiC whiskers are produced by heating coked rice hulls, or by Chemical vapor deposition method [10] as SiC fibers [11] which can be produced also by use the Chemical vapor deposition method [10–14] where SiC is deposited from the gas phase on a tungsten wire. Chemical vapor deposition (CVD) method has been used to synthesis silicon carbide [14], [15], [16–18]. It has been used to produce pure bulk materials and powders of solids and semiconductor materials [19].The materials which are deposited by CVD have very high purity, and the impurities can be removed from gases by using distillation techniques. Silicon carbide also has been used in photovoltaic solar cell. However, the band gap of SiC ranges from 2.3 eV to 3.3 eV (see table 1-2), which are higher than what is suitable for efficient solar energy absorption. Efficient solar conversion requires a band gap of less than 1.5eV, so it is necessary to have tunable band gap in SiC. The non-stoichiometric SiC may provide that option, so we studied Si rich SiC for this thesis. In the limit of all C atoms replaced by Si atoms, the band gap should approach to pure Si gap which is 1.1 eV. However, we would like to avoid the indirect band gap problem which a short coming of pure Si solar cell devices.

1.2 Silicon Rich Silicon Carbide

Increasing the atoms of silicon and decreasing the carbon atoms in silicon carbide will help to lower the band gap which is necessary for the photovoltaic applications. The experimental result shows that the band gap changes as the silicon concentration increases. In silicon carbide material, if the carbon atoms are added [20], it will increase the band gap which is not good in the photovoltaic, whereas when more silicon are deposited, which lower the band gap from 2.05 eV to 1.49 eV [20]. For example, Si-rich a-$Si_{1-x}C_x$ thin film has become an attractive material due to its band gap. It can be used in many applications such as nanotubes and the light emitting diodes [20–25]. It has been used as a layer to improve the efficiency of amorphous silicon which is used in solar cells. The fraction of the carbon in Si-rich amorphous-$Si_{1-x}C_x$ thin film can be varied because the carbon affects the structural and the properties of the material negatively. Changing the fraction of the carbon would be great to improve the devices and the performance [22], [26]. The silicon rich $Si_{1-x}C_x$ films has been synthesized by using low temperature and low power plasma enhanced CVD (PECVD) method in a system which is rich by the inorganic compound silane [27]. Moreover, Si-rich Si_xC_{1-x} has existed as nonstoichiometric matrix which corresponds to Si fabricating technology to keep the Si-quantum dots (QDs) [25,28]. The use of silicon rich silicon carbide has been expanded. For instance, silicon carbide/silicon rich carbide multilayers are used to produce silicon nanodots which is utilized in the application of photovoltaic [29]. Solar cells are encountered with losing the power in the band gap when the photons with energy higher than the band gap can lose

the extra energy by thermalization, but the photons which has energy lower the band gap cannot [30]. This obstacle can be overcome by using the multi-junction where materials with different band gaps can be stacked together [31–33]. Silicon nano-crystals used as absorbers in all-Si multi-junction solar cell. It is expected that this will increase the efficiency, and decrease the cost of photovoltaic [31,34,35]. Silicon rich silicon carbide film would provide a great potential when it is used in photovoltaic solar cell and in the light emitting applications [36].

1.3 Photovoltaic

Photovoltaic device is a unique device, which is made of semiconductor material, that produces electrical energy from sunlight. Photovoltaic word came from two parts, word photo which means light and voltaic which means the electricity. The effect of photovoltaic was discovered by the French scientist Alexandre-Edmond Becquerel in 1839 [37]. He observed that if one side of a simple battery cell is exposed to light, the generated current could rise [38,39]. Electricity can be generated directly using photovoltaic device by the direct conversion of sunlight, or by using concentrated solar power [39,40]. Some materials have a property which is known as photoelectric effect such as silicon. This property increases the ability to absorb photons of light and then release electrons, when the free electrons are captured, the electric current which is produced can be utilized as electricity. Photovoltaic which is called solar cells as well are composed in most cases of silicon which is considered as the significant component of photovoltaic device. Photovoltaic devices need efficient materials which have high stability and suitable band gap to work efficiently. In the past, photovoltaic was used in the satellites and spacecraft, but nowadays, it has been used to generate the electricity for everyday use, such as in the industrial and residential purposes. Generating electricity from solar energy is an impotant because it does not increase CO_2 emission production. Furthermore, photovoltaic systems considered to be the most important renewable energy resources, and has taken places in all the world [41,42]. Photovoltaic is made by crystalline material such as single crystalline silicon and polycrystalline silicon. Polycrystalline

silicon would be better to use than single crystalline silicon due to its strength and the lower costs of polycrystalline silicon [43]. Also, the photovoltaic device can be made of thin film of semiconductor materials, and the process would be faster, easier and less energy will be lost. However, there is main obstacle is that the efficiency of thin film is lower than the crystalline materials [44]. It is an ongoing challenge to develop suitable photovoltaic materials.

Chapter 2

Methodology

Density functional theory (DFT) is considered as one of the most important methods which is used to treat the problem of many body system by using the electron density. While the wave function Ψ of an N-electron system contains 3N variables, the electron density ρ depends on three variables x, y, and z. DFT has been used due to the significant results which are provided by it. DFT describes the ground state properties, and it gives important concepts such as the chemical potential.

2.1 Schrödinger Equation

Schrödinger equation has become the starting point of the studies in quantum mechanics. Schrödinger equation can be used to solve simple systems, and determine the wave functions of the system. Then, the energies and properties can be obtained. Schrodinger equation which is the eigen values equation, is given by

$$H\Psi = E\Psi \tag{2.1}$$

Where H is the Hamiltonian, Ψ presents the wave function, and E is the energy of the system.

The Hamiltonian H is given by the following equation

$$H = T_e + T_N + V_{ee} + V_{eN} + V_{NN} \tag{2.2}$$

where T_e is the kinetic energy of the electrons:

$$T_e = -\sum_{i=1}^{N} \frac{1}{2} \nabla_i^2 \quad (2.3)$$

T_N is the kinetic energy of the nucleus:

$$T_N = -\sum_{\alpha=1}^{M} \frac{1}{2M_\alpha} \nabla_\alpha^2 \quad (2.4)$$

V_{ee} is the electron-electron repulsion energy:

$$V_{ee} = \sum_{i=1}^{N} \sum_{j>1}^{N} \frac{1}{|\vec{r}_i - \vec{r}_j|} \quad (2.5)$$

V_{eN} is the energy of interaction between electrons and nucleus:

$$V_{eN} = \sum_{i=1}^{N} \sum_{\alpha=1}^{M} \frac{Z_\alpha}{|\vec{r}_i - \vec{R}_\alpha|} \quad (2.6)$$

V_{NN} is the energy repulsion between the nucleus:

$$V_{NN} = \sum_{\alpha=1}^{M} \sum_{\beta>\alpha}^{M} \frac{Z_\alpha Z_\beta}{|\vec{R}_\alpha - \vec{R}_\beta|} \quad (2.7)$$

Where i , j are related to the electrons, and α, β are related to the nucleus.

M_α is the ratio of the of mass of nucleus α to the mass of the electron, and Z_α , Z_β are the atomic number of nucleus α and nucleus β respectively.

$|\vec{r}_i - \vec{r}_j|$ is the distance between electron i and electron j.

$|\vec{r}_i - \vec{R}_\alpha|$ is the distance between electron i and nucleus α.

$|\vec{R}_\alpha - \vec{R}_\beta|$ is the distance between nucleus α and nucleus β.

However, Schrödinger equation can't be solved for N-body system.

2.2 N-body system

For many body problems, using Schrödinger equation (2.1) with the Hamiltonian, which is given above by equation (2.2), is very complicated and might be impossible. It requires using some approximation to solve it. Born-Oppenheimer

approximation is one of the important approximations which is used and could handle solving many-body system. Born-Oppenheimer approximation assumed that we can separate the nuclei motion and the electronic motion in the molecules.

$$\Phi(x,\vec{R}) = \Psi(x,\vec{R})\chi(\vec{R}) \tag{2.8}$$

Where $\Psi(x,\vec{R})$ is the electronic wavefunction, and $\chi(\vec{R})$ is the nuclear wave-function. It allows us to neglect the nuclear terms due to the mass of nucleus which is very heavy when we compare it with the mass of electron. Since the electrons move faster than nuclei, Born-Oppenheimer approximation eliminates the nuclei kinetic energy, and considers the repulsion energy between nuclei as a constant.

2.3 Density Functional Theory

Density functional theory (DFT) is one of the most common computational methods. It has been used to determine the ground state properties and the electronic structure of the materials. Density functional theory has been used to solve many body system problems.

2.3.1 Thomas-Fermi Model

In 1926, Thomas and Fermi formulated the first density functional theory [45]. The main idea of Thomas-Fermi theory is to determine the ground state of energy as a function of the electron density instead of wave-function [46]. Thomas-Fermi method works better for a homogenous system. It gives roughly correct energies with error about 10 % [46]. However, Thomas-Fermi method failed to predict most of properties of many body system. It prevents the molecules

of the system to bind with each other, and it will fail to find the binding energies in the system. According to Thomas-Fermi model, the total energy of the system is given by

$$E_{TF} = C_1 \int d^3r\, \rho(r)^{5/3} + \int d^3r\, V_{ext}\rho(r) + C_2 \int d^3r\, \rho(r)^{4/3} + \frac{1}{2}\int d^3r d^3r' \frac{\rho(r)\rho(r')}{|r-r'|} \quad (2.9)$$

Where $C_1 = \left(\frac{3}{10}\right)(3\pi^2)^{2/3}$ and $C_2 = -\left(\frac{3}{4}\right)(3/\pi)^{1/3}$

The first term of the above equation describes the kinetic energy of the system, the 2nd term is for the electron-nuclei interaction, and the following terms are for the exchange and the Hartree term respectively. The kinetic energy and exchange correlation terms are calculated assuming the many-electron system to be a homogenous electron gas. This assumption is also very important for the density functional theory. However, the TF model assumes the homogenous electron gas to be non-interacting/weakly interacting.

2.3.2 Hohenberg-Kohn Theorem

The modern density functional theory has proved that for many-body problem, we can determine exact solution using the density functional [46]. In 1964, Hohenberg and Kohn proved that all properties which observe in any system can be determined by using the electron density [46], and the electron density is corresponding to the ground state wavefunction of many electrons [47–49]. Hence, it leads to know that the properties can be written as a functional of the electron density where $\rho(r)$ is given by

$$\rho(r) = N \int d^3r_1 \dots d^3r_N \mid \Psi(x_1, x_2, x_3, \dots\dots\dots, x_N) \mid^2 \delta(r - r_1) \quad (2.10)$$

Hohenberg and Kohn introduced other theorem which clarifies that the density which minimize the energy is the ground state density,

$$E_0 \leq E_v(\rho) \quad (2.11)$$

where E_0 is the ground state energy, and $E_v(\rho)$ presents the energy functional which is given by the following equation,

$$E_v(\rho) = T[\rho] + V_{ee}[\rho] + V_{ne}[\rho] \quad (2.12)$$

$$E_v(\rho) = \int d^3r\, \rho(r)\, V_{ext} + F_{HK} \quad (2.13)$$

Where

$$F(\rho) = T[\rho] + V_{ee}[\rho] \quad (2.14)$$

and where $V_{ee}[\rho]$ is the classical electron-electron interaction under the physical constraints [46,49] such that

$$\int d^3r\, \rho(r) = N \quad (2.15)$$

and

$$\rho(r) \geq 0 \quad (2.16)$$

and it is given by

$$V_{ee}[\rho] = \frac{\frac{1}{2}\int\int d^3r\, d^3r`\rho(r)\rho(r`)}{|r - r`|} \quad (2.17)$$

In 1965, Hohenberg and Kohn considered two significant problems. The first issue was that the exact kinetic energy cannot be found, and the second one is that the interaction between the electrons approximated without considering the Pauli Exclusion Principle, which should have been respected when the electrons distribute considering the correlation of all electrons.

2.3.3 Kohn-Sham Formulation

The basic idea of Kohn-Sham theorem is to map the many particle problem onto a system of non-interacting particles, where the non-interacting system has the same ground state density as the many-electron system.

Kohn and Sham included the correlation term to the functional energy, and it takes form as the following equation,

$$E_v(\rho) = T_0[\rho] + \int \left(V_{ext}(r) + \frac{1}{2}\emptyset(r)\right)\rho(r)\, dr + E_{xc}[\rho] \tag{2.18}$$

where the first term is non-interacting electron kinetic energy functional. $V_{ext}(r)$ is the external potential energy, and $\emptyset(r)$ is the classical coulomb potential of electrons which is given by

$$\emptyset(r) = \int \frac{\rho(r')}{|r'-r|} dr' \tag{2.19}$$

The third term $E_{xc}[\rho]$ presents the exchange-correlation energy which includes the non-classical electron-electron interaction and the correction to $T_0[\rho]$. When the functional energy minimizes with respect to the electron density, the chemical potential in density functional theory [49] will be

$$\mu = \frac{\delta E[\rho(r)]}{\delta\rho(r)} \tag{2.20}$$

Minimizing the energy functional,

$$\mu = \frac{\delta E[\rho(r)]}{\delta\rho(r)} = \frac{\delta T_0[\rho]}{\delta\rho(r)} + \frac{\delta}{\delta\rho(r)}\left[\int \left(V_{ext}(r) + \frac{1}{2}\emptyset(r)\right)\rho(r)\, dr\right] + \frac{\delta E_{xc}[\rho]}{\delta\rho(r)} \tag{2.21}$$

$$\mu = \frac{\delta T_0[\rho]}{\delta\rho(r)} + V_{ext}(r) + \emptyset(r) + \frac{\delta E_{xc}[\rho]}{\delta\rho(r)} \tag{2.22}$$

$$\mu = \frac{\delta T_0[\rho]}{\delta \rho(r)} + V_{eff}(r) \tag{2.23}$$

where $V_{eff}(r)$ is the Kohn-Sham effective potential [49,50], and it is given by

$$V_{eff}(r) = V_{ext}(r) + \emptyset(r) + \frac{\delta E_{xc}[\rho]}{\delta \rho(r)} \tag{2.24}$$

By solving the following equation for N-electrons equation, the electron density will be determined.

$$\left[-\frac{1}{2}\nabla^2 + V_{eff}(r)\right]\psi_i = \varepsilon_i\,\psi_i \tag{2.25}$$

and

$$\rho(r) = \sum_i^N |\psi_i(r)|^2 \tag{2.26}$$

After guessing the electron density $\rho(r)$, $V_{eff}(r)$ the effective potential can be determined by using the above equation (2.24), and then by applying equation (2.25) and (2.26), new $\rho(r)$ can be calculated. The self-consistent field (SCF), which means that the cycle is repeated until consistent result is appeared and the changes becomes negligible, can be utilized to determine both $\rho(r)$ and $V_{eff}(r)$ [46].

Thus, the energy functional of the system can be determined using equation (2.17), and $T_0[\rho]$ can be obtained by the following equation,

$$T_0[\rho] = \frac{1}{2}\sum_{i=1}^N < \psi_i \left|\nabla_i^2\right| \psi_i > \tag{2.27}$$

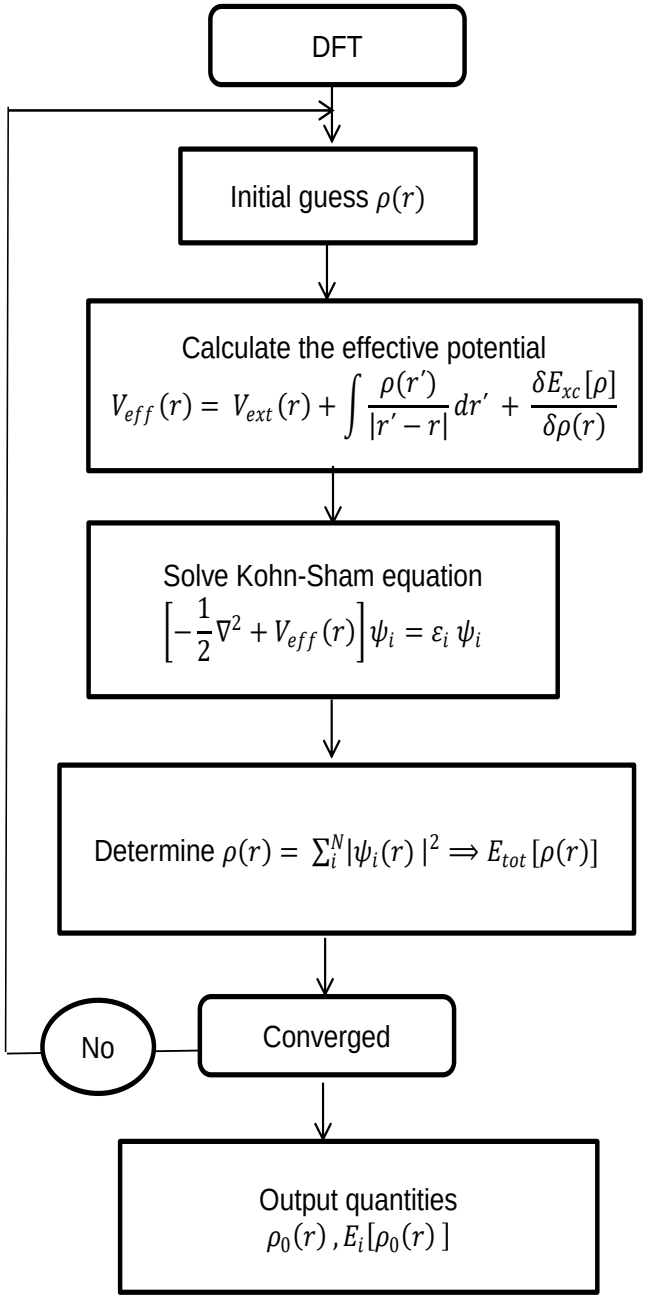

Figure 2-1 The flow chart of DFT

It can be clearly seen that the Kohn-Sham method is more powerful compared to other methods since it considered the exchange correlation energy, and includes it in the energy functional [49]. Including $E_{xc}[\rho]$ in DFT will help to obtain the ground state properties of many body systems in proper way.

2.4 The Exchange Correlation

2.4.1 Local Density Approximation

Local density approximation (LDA) is one of the approximations was used to the exchange-correlation energy functional of the electron density $\rho(r)$. By using a homogeneous electron gas, an accuracy approximation is determined. In local density approximation, the exchange-correlation energy functional is given by the following equation,

$$E_{xc}^{LDA}[\rho(r)] = \int d^3r \ \varepsilon_{xc}[\rho(r)] \tag{2.28}$$

where the exchange-correlation energy functional divided into two terms as the following equation,

$$E_{xc}^{LDA}[\rho(r)] = E_x[\rho(r)] + E_c[\rho(r)] \tag{2.29}$$

The first term is the exchange energy, and the second term is the correlation energy.

Local spin density approximation (LSDA) is similar with the local density approximation. The spin density is separated to spin-up and spin-down [46] , LSDA equation is written as

$$E_{xc}^{LDA}[\rho(r)] = \int d^3r \ \varepsilon_{xc}[\rho \uparrow (r), \rho \downarrow (r)] \tag{2.30}$$

Vibrational properties and the ground state geometries can be determined accuracy using the local density approximation. However, the drawback of LDA is that the approximation results smaller lattice parameter than what is expected, and it underestimates the band gap of semiconductor materials.

2.4.2 Generalized Gradient Approximation

Generalized Gradient Approximation (GGA) is an approximation which includes the gradient of the electron density. In GGA, the heterogeneous of the electron density has been considered, and it has been used due to the fact it determines more accurate results in the chemical properties such as atomization energies [46,49]. GGA works very well to calculate the formation energies, and determine the electronic structure and properties of the system. Generalized gradient approximation equation is given as shown

$$E_{xc}^{GGA}[\rho(r)] = \int d^3r\, \varepsilon_{xc}[\rho\uparrow(r), \rho\downarrow(r), |\nabla\rho\uparrow(r)|, |\nabla\rho\downarrow(r)|] \quad (2.31)$$

2.5 Computational Details

The calculations of the research are done completely by using a standard projector wave method DFT in Vienna ab initio simulation package (VASP) [51,52]. VASP is a computer program which has been utilized to determine the ground state electronic structures and properties of many-body system with first principle calculation.

We have utilized the Projector augmented wave (PAW) [53]. PAW has been known as a generalization of the pseudopotential, and augmented wave.

We have utilized the generalized gradient approximation. The Perdew–Burke–Ernzerhof (PBE) is applied. PBE is an exchange-correlation functional which belongs to GGA [54,55]. It does not include experimental fitted parameters which makes it useful in several of systems [55].

We fully relaxed all structures, and then calculated the total energies. Then, we calculated the formation energies of our structures to examine the stability of these structures. The formation enthalpy is written as

$$\Delta H_f = E(Si_xC_y) - xE(Si) - yE(C) \quad (2.32)$$

where ΔH_f is the formation enthalpy (Enthalpy), and $E(Si_xC_y)$ is the total energy of the unit cell. $E(Si)$ is the total energy of stable bulk phase per Si atom, and $E(C)$ is the total energy of stable bulk phase per C atom. x and y present the total number of Si atoms and C atoms respectively.

We include Van der Waals forces in our calculation to determine the total energy of bulk Graphite to find the energy of carbon per atom [56,57].

We have worked on a software program visualization for electronic and structural analysis (VESTA) to visualize the structures which is used in the research [58].

We have used tetrahedron method to plot the density of states (DOS) with different meshes taking the size of unit cell into account. However, when tetrahedron method was not applicable with some hexagonal structures with large cells, we used Gaussian smearing.

Chapter 3

Pristine Silicon Carbide

In the first, we have utilized some sources such as Material project website, and American Mineralogist Crystal Structure Database [59] to collect information about different structures of silicon carbide. These sources provide the lattice parameters and initial coordinates of 2H, 4H, 6H, Diamond structure, FeSi structure and wurtzite structure of silicon carbide.

2H is a hexagonal structure which has 2 atoms of silicon and 2 atoms of carbon. Figure 3-1 shows the unit cell of 2H structure of SiC after the relaxation from our calculation using DFT.

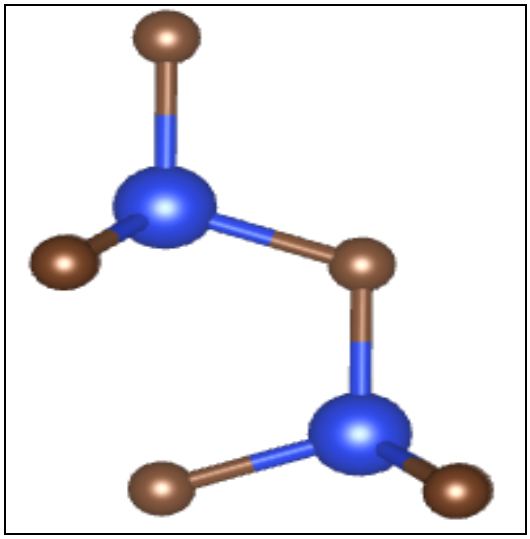

Figure 3-1 The unit cell of 2H structure of SiC after the relaxation using DFT

4H is also a hexagonal structure which is same as 2H, but 4H is larger than 2H where it contains 4 atoms of silicon and 4 atoms of carbon. Figure 3-2 demonstrates the relaxed structure of 4H of SiC using DFT.

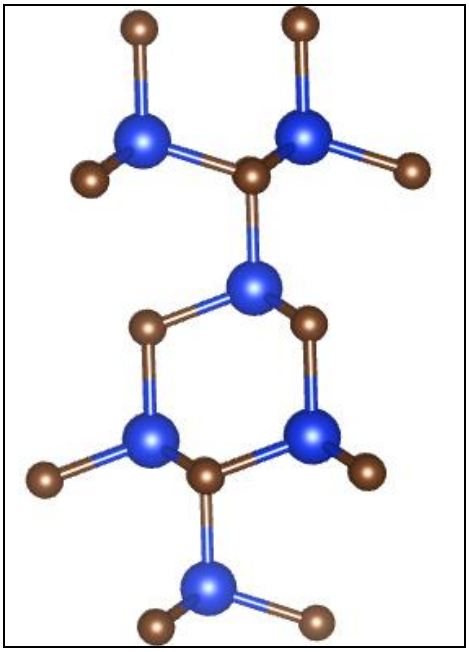

Figure 3-2 The unit cell of 4H structure of SiC after the relaxation using DFT

6H is a hexagonal structure as 2H and 4H, but it is lager two times than 4H and three times than 2H. It has 6 atoms of silicon and 6 atoms of carbon. Figure 3-3 is the unit cell of 6H structure after the relaxation using DFT.

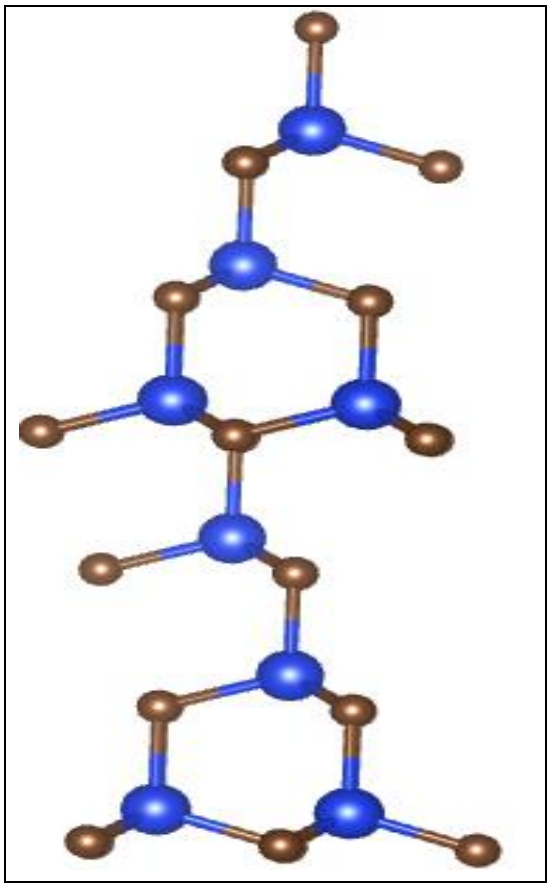

Figure 3-3 The unit cell of 6H structure of SiC after the relaxation using DFT

In 2H, 4h, and 6H structures, the lattice parameter a is equal to b, but the lattice parameter c is different and lager than a and b. The main difference between these structures is in the lattice parameter c where 2H has the smallest number, and 6H has the largest number. However, these hexagonal structures have the same angel parameters where $\alpha = \beta = 90°$ and $\gamma = 120°$.

Also, we utilized wurtzite structure of zinc sulfide [59] with replacing zinc atoms with silicon atoms and replacing the sulfide atoms with carbon atoms.

Wurtzite structure has similarity with hexagonal structures especially with 4H structure where it can be noticeable that the lattice parameters are almost same. Also, the angel parameters are same as in the hexagonal structures. Figure 3-4 shows the unit cell of wurtzite structure of SiC from our calculation after the relaxation using DFT.

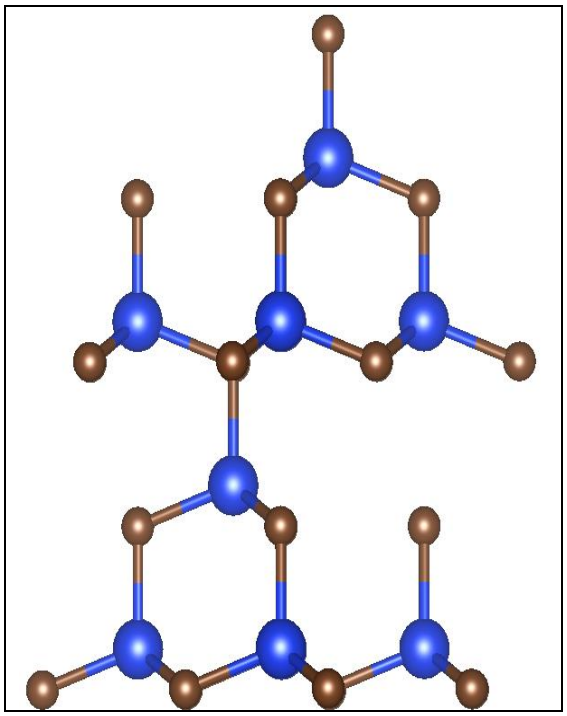

Figure 3-4 The unit cell of wurtzite structure of SiC after the relaxation using DFT

Naquite structure of FeSi [60] is used where iron is replaced by silicon and the silicon, which is in FeSi, is replaced by carbon. FeSi structure has cubic structure where the lattice parameters a, b, and c are equal, and the angel

parameters are also equal $\alpha = \beta = \gamma$. Figure 3-5 is the unit cell of FeSi structure of SiC after the relaxation using DFT. The lattice parameter in FeSi is lager in FeSi structure than the other structures about 1.28 A°, and a is almost same in all other structures.

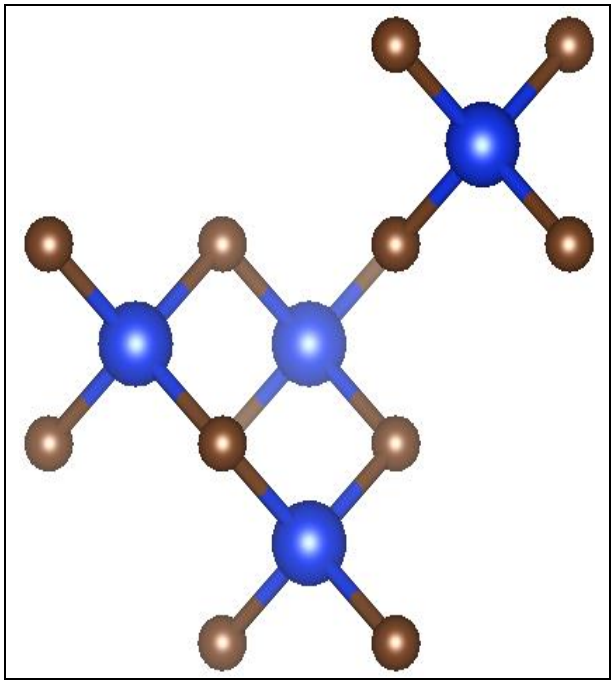

Figure 3-5 The unit cell of FeSi structure of SiC after the relaxation using DFT

Diamond structure similar to FeSi structure which has cubic structure and the lattice parameters a, b, and c are equal. Also, the angel parameters are equal $\alpha = \beta = \gamma$. Figure 3-6 demonstrates the relaxed diamond structure of SiC after using DFT.

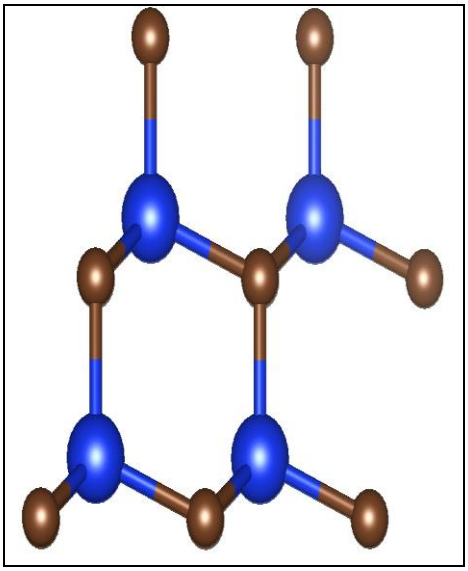

Figure 3-6 The unit cell of diamond structure of SiC after the relaxation using DFT

3.1 Relaxing the Structures of Pristine Silicon Cabide

When the information, the lattice parameters, and the crystal structures of different phases of silicon carbide, are collected from the sources, we used density functional theory (DFT) to relax the systems. When the systems were fully relaxed, we obtain the relaxed volumes. Table 3-1 shows the relaxed volumes of unit cell (1x1x1) of 2H which has 2 atoms of silicon and 2 atoms of carbon, 4H with 4 atoms of silicon and 4 atoms of carbon, 6H with 6 atoms of silicon and 6 atoms of carbon, Diamond structure with 1 atom of silicon and 1 atom of carbon, FeSi structure with 4 atoms of silicon and 4 atoms of carbon, and wurtzite structure of SiC with 4 atoms of silicon and 4 atoms of carbon.

Table 3-1 shows the volume of unit cell of SiC. 2H, 4H, 6H, Diamond structure, FeSi structure, and wurtzite structure (1x1x1). It can be clearly seen that the volumes of these structures are different due to the number of atoms which is 2 atoms of silicon and 2 atoms of carbon in 2H structure, and 4 atoms of silicon and 4 atoms of carbon in 4H, wurtzite, diamond and FeSi structure, and 6 atoms of silicon and 6 atoms of carbon in 6H structure. We calculated the volume per pair and noticed that diamond structure has the largest volume with different about 0.005 $A^{\circ 3}$ comparing to 2H structure which has the second highest volume. 2H structure is larger than FeSi structure with difference about 0.005 $A^{\circ 3}$, but FeSi structure is larger than the wurtzite structure about 0.003 $A^{\circ 3}$.

Table 3-1 The relaxed volume of unit cell of SiC. 2H, 4H, 6H, Diamond structure, FeSi structure, and wurtzite structure (1x1x1)

Structure of SiC (1x1x1)	Volume of cell ($A^{\circ 3}$)	Volume per pair ($A^{\circ 3}$)
Diamond (1Si1C)	20.900	20.900
2H (2Si2C)	41.790	20.895
4H (4Si4C)	83.530	20.882
6H (6Si6C)	125.310	20.885
Fesi (4Si4C)	83.560	20.890
Wurtzite (4Si4C)	83.550	20.887

Table 3-2 presents the optimized lattice parameters with lowest energies of our structures. It is shown in the table that in 2H, 4h, 6H, Wurtzite structure have the lattice parameters a = b, and for Diamond structure and FeSi structure, the lattice parameters a = b = c after the relaxation.

The lattice angels are depending on the structures. When the structures were fully relaxed, the angels of hexagonal structure and wurtzite structure were $\alpha = \beta = 90°$ and $\gamma = 120°$, for Diamond structure, $\alpha = \beta = \gamma = 60°$, and FeSi structure, $\alpha = \beta = \gamma = 90°$. It means the symmetry for all the structures did not break through the calculation processes.

Table 3-2 Lattice parameters of diamond structure, 2H, 4H, 6H, FeSi, Wurtzite, of SiC after relaxation (1x1x1) using DFT

Structure	Lattice parameters			The angels		
	a (A°)	b (A°)	c (A°)	α (°)	β (°)	γ (°)
Diamond	3.091	3.091	3.091	60	60	60
2H	3.086	3.086	5.065	90	90	120
4H	3.088	3.088	10.111	90	90	120
6H	3.089	3.089	15.158	90	90	120
FeSi	4.371	4.371	4.371	90	90	90
Wurtzite	3.089	3.089	10.108	90	90	120

Comparing our result with the experimental result of determining the lattice parameters of 2H, 4H, and 6H structures, we can see that in 2H at T = 300 K, the lattice parameter a = b =3.0763 A° which is very close to our calculation with different about 0.009 A°, and c = 5.065 A° with different about 0.017 A° [61]. However, in 4H structure at T = 300 K, the lattice parameters a = b = 3.0730 A° which means there is different around 0.015 A° comparing to our result, and c = 10.053 A° with different about 0.058 A° [61] . On the other hand, In 6H structure at T = 297 K, the experimental lattice parameters a = b = 3.0806 A° which demonstrates that there is different with our calculation about 0.008 A°, and c = 15.1173 A° with different about 0.041 A° [61] .

We did the same steps but with supercell (2x2x2) of Diamond structure, Wurtzite, FeSi and 6H structure of silicon carbide. We have examined and forced on these structures since they gave accurate results as it will be shown later in the next chapter. The supercell of 6H has 48 atoms of silicon and 48 atoms of carbon, and diamond structure, FeSi structure, and wurtzite structure of SiC have 32 atoms of silicon and 32 atoms of carbon.

The 3-7, 3-8, 3-9, and 3-10 shows the structures of Diamond structure, 6H, FeSi structure and wurtzite structure of supercell (2x2x2) when the structures fully relaxed.

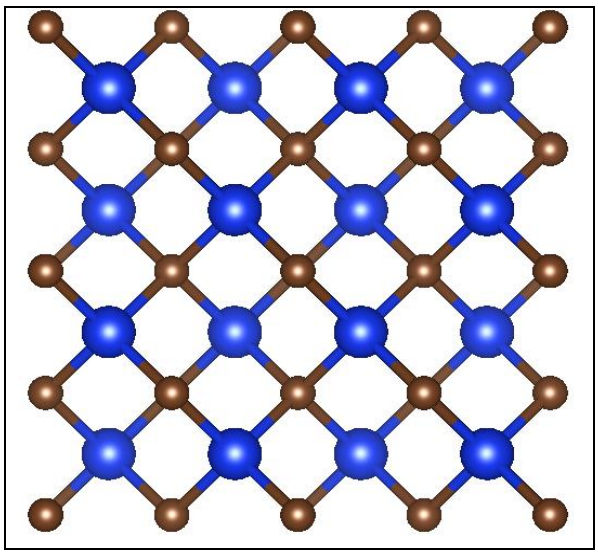

Figure 3-7 The supercell of diamond structure of SiC after the relaxation using DFT

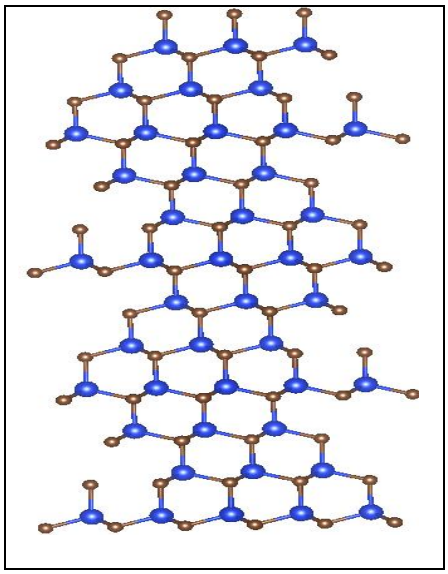

Figure 3-8 The supercell of 6H structure of SiC after the relaxation using DFT

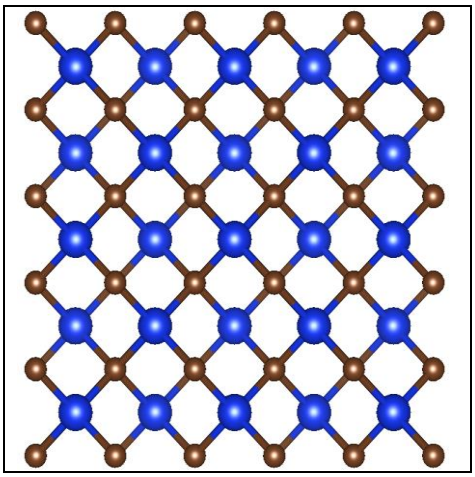

Figure 3-9 The supercell of FeSi structure of SiC after the relaxation using DFT

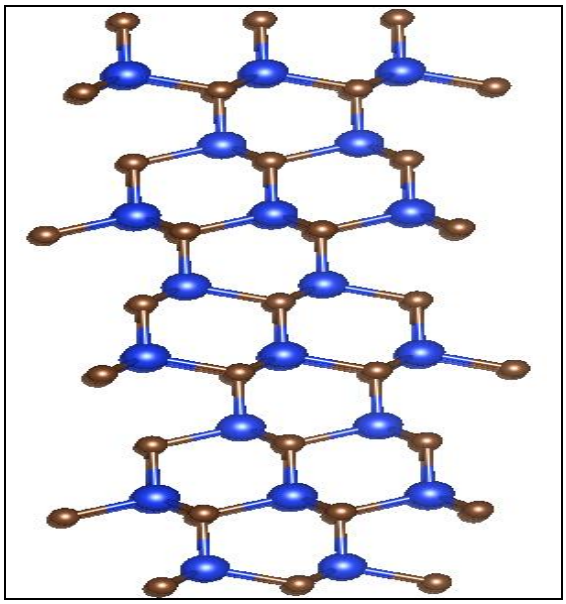

Figure 3-10 The wurtzite structures of the supercell of SiC after the relaxation using DFT

The volumes of the above structures were determined which are shown in table 3-3. The structure have similar volumes per pair with very slight different. The largest relaxed volume per pair is the volume of diamond structure with different about 0.005 $A^{\circ 3}$ comparing to 6H structure, and 0.003 $A^{\circ 3}$ comparing with FeSi structure and 0.006 $A^{\circ 3}$ when we compare it with wurtzite structure.

Table 3-3 The relaxed volume of supercell of 6H, Diamond structure, FeSi structure, wurtzite structure of SiC (2x2x2)

Structure of SiC (2x2x2)	Volume of cell $A^{\circ 3}$)	Volume per pair ($A^{\circ 3}$)
Diamond (32Si32C)	668.510	20.890
6H (48Si48C)	1002.500	20.885
Fesi (32Si32C)	668.410	20.887
Wurtzite (32Si32C)	668.30	20.884

Table 3-4 demonstrates the lattice parameters and the angels of supercell of diamond structure, 6H, FeSi, and wurtzite after the relaxation. It can be clearly seen that 4H, 6H, wurtzite structure have the lattice parameters a = b, and for Diamond structure and FeSi structure, the lattice parameters a = b = c after the relaxation which is same as in unit cell (1x1x1).

Also, when the structures relaxed, the symmetry did not break through calculation where the lattice angels in hexagonal structure and wurtzite structure were $\alpha = \beta = 90°$ and $= 120°$, for Diamond structure, $\alpha = \beta = \gamma = 90°$, and FeSi structure, $\alpha = \beta = \gamma = 90°$.

Table 3-4 Lattice parameters of supercell of diamond structure, 6H, FeSi, and wurtzite after relaxation (2x2x2) using DFT

Structure	Lattice parameters			The angels		
	a (A°)	b (A°)	c (A°)	α (°)	β (°)	γ (°)
Diamond	8.743	8.743	8.743	90	90	90
6H	6.179	6.179	30.314	90	90	120
FeSi	8.743	8.743	8.743	90	90	90
Wurtzite	6.177	6.177	20.219	90	90	120

Comparing the lattice parameters of diamond structure from our calculation with the experimental result with considering that the experimental lattice parameters for unit cell 1x1x1 while our calculation with 2x2x2 supercell, we can see that a= b= c = 4.359 A°, if we think of making our result for 1x1x1 unit cell, we can see that a = b = c = 4.371 A° which means that there is different about 0.011 A° [61].

3.2 Calculating the Lowest Energies of Structures and the Formation Enthalpies of Pristine Structures

When the structures were fully relaxed, we calculated the total energies of all the structures mentioned above by using density functional theory. We have calculated also the energy of bulk diamond phase of Si and graphite to calculate the formation enthalpies of the structures of SiC using the following equation

$$\Delta H_f = E(Si_xC_y) - xE(Si) - yE(C)$$

We utilized Van der Waals forces to calculate the energy of graphite due to the weak bonds between the layers in it. In table 3-5 we present the volume and the energies of bulk phase of Si and graphite after relaxation using DFT.

Table 3-5 The volume and the energies of bulk phase of Si and Graphite after relaxation using DFT

1x1x1	C only (4C)	Si only (2Si)
Volume of cell (A°)	34.260	40.880
Total energy (eV)	-37.232	-10.849
The energy per atom (eV)	-9.308	-5.424

Then, we determined the formation enthalpies per atom by using the energy per atom of silicon and the energy per atom of carbon, and by the total energy of SiC which is calculated by DFT.

Table 3-6 shows the total energies and the formation enthalpiees per atom of unit cell (1x1x1) of 2H, 4H, 6H, diamond structure, FeSi structure, wurtzite structure of SiC. It can be clearly seen that 4H and 6H structures have the same formation enthalpies per atom, and it is noticeable that 4H and 6H structures have the lowest formation enthalpies which is -0.166 eV which means that they are most stable structure among all structures. Also, diamond structure and FeSi structure have the same formation enthalpies, and have the second lowest formation enthalpies with -0.165 eV comparing to the other structures which means that they are more stable than 2H structure which has the formation enthalpy -0.162 eV, and lastly the wurtzite structure has the highest formation enthalpy which is -0.153 eV. It can be noticeable to see that the difference between the first lowest formation enthalpy and the second lowest formation enthalpy is 0.001 eV which is very small.

Table 3-6 The total energies and the formation enthalpies per atom of unit cell 2H, 4H, 6H, diamond structure, FeSi structure and wurtzite structure of SiC (1x1x1)

Structure (1x1x1)	Total energy (ev)	The formation enthalpy (ev)	The formation enthalpy per atom (ev)
Diamond (1Si1C)	-15.063	-0.331	-0.165
2H-SiC (2Si2C)	-30.114	-0.325	-0.162
4H-SiC (4Si4C)	-60.258	-0.332	-0.166
6H-SiC (6Si6C)	-90.387	-0.332	-0.166
Fesi (4Si4C)	-60.253	-0.331	-0.165
Wurtzite (4Si4C)	-60.159	-0.307	-0.153

We have focused more on 6H structure, diamond structure, FeSi structure, and wurtzite structure, and calculated supercell (2x2x2) of these structures. We have calculated the total energies and then the formation enthalpies per atom of supercell of diamond structure, 6H structure, FeSi structure, and wurtzite structure (2x2x2) with the same steps which was used to calculate for (1x1x1) structures. Table 3-7 demonstrates the total energies and the formation enthalpies per atom of supercell of diamond structure, 6H, FeSi structure, and wurtzite structure of SiC (2x2x2). We have seen that with the large structure, diamond structure and FeSi structure keep the same formation energy -0.165 eV while in 6H structure, the formation energy increases about 0.003 eV. However, in wurtzite structure, the formation energy in 2x2x2 structure decreases about 0.01 eV comparing to 1x1x1

structure and became -0.163 eV which is exactly same as the 6H structure. We have examined deeply the wurtzite structures of 1x1x1 and 2x2x2 to know the reasons behind getting different total energies although they are same structures of pristine SiC. In 1x1x1 and 2x2x2 wurtzite structures, we have two bond lengths along Z axis, in 1x1x1 the first bond length is 1.904 A°, and the second one is 1.891 A° while the first bond lend length in 2x2x2 structure is 1.902 A°, and the second bond length is 1.895 A°. The difference between the two bond lengths in 1x1x1 structure is 0.013 A°, but the difference in 2x2x2 structure is 0.007. It can be noticeable that the difference between the two bond lengths in1x1x1 higher than in 2x2x2 structure, and it is almost the double comparing to 2x2x2. Also, the lattice parameters a and c show a slight difference when we compare 1x1x1 with 2x2x2 structure. It shows that a = b 3.089 A° and c = 10.108 A° in 1x1x1 structure where it should be in 2x2x2 a =b= 6.179 A°, and c = 20.217 A°. However, the result of the calculation of 2x2x2 structure shows that the lattice parameters are a = b = 6.177 A°, and c = 20.219 A°. This means 2x2x2 structure has a slight different in a,b about 0.011 A° which is lower than the expectation from 1x1x1 structure, and the lattice parameter c has different about 0.001 A° which is higher than the expectation from 1x1x1 structure. Lastly, the comparing of the volumes of these structures shows slightly different about 0.003 $A^{\circ 3}$ in 1x1x1 structure higher than 2x2x2 structure. It can be concluded that the energy became more accurate in 2x2s2 structure due to the atomic arrangement. 2x2x2 structure has more atoms which have the freedom to move around in the structure where the structure is bigger than 1x1x1

structure. It allows the structure to get on more relaxation, and then get better result. These results indicate that diamond structure and FeSi structure are the most favorable structures comparing to 6H and wurtzite structures.

Table 3-7 The total energies and the formation enthalpies per atom of supercell of diamond structure, 6H, FeSi structure, and wurtzite structure of SiC (2x2x2)

Structure of SiC (2x2x2)	The total energy (eV)	The formation enthalpy (eV)	The formation enthalpy per atom (ev)
Diamond (32Si32C)	-482.029	-10.605	-0.165
6H (48Si48C)	-722.833	-15.697	-0.163
Fesi (32Si32C)	-482.027	-10.603	-0.165
Wurtzite (32Si32C)	-481.890	-10.466	-0.163

3.3 Electronic Properties of Pristine structures

Density of state (DOS) is one of the most important electronic properties which we have studied. We have calculated the DOS of diamond structure, 6H structure, FeSi structure, and wurtzite structure of SiC (1x1x1) using density functional theory and then we plot the partial DOS of silicon, partial DOS of carbon and the total DOS of silicon carbide. In all DOS plots, we have considered the spin up contribution and spin down contribution.

Figure 3-11 demonstrates the total DOS plot of diamond structure of SiC (1x1x1). It is noticeable that the bottom of conduction band starts with the contribution from silicon p orbital and carbon p orbital. Also, there is a band gap between the fermi level and the bottom of the conduction band around 1.391 eV. It can be seen the main contribution in the total dos is from p orbitals.

Figure 3-12 shows the partial DOS plot of silicon in diamond structure of SiC (1x1x1). It can be clearly seen that from fermi level to the bottom of the conduction band, there is a gap around 1.391 eV. The bottom of the conduction band with is near the fermi level, there is starting contribution of silicon s orbital and silicon p orbital. P orbital has higher contribution than s orbital, but around 5.5 eV s orbital has more contribution than p orbital. However, the contribution from p orbital increases till it gives the prominent peak around 13.2 eV. On the other side, in the valance band, the most contribution near fermi level is from p orbital, and it increases till it reaches to the highest peak at -3.09 eV. Also, it is noticeable that the highest peak in the valance band is from s orbital at -7.225 eV.

Lastly, in figure 3-13 presents the partial DOS plot of carbon in diamond structure of SiC (1x1x1). We can see that between the fermi level and the bottom of the conduction band, there is a gap which is around 1.391 eV. Then, the most contribution comes from p orbital, and the contribution increases till it gives the highest peak at 10.90 eV. On the other hand, the valance band has the highest contribution from p orbital around -1.66 eV.

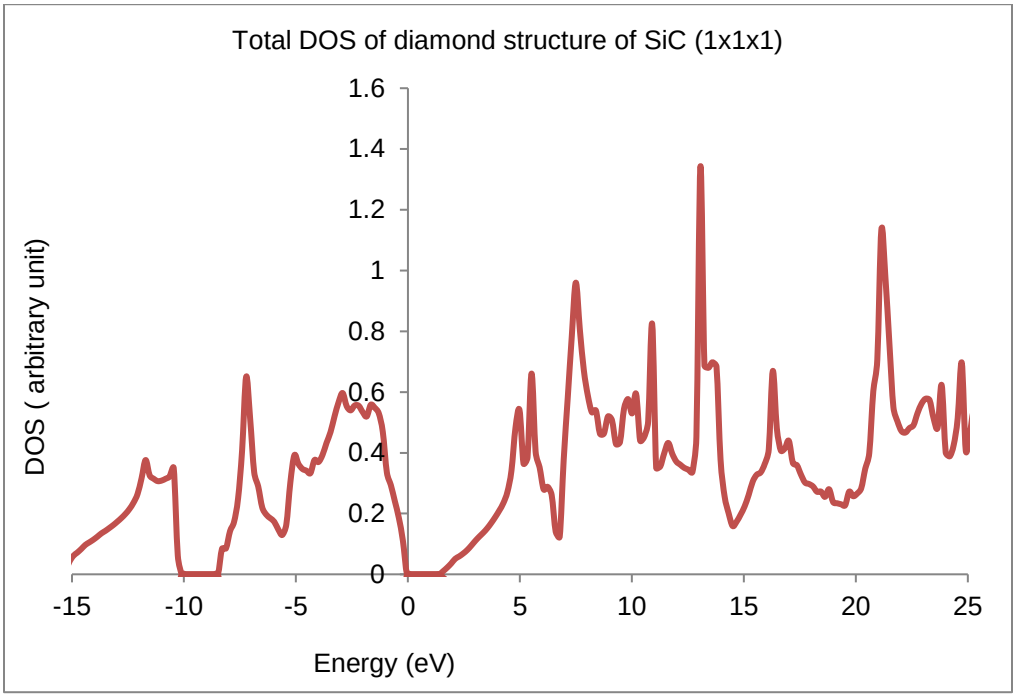

Figure 3-11 The total DOS plot of diamond structure of SiC (1x1x1)

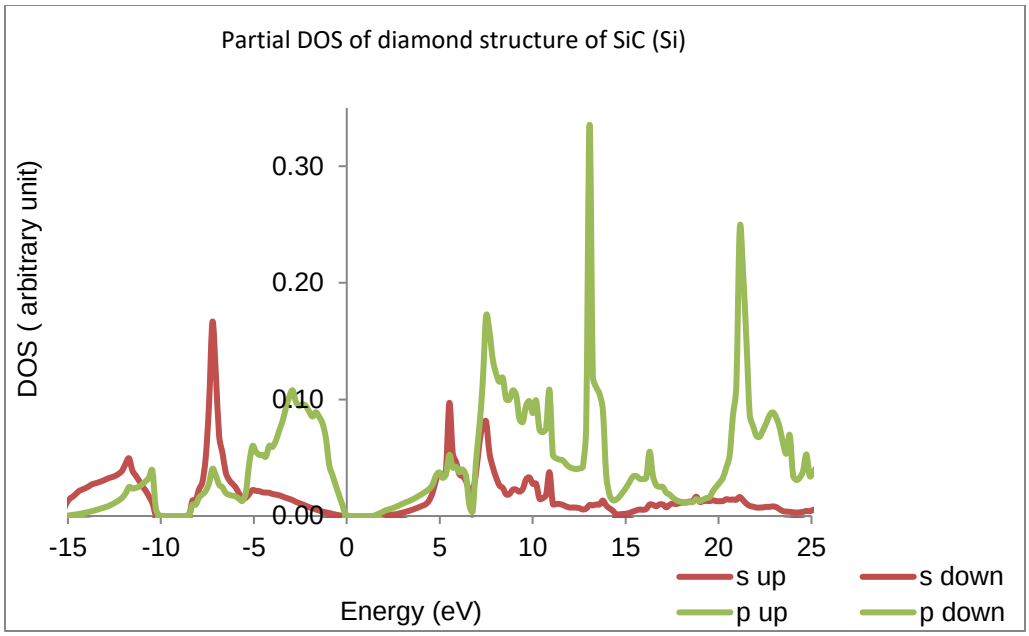

Figure 3-12 The partial DOS plot of diamond structure of SiC (1x1x1) (Si)

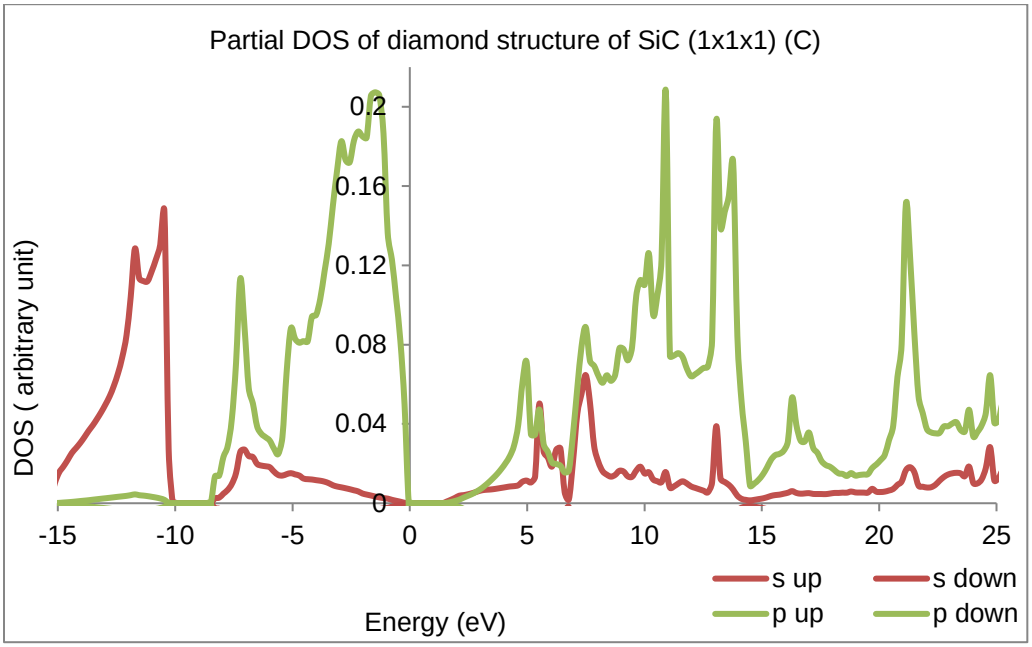

Figure 3-13 The partial DOS plot of diamond structure of SiC (1x1x1) (C)

Figure 3-14 demonstrates the total DOS plot of 6H structure of SiC (1x1x1). The plot has band gap between the fermi level and the conduction band around 2.034 eV which also the partial DOS of silicon and the partial DOS of carbon of 6H-SiC have, shown in figure 3-15 and 3-16. It is visible that the most contribution in 6H DOS plot is from p orbital as in diamond structure of SiC. However, when we compare the band gap which 6H structure and diamond structure have, we can see that there is a difference about 0.643 eV.

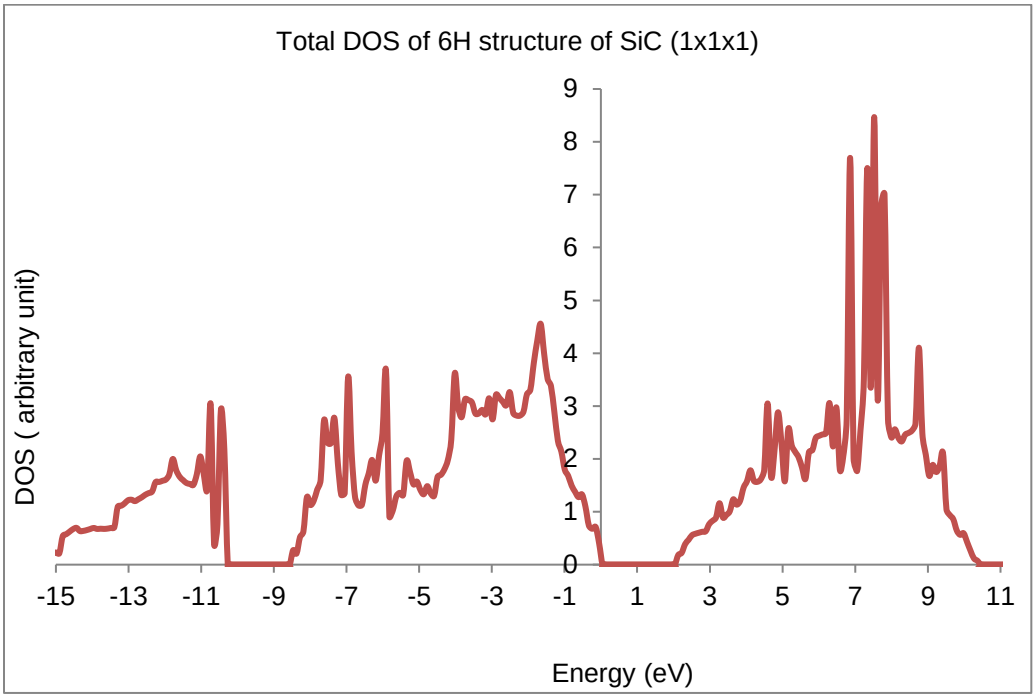

Figure 3-14 The total DOS plot of 6H structure of SiC (1x1x1)

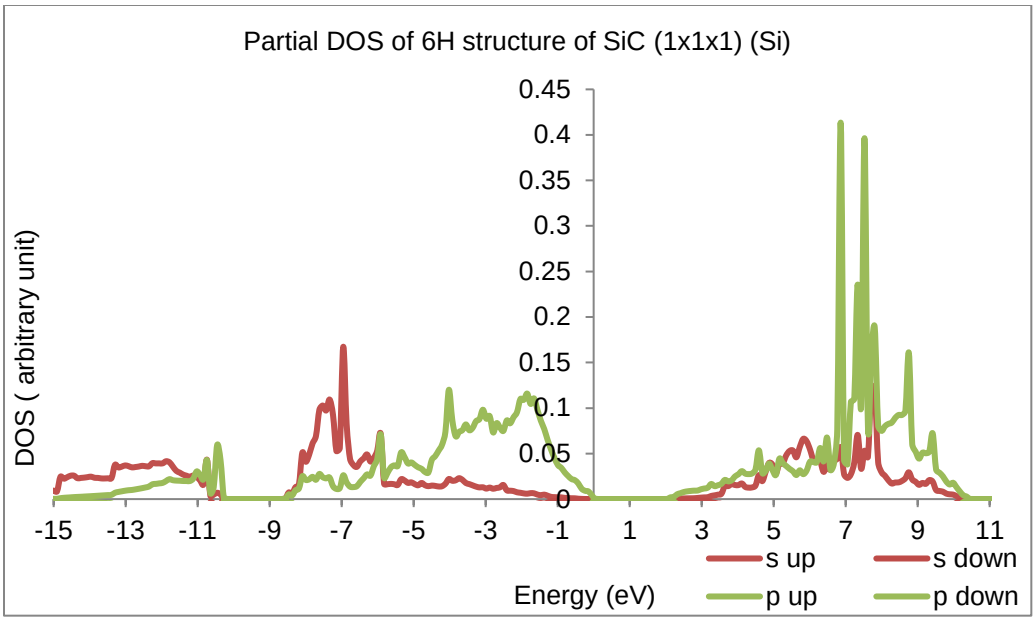

Figure 3-15 The partial DOS plot of 6H structure of SiC (Si) (1x1x1)

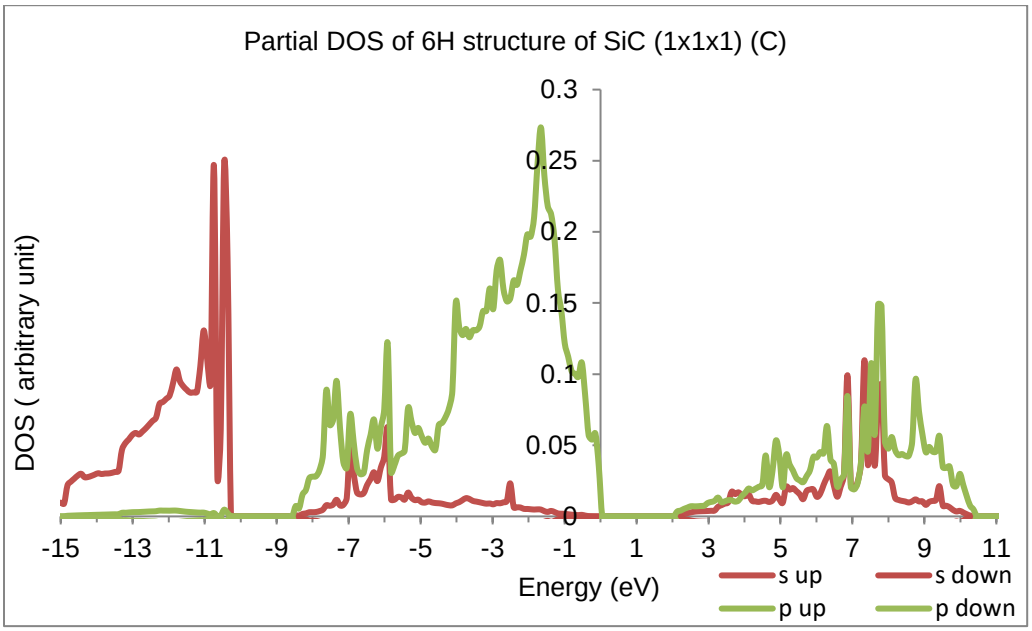

Figure 3-16 The partial DOS plot of 6H structure of SiC (C) (1x1x1)

Figure 3-17 shows the total DOS plot of FeSi structure of SiC (1x1x1). It can be noticeable that the total DOS of FeSi structure, and the partial DOS of silicon and the partial DOS of carbon which are shown in figure 3-18 and 3-19, also have band gap about 1.275 eV. This band gap is lower than what we have in diamond structure about 0.116 eV, and lower than 6H structure about 0.759 eV. Moreover, we can see that FeSi structure has contribution mostly from p orbital as it is in 6H and diamond structure.

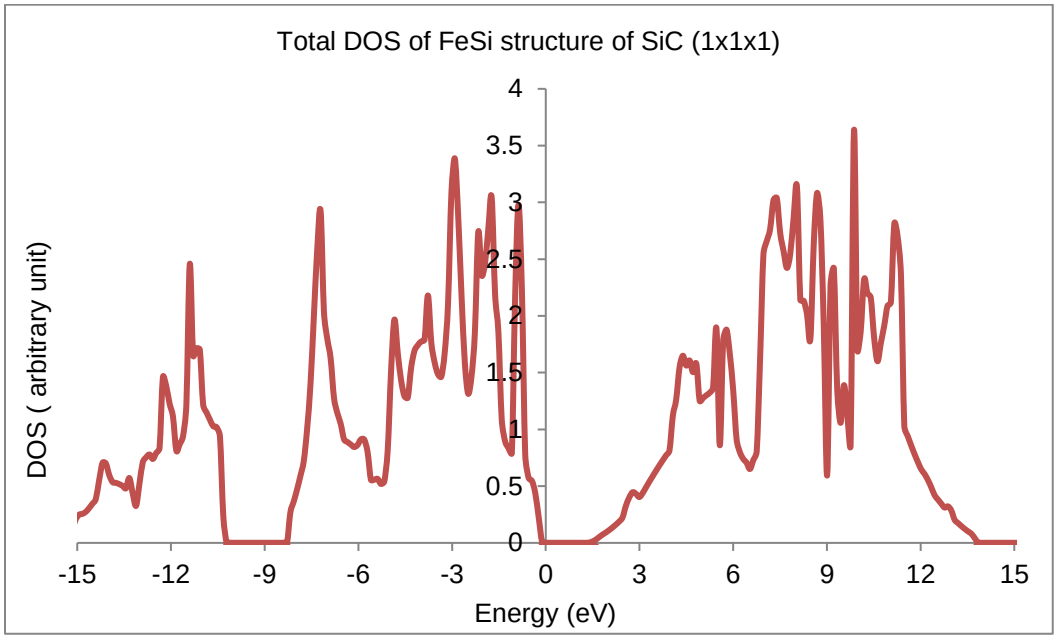

Figure 3-17 The total DOS plot of FeSi structure of SiC (1x1x1)

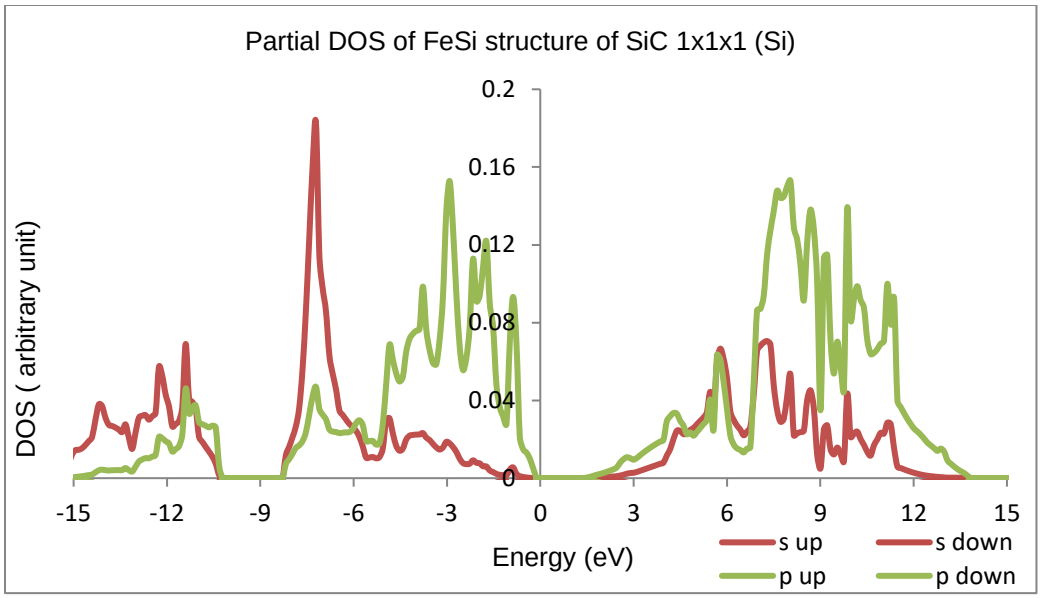

Figure 3-18 The partial DOS plot of FeSi structure of SiC (1x1x1) (Si)

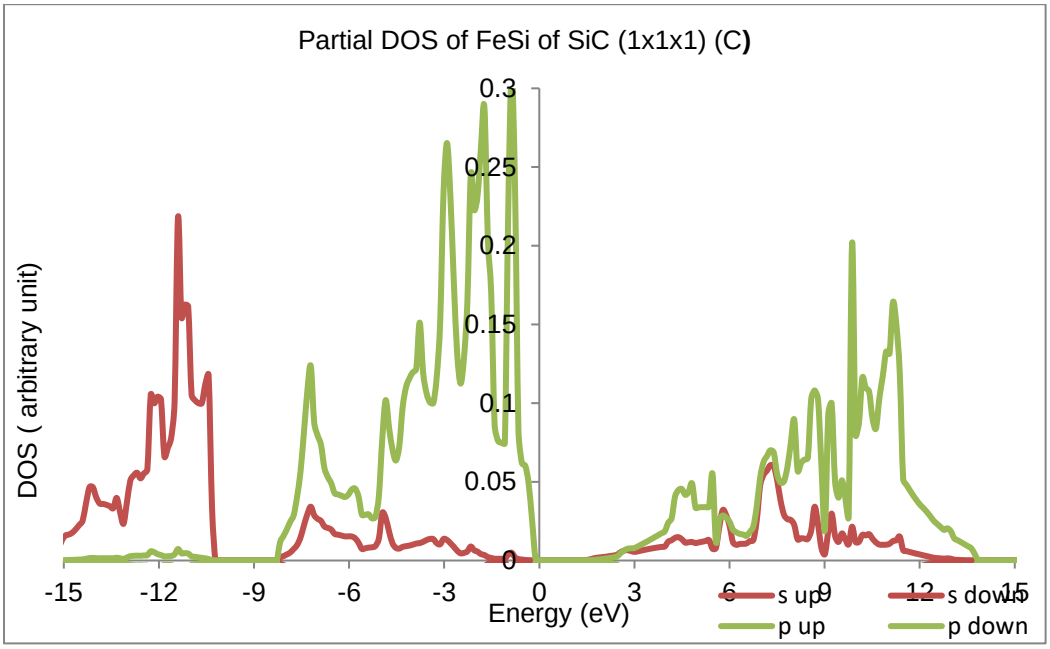

Figure 3-19 The partial DOS plot of FeSi structure of SiC (1x1x1) (C)

Lastly, the total DOS plot of wurtzite structure of SiC (1x1x1) is shown by figure 3-20 where we have band gap around 2.401 eV. This band gap is larger than what we have in 6H structure by about 0.366 eV, larger than the gap of diamond structure around 1.01 eV, and larger than FeSi structure about 1.126 eV. In figure (3-21) which is the partial DOS plot of silicon wurtzite structure of SiC, we have the same gap as in the total DOS plot of wurtzite structure of SiC, and the partial DOS plot of carbon wurtzite structure of SiC, which is shown in figure 3-22, has the same band gap as well. Also, as the previous structures, the DOS plots of wurtzite structure of SiC have the most contribution from p orbital.

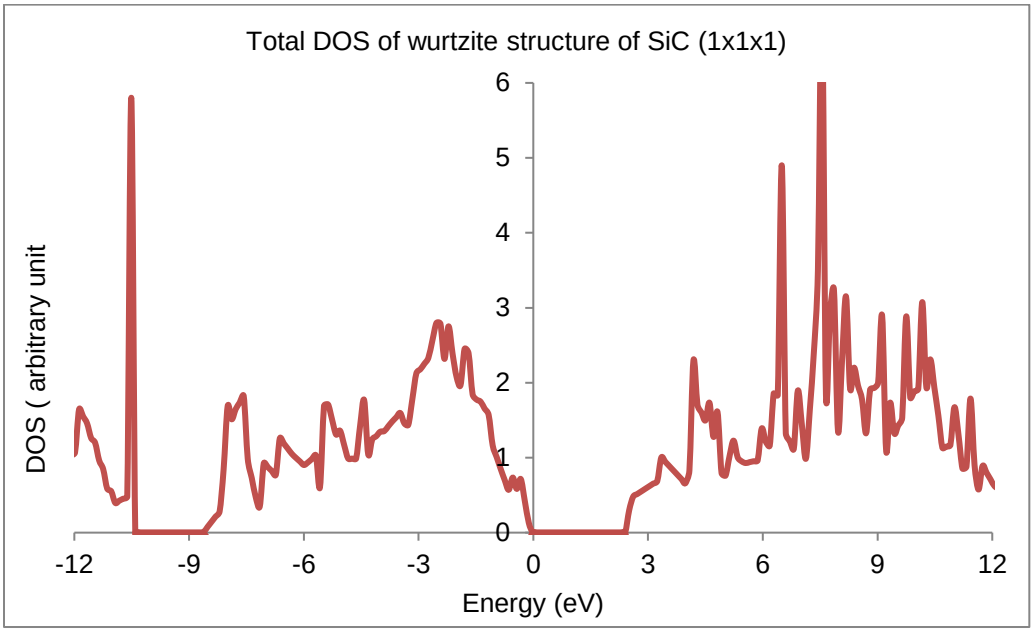

Figure 3-20 The total DOS plot of wurtzite structure of SiC (1x1x1)

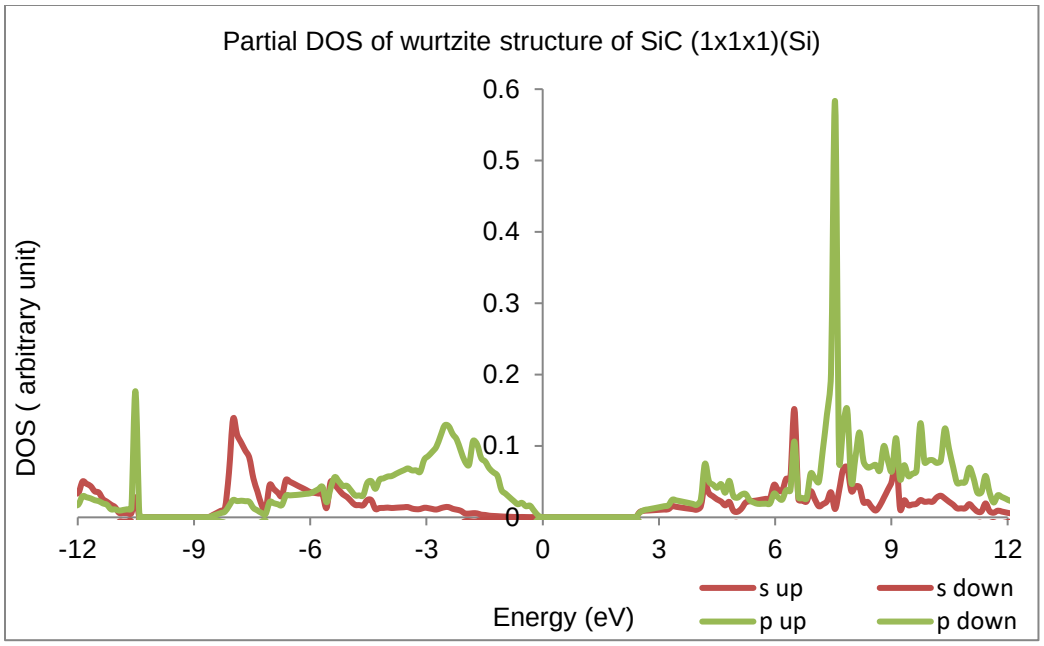

Figure 3-21 The partial DOS plot of wurtzite structure of SiC (1x1x1) (Si)

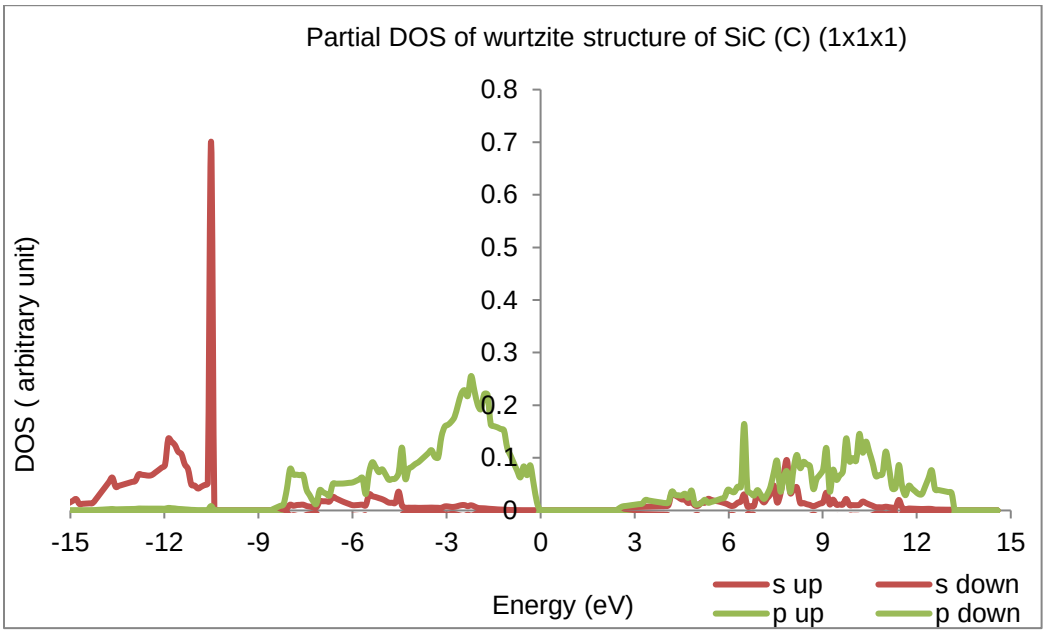

Figure 3-22 The partial DOS plot of wurtzite structure of SiC (1x1x1) (C)

By comparing the partial DOS of these four structures of carbon atom in silicon carbide, it can be noticeable that in diamond structure and FeSi structure, the contribution from p orbital goes highly very quick in the valance band while in wurtzite structure and 6H structure, it takes a while to reach the highest contribution in valance band. However, the p orbital in the conduction band in diamond structure and FeSi structure goes very slowly till it reaches to the first peak which is around 4.981 eV in diamond structure and 4.605 eV in FeSi structure. On the other side, in 6H structure and wurtzite structure, there is a strong hybridization between s orbital and p orbital in the conduction band. it can be clearly seen that in diamond structure and FeSi structure, the s orbital and p orbital in the partial DOS of carbon atom act similarly with slight different, and 6H structure and wurtzite structure have some similarity in the behave of s orbital and p orbital except that in the valance band of 6H, there is very long peak which wurtzite structure does not have.

Comparing the partial DOS of silicon in silicon carbide of the above structures, we can see that in wurtzite structure, s orbital and p orbital coupled with each other in the conduction band which is the situation in 6H structure, and both 6H structure and wurtzite structure in the valance band p orbital takes time to increase where it increases more quickly in FeSi structure. The hybridization between s orbital and p orbital in the conduction band is higher in wurtzite structure than in FeSi structure. Diamond structure and FeSi structure shows that there is a huge peak in the valance band around -7.22 eV from s orbital and in

6H structure it is around -6.95 eV while in wurtzite structure it comes from p orbital around -10.51 eV.

Chapter 4

Silicon Rich Silicon Carbide

The main aim in this chapter to study different structures of silicon rich silicon carbide structures, and see which structures are thermodynamically stable. Silicon rich silicon carbide means that the number of silicon atoms in silicon carbide is larger than the number of the carbon atoms in the structure. Our work mainly based on taking off the carbon atoms and replace it by silicon to get structure which has silicon atoms more than the carbon atoms which is considered as one of the impurities in silicon carbide.

We started with 2H structure of silicon carbide with replacing one carbon by one silicon. We did the relaxation of two different sizes of 2H structure, one of them with 5 atoms of silicon and 3 atoms of silicon 1x1x2 structure, and the second one when we have 17 atoms of silicon and 15 atoms of carbon 2x2x2 super cell. When the systems were fully relaxed, we obtain the volume of these structures, and then, we determined the total energy of each structure of 2H-SiC. Lastly, we calculated the formation enthalpies of both structures. Table 4.1 shows the volume after relaxation and the total energies of 2H structures of Si_c:SiC 1x1x2 and 2x2x2. In 1x1x2 structure, the formation enthalpy was above zero which means that the structure is not stable. However, in 2x2x2 structure, it gives lower formation energy about 0.233 eV, but it is still not stable comparing to other structures such 6H, diamond structure which will be discussed deeply later.

Table 4-1 The volume after relaxation and the total energies of 2H of Si_C:SiC

2H of Si_C:SiC	Volume of cell ($A^{\circ 3}$)	Volume per pair ($A^{\circ 3}$)	Total energy (eV)	The formation enthalpy (eV)
(5Si3C) 1x1x2	97.760	24.440	-52.887	+2.157 (+0.269 per atom)
(17Si15C) 2x2x2	351.200	21.950	-232.917	-1.089 (-0.036 per atom)

Also, we have examined 4H of Si_C:SiC as well to see if it would give stable structures of silicon rich silicon carbide. We obtained the volume of 4H of Si_C:SiC after the relaxation, and the energies of 4H structures with different number of atoms, shown in table 4-2. Then, the formation enthalpies are calculated per atom. It can be clearly seen that in 1x1x1 structure of 4H of Si_C:SiC, the structure need large volume to fully relax, and it gives formation enthalpy above zero which means that the structure is not stable. We calculated also 2x2x1 structure of 4H of Si_C:SiC, and it gives a formation enthalpy -0.037 eV, but it is still not good as the other structures. We went up to taking three carbon atoms and replaced them by silicon atoms, but the stability of 4H structure is less accurate than the other structure which will be discussed later in this chapter. Table 4-3 and 4-4 show the volume after relaxation and the total energies of 4H of $2Si_C$:SiC and the volume after relaxation and the total energies of 4H of $3Si_C$:SiC respectively.

Table 4-2 The volume after relaxation and the total energies of 4H of Si_C:SiC

4H of Si_C:SiC	Volume of cell ($A^{\circ 3}$)	Volume per pair ($A^{\circ 3}$)	Total energy (eV)	The formation enthalpy (eV)
(5Si3C) 1x1x1	95.880	23.970	-54.107	+0.937 (+0.117 per atom)
(17Si15C) 2x2x1	350.950	21.934	-232.944	-1.116 (-0.037 per atom)
(33Si31C) 2x2x2	684.730	21.397	-473.866	-6.326 (-0.098 per atom)

Table 4-3 The volume after relaxation and the total energies of 4H of $2Si_C$:SiC

4H of $2Si_C$:SiC 2x2x2	Volume of cell ($A^{\circ 3}$)	Volume per pair ($A^{\circ 3}$)	Total energy (eV)	The formation enthalpy (eV)
(far) (34Si-30C)	701.920	21.935	-466.032	-2.376 (-0.0742 per atom)

Table 4-4 The volume after relaxation, total energies, and the formation enthalpies of 4H of $3Si_C$:SiC

4H of $3Si_C$:SiC 2x2x2	Volume of cell ($A^{\circ 3}$)	Volume per pair ($A^{\circ 3}$)	Total Energy (eV)	The formation enthalpy (eV)
3near (35Si29C)	714.520	22.328	-459.75	0.022 0.0003 per atom
3far (35Si29C)	718.190	22.443	-458.879	0.893 0.013 per atom
2near 1far (35Si29C)	714.910	22.340	-459.810	-0.038 -.0005 per atom

4.1 Relaxing the Structures of Silicon Rich Silicon Carbide

From the above results, we excluded 2H, and 4H structures from this studies in this thesis. We decide to examine 6H structure, diamond structure, FeSi structure and wurtzite structure deeply. We worked on supercell structures 2x2x2 where diamond structure, FeSi structure and wurtzite structure have 32 atoms of silicon atoms, and 32 atoms of carbon, and 6H structure has 48 atoms of silicon and 48 atoms of carbon without defect. Then, we started to change the structure and make it silicon rich silicon carbide by taking off one carbon atom and replaced it by one silicon atom. We relaxed the structures fully, and we got on the structures. Figure 4-1 shows the relaxation structure of diamond, FeSi, 6H and wurtzite structure of silicon rich silicon carbide (Si_C:SiC) respectively.

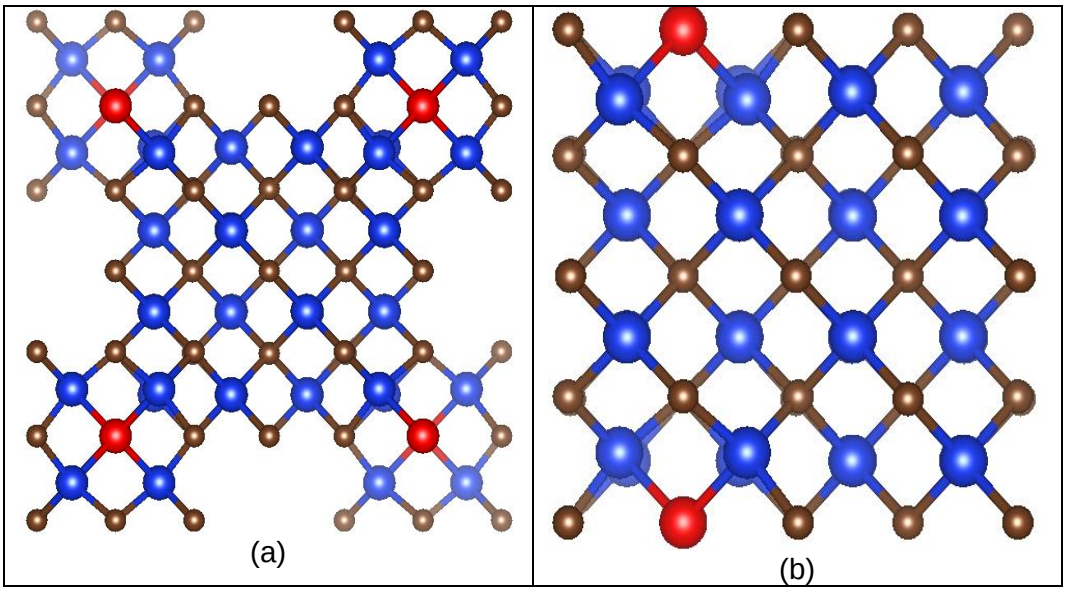

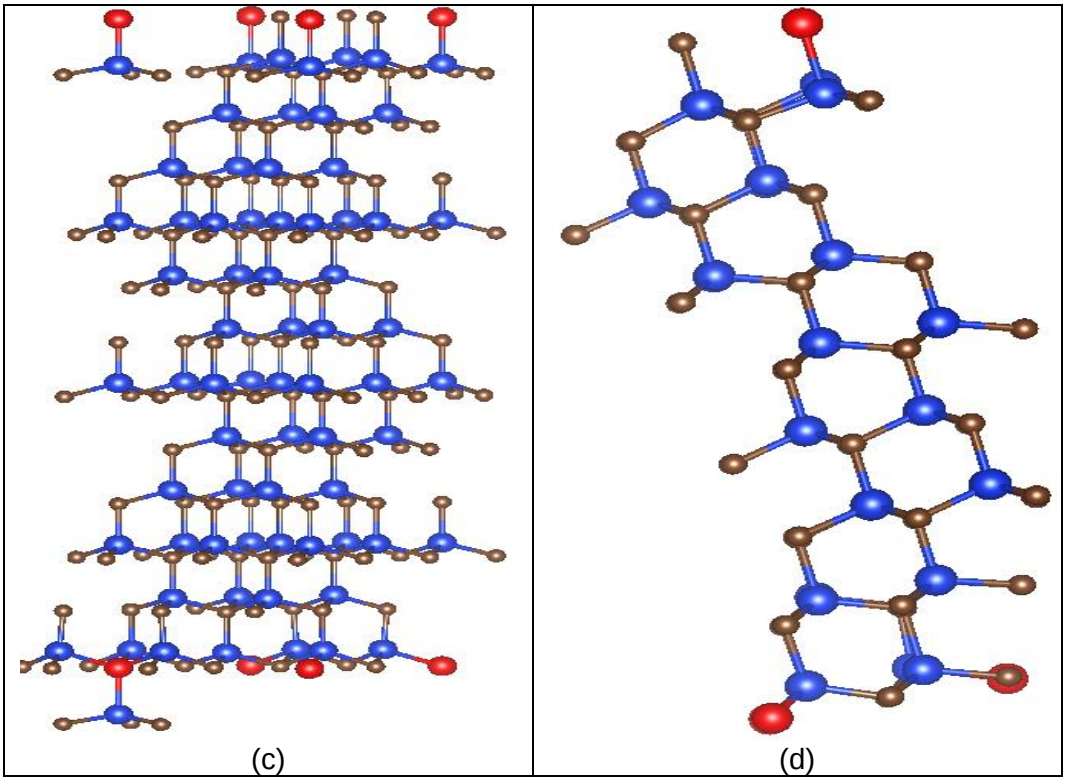

Figure 4-1 Silicon rich silicon carbide of (a) diamond structure, (b) FeSi structure, (c) 6H structure, and (d) wurtzite structure

Table 4-5 shows the volume after the relaxation of diamond, FeSi, wurtzite, and 6H structure supercell 2x2x2 using DFT. It can be clearly seen that 6H structure has the lowest relaxation volume while wurtzite structure has the highest volume with different about 0.186 $A^{\circ 3}$ when we compare it with 6H structure, and 0.011 $A^{\circ 3}$ comparing to FeSi structure and around 0.013 $A^{\circ 3}$ different with diamond structure.

Table 4-5 The volume after relaxation of diamond, FeSi, wurtzite, and 6H structure of Si_C:SiC supercell 2x2x2 using DFT

structure of Si_C:SiC	Volume ($A^{\circ 3}$)	Volume per pair ($A^{\circ 3}$)
diamond	684.40	21.387
FeSi	684.45	21.389
wurtzite	684.83	21.400
6H	1018.31	21.214

Table 4-6 The lattice parameters and the angels of diamond, FeSi, wurtzite, and 6H structures of Si_C:SiC supercell 2x2x2

Structure of Si_C:SiC	Lattice parameters			The angels		
	a (A°)	b (A°)	c (A°)	α (°)	β (°)	γ (°)
Diamond	8.812	8.812	8.812	90	90	90
FeSi	8.812	8.812	8.812	90	90	89.999
Wurtzite	6.226	6.226	20.396	90	90	120
6H	6.210	6.210	30.485	90	90	120

Table 4-6 demonstrates the lattice parameters and the angels of diamond, FeSi, wurtzite, and 6H structures supercell 2x2x2. It can be clearly seen that diamond structure and FeSi structure has the same lattice parameters where a = b = c, but comparing the angels of diamond structure and FeSi structure, we can see very slight different in γ angel about 0.001. On the other side, it can be

noticeable that the angels in wurtzite structure and 6H structure did not change through the calculation, and there is different about 0.016 A° in the lattice parameters a and b when we compare 6H structure with wurtzite structure.

After taking one atom of carbon and replaced it by silicon, we went farther and take off two carbon atoms and added two silicon atoms to our structures. We take into an account the configuration of the carbon atoms which are replaced by silicon. We considered both situation when the atoms near each other and far from each other to examine when the structures would give more accurate results and become stable structures. We did the comparison of near atoms and far atoms on 6H structure and diamond structure, and determined the relaxation volume of the. Figure 4-2 shows diamond structure of $2Si_C$:SiC when 2 atoms of carbon are near each and when the two atoms of carbon are far from each other, and figure 4-3 shows for 6h structure.

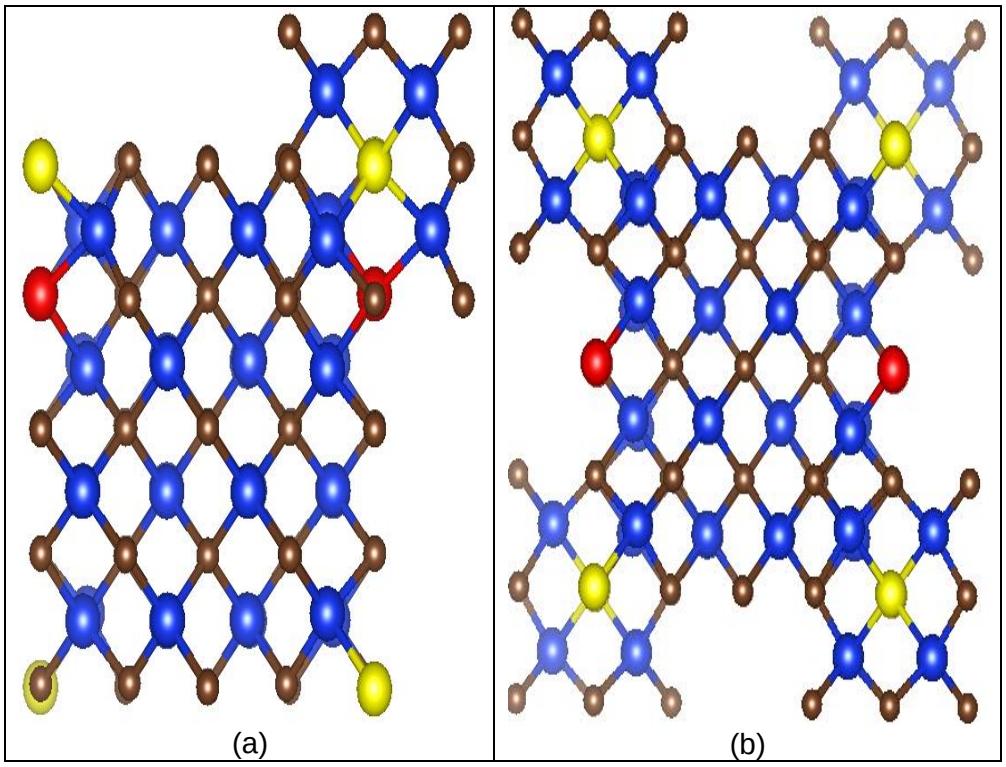

Figure 4-2 Diamond structure of $2Si_C$:SiC (a) is diamond structure of $2Si_C$:SiC (2 extra silicon atoms near each and (b) diamond structure of $2Si_C$:SiC (2 extra silicon atoms far from each other)

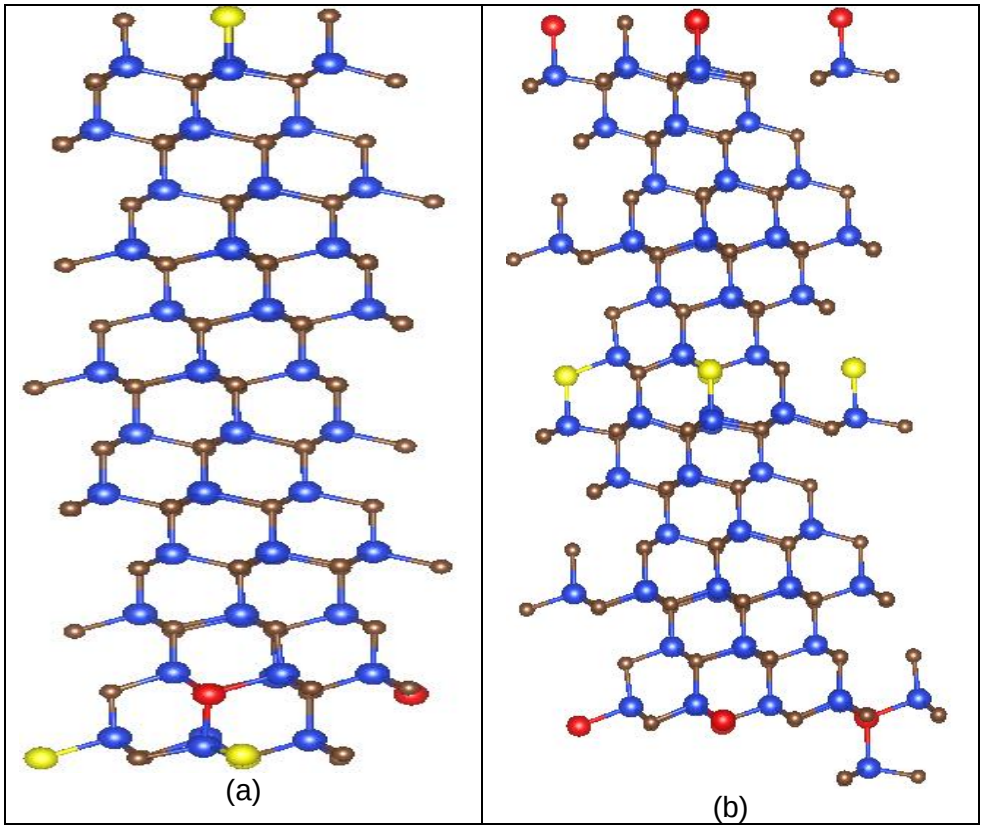

Figure 4-3 6H structure of $2Si_C$:SiC (a) is 6H structure of $2Si_C$:SiC (2 extra silicon atoms near each and (b) 6H structure of $2Si_C$:SiC (2 extra silicon atoms far from each other)

Table 4-7, and 4-9 demonstrate the relaxed volume of diamond $2Si_C$:SiC structure and 6H structure supercell 2x2x2 using DFT respectively. It shows that both diamond and 6H structure need less volume to fully relax when the carbon atoms near each other. Table 4-8, and 4-10 shows the lattice parameters and the angels of diamond $2Si_C$:SiC structure, and 6H structure $2Si_C$:SiC supercell 2x2x2 using DFT respectively. It can be clearly seen that when the carbon atoms near

each other, the angel α changed about 0.193 in diamond structure, and around 0.030 6H structure.

Table 4-7 The relaxed volume of diamond $2Si_C$:SiC structure supercell 2x2x2 using DFT

Diamond structure (34Si30C)	Volume (A°)
$2Si_C$:SiC (2 extra silicon atoms near each other)	700.010
$2Si_C$:SiC (2 extra silicon atoms far from each other)	700.319

Table 4-8 The lattice parameters and the angels of diamond $2Si_C$:SiC structure supercell 2x2x2 using DFT

Diamond Structure	Lattice parameters			The angels		
	a (A°)	b (A°)	c (A°)	α (°)	β (°)	γ (°)
$2Si_C$:SiC (2 extra silicon atoms near each other)	8.887	8.874	8.874	90.193	90	90
$2Si_C$:SiC (2 extra silicon atoms far from each other)	8.879	8.879	8.883	90	90	90

Table 4-9 The relaxed volume of 6H $2Si_C$:SiC structure supercell 2x2x2 using DFT

6H structure (50Si46C)	The volume ($A^{\circ 3}$)
$2Si_C$:SiC (2 extra silicon atoms near each other)	1034.360
$2Si_C$:SiC (2 extra silicon atoms far from each other)	1035.420

Table 4-10 The lattice parameters and the angels of 6H $2Si_C$:SiC structure supercell 2x2x2 using DFT

6H Structure	Lattice parameters			The angels		
	a (A°)	b (A°)	c (A°)	α (°)	β (°)	γ (°)
$2Si_C$:SiC (2 extra silicon atoms near each other)	6.246	6.240	30.647	90.137	90	120.030
$2Si_C$:SiC (2 extra silicon atoms far from each other)	6.244	6.244	30.663	90	90	120

The results indicate that when the carbon atoms, which are replaced by silicon, are near each other, it tends to give accurate results than when they are far from each other.

Based on the results of diamond structure and 6H structure, we considered the situation where the carbon atoms near each other in the rest structures, wurtzite structure and FeSi structure. Figure 4-4 shows the relaxed structure of FeSi structure and wurtzite structure.

We got on the relaxed volumes in all structures where the carbon atoms near each other shown in table 4-11. We can see that 6H structure has the lowest volume comparing to other structures, and wurtzite structure has the highest relaxed volume. Also, it can be noticeable that diamond structure and FeSi structure have slight different comparing to each other about 0.017 $A^{\circ 3}$.

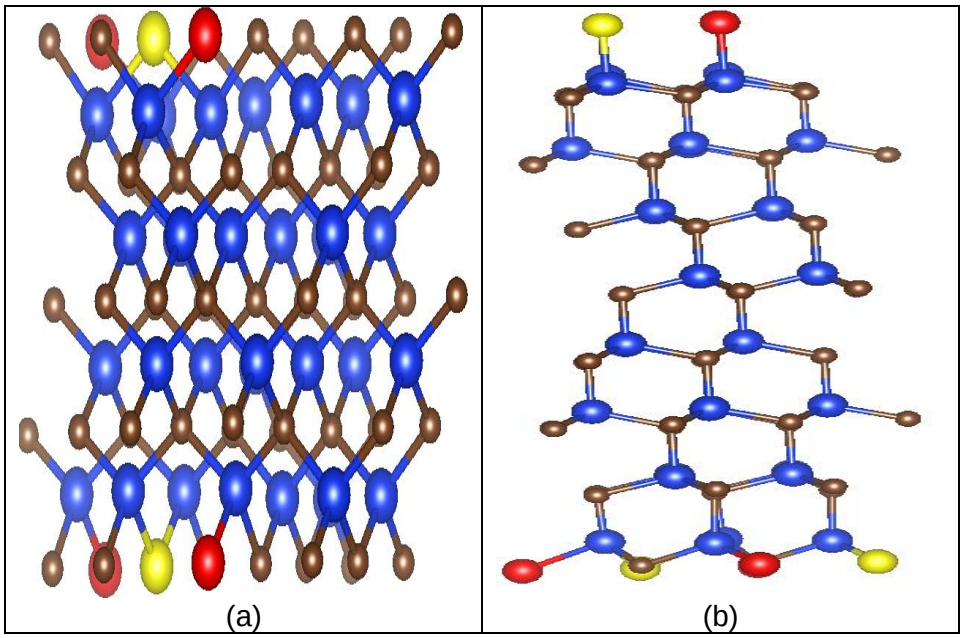

Figure 4-4 FeSi structure and wurtzite strucutre of $2Si_C$:SiC (a) is FeSi structure of $2Si_C$:SiC (2 extra silicon atoms near each other, and (b) wurtzite structure of $2Si_C$:SiC (2 extra silicon atoms near each other)

Table 4-11 The volume after relaxation of diamond, FeSi, wurtzite, and 6H structure of $2Si_C$:SiC supercell 2x2x2 when the carbon atoms near each other using DFT

structure of $2Si_C$:SiC	Volume ($A^{\circ 3}$)	Volume per pair ($A^{\circ 3}$)
diamond	700.010	21.875
FeSi	700.550	21.892
wurtzite	698.330	21.822
6H	1034.360	21.549

Table 4-12 Shows the lattice parameters and the angels of diamond, FeSi, wurtzite, and 6H structure of $2Si_C$:SiC supercell 2x2x2 when the carbon atoms, which are replaced by silicon, are near each other. It is visible that in all structures the lattice parameters a and b became not equal where it supposes to be equal, and diamond structure and FeSi structure have very close lattice parameters with very small different. Also, the angel α in diamond structure and 6H structure became larger, but it became smaller in FeSi structure

Table 4-12 The lattice parameters and the angels of diamond, FeSi, wurtzite, and 6H structure of $2Si_C$:SiC supercell 2x2x2 when the carbon atoms near each other

Structure of $2Si_C$:SiC	Lattice parameters			The angels		
	a (A°)	b (A°)	c (A°)	α (°)	β (°)	γ (°)
Diamond	8.887	8.874	8.874	90.193	90	90
FeSi	8.884	8.880	8.879	89.998	90.001	90.001
Wurtzite	6.266	6.209	20.661	90	90	119.700
6H	6.246	6.240	30.647	90.137	90	120.030

We did the same procedure with taking off three atoms of carbon and replaced them by silicon atoms in diamond structure and 6H structure, and we did comparison when the three atoms near each other, far from each other, and when 2 atoms near each other and the third one is far from the other two. Figure 4-5 shows how the extra silicon atoms distributed in diamond structure of $3Si_C$:SiC, in figure 4-5 (a) shows how the three atoms near each other with lowest between them, and (b) shows when two atoms are near each other but the third one far from them, and the last figure 4-5(c) shows how the extra silicon atoms far from each other.

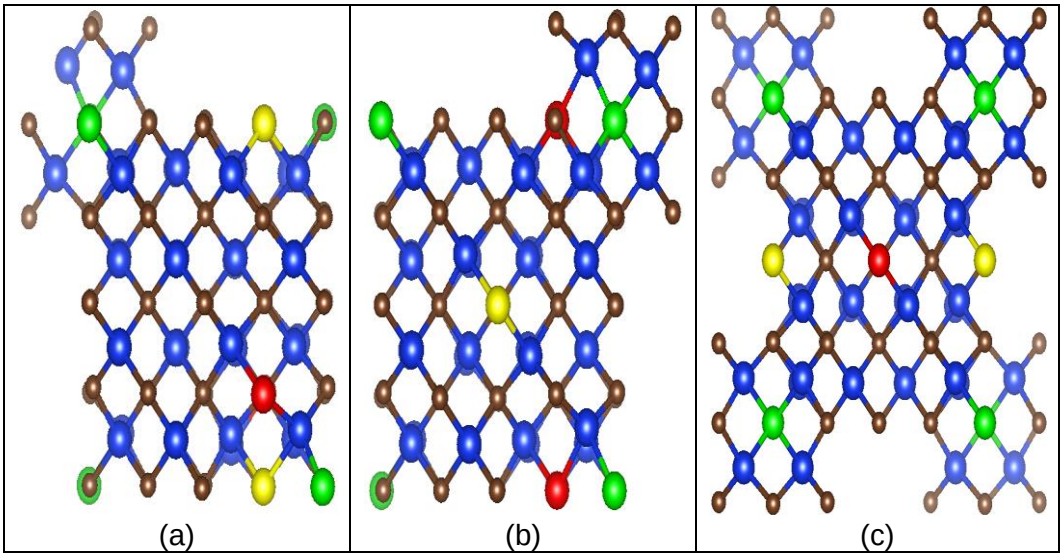

Figure 4-5 Diamond structure of $3Si_C$:SiC (a) Diamond structure of $3Si_C$:SiC (3 extra silicon atoms near each other), (b) Diamond structure of $3Si_C$:SiC (2 extra silicon atoms near each other and the third one far from them), and (c) Diamond structure of $3Si_C$:SiC (3 extra silicon atoms far from each other)

Table 4-13 demonstrates the relaxed volume of diamond $3Si_C$:SiC structure supercell 2x2x2 with different configuration of the extra silicon atoms using DFT. It shows that when the atoms of silicon are near each other, it gives small volume to fully relax, while it can be see that when two extra silicon near each other and the third one far gives the highest volume.

Table 4-13 The relaxed volume of diamond $3Si_C$:SiC structure supercell 2x2x2 using DFT

Diamond structure	volume (A°)
$3Si_C$:SiC (3 extra silicon atoms near each other)	716.350
$3Si_C$:SiC (2 extra silicon atoms near each other and the third one far from them)	717.210
$3Si_C$:SiC (3 extra silicon atoms far from each other)	717.340

Table 4-14 the lattice parameters and the angels of diamond $3Si_C$:SiC structure supercell 2x2x2 using DFT with different distribution of the extra silicon atoms. It is noticeable that in all configuration the lattice parameters and the angels changed.

Table 4-14 The lattice parameters and the angels diamond $3Si_C$:SiC structure supercell 2x2x2 using DFT

Diamond Structure	Lattice parameters			The angels		
	a (A°)	b (A°)	c (A°)	α (°)	β (°)	γ (°)
$3Si_C$:SiC (3 extra silicon atoms near each other)	8.947	8.947	8.947	90.207	90.207	89.792
$3Si_C$:SiC (2 extra silicon atoms near each other and the third one far from them)	8.95015	8.962	8.941	90.003	90.17	89.991
$3Si_C$:SiC (3 extra silicon atoms far from each other)	8.956	8.956	8.942	90	90	90

Figure 4-6 shows 6H structure of $3Si_C$:SiC with different arrangement of the extra silicon atoms where in figure (a) 2 extra silicon atoms are near each other and the third one far from them), (b) all the extra silicon far from each other), and (c) all the extra silicon near each other. Table 4-15, and 4-16 show the relaxed volume and the lattice parameters and the angels of 6H $3Si_C$:SiC structure supercell 2x2x2 using DFT respectively. It can be clearly seen that the smallest relaxed volume is when the extra silicon atoms are near each other as in diamond

structure, and the lattice parameters and the angels have been changed in all configuration due to the changes of the carbon atoms' number and the silicon atoms' number in the structure.

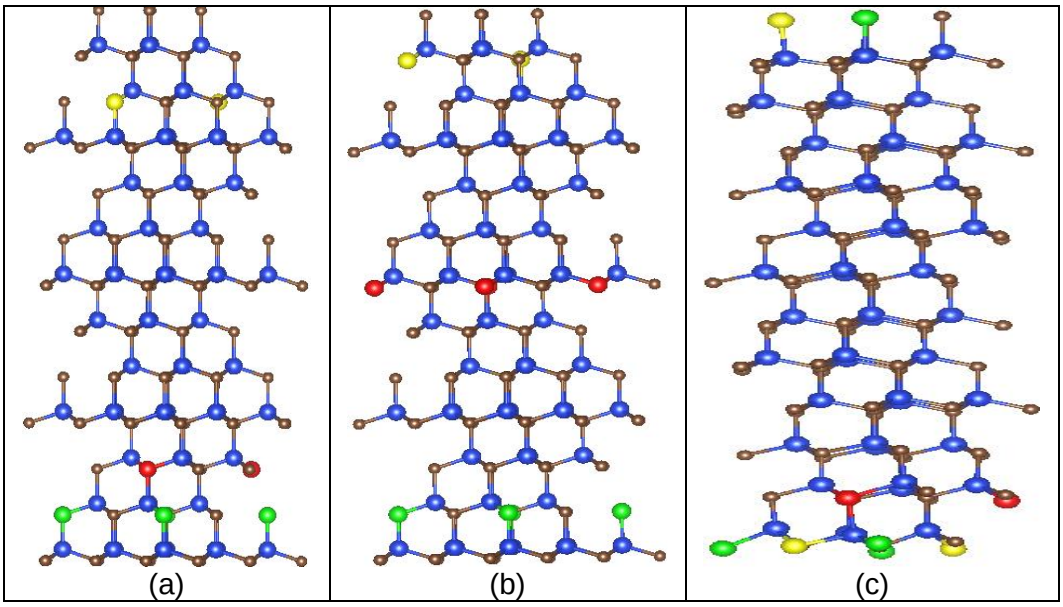

Figure 4-6 6H structure of $3Si_C$:SiC. (a) 6H structure of $3Si_C$:SiC (2 extra silicon near to each other and the third one far from them), (b) 6H structure of $3Si_C$:SiC (3 extra silicon far from each other), and (c) 6H structure of $3Si_C$:SiC (3 extra silicon near each other)

Table 4-15 The relaxed volume of 6H $3Si_C$:SiC structure supercell 2x2x2 using DFT

6H structure	Volume ($A^{\circ 3}$)
$3Si_C$:SiC (3 extra silicon atoms near each other)	1047.92
$3Si_C$:SiC (2 extra silicon atoms near each other and the third one far from them)	1051.401
$3Si_C$:SiC (3 extra silicon atoms far from each other)	1052.074

Table 4-16 The lattice parameters and the angels of 6H $3Si_C$:SiC structure supercell 2x2x2 using DFT

6H Structure $3Si_C$:SiC	Lattice parameters			The angels		
	a (A°)	b (A°)	c (A°)	α (°)	β (°)	γ (°)
(3 extra silicon atoms near each other)	6.272	6.229	30.893	90	90.172	119.773
(2 extra silicon near each other and the third one far from them)	6.280	6.2750	30.816	90.134	90.005	120.034
(3 extra silicon atoms far from each other)	6.278	6.277	30.821	90.009	90	120.004

We obtained the volumes, the lattice parameters, and the angels of FeSi structure of $3Si_C$:SiC and the wurtzite structure of $3Si_C$:SiC when the extra silicon atoms are near each other shown in figure 4-7 and compare it with 6H structure

and diamond structure shown in table 4-17 and table 4-18. It can be clearly seen that still 6H structure kept the lowest relaxed volume comparing to the other structures. The second lowest volume belongs to wurtzite structure with different about 0.31 $A^{\circ 3}$ comparing to the highest volume which belongs to FeSi structure. Looking to the lattice parameters of wurtzite structure, it is clear that a = b, and the angels are 90°, 90°, and 120° which means that the lattice and the angels presents the ideal structure while in diamond structure α, β, and γ become larger than the ideal angels.

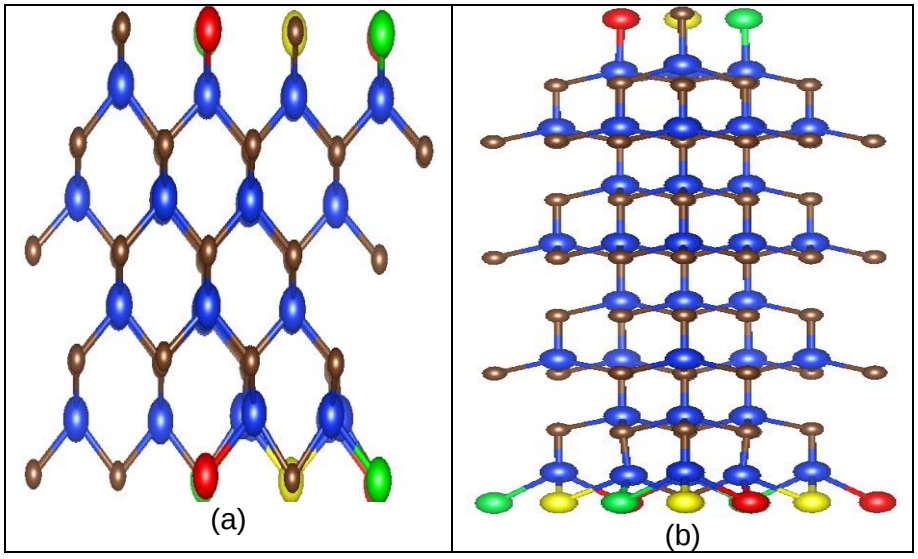

Figure 4-7 The structure of $3Si_C$:SiC. (a) FeSi structure of $3Si_C$:SiC (3 extra silicon atoms near each) (b) Wurtzite structure of $3Si_C$:SiC (3 extra silicon atoms near each other)

Table 4-17 The volume after relaxation of diamond, FeSi, wurtzite, and 6H structure of $3Si_C$:SiC supercell 2x2x2 when the extra silicon atoms near each other using DFT

structure of $3Si_C$:SiC	Volume ($A^{\circ 3}$)	Volume per pair ($A^{\circ 3}$)
diamond	716.350	22.385
FeSi	716.940	22.498
wurtzite	710.040	22.188
6H	1047.920	21.831

Table 4-18 The lattice parameters and the angels of diamond, FeSi, wurtzite, and 6H structure of $3Si_C$:SiC supercell 2x2x2 when the extra silicon atoms near each other

Structure of $3Si_C$:SiC	Lattice parameters			The angels		
	a (A°)	b (A°)	c (A°)	α (°)	β (°)	γ (°)
Diamond	8.947	8.947	8.947	90.207	90.207	89.792
FeSi	8.954	8.941	8.954	89.999	90	90
Wurtzite	6.241	6.241	21.044	90	90	120
6H	6.272	6.229	30.893	90	90.172	119.773

Also, we examined different configuration of four extra silicon which take the position of 4 carbon atoms in the four structures we have. We considered different configuration such as when the four atoms near each other and when two

atoms near each other and the other two are near each other in 6H structure and diamond structure. Also, we tried numerous arrangement of extra silicon atoms in diamond structure because it tends to give unstable structure when we take off four atoms of silicon and replaced it by 4 atoms of silicon. Also, FeSi structure becomes unstable structure with replacing four silicon atoms in the position of carbon atoms. However, in 6H structure, it gives stable structure when we add extra four silicon atoms instead of 4 atoms of carbon, and it is the same in wurtzite structure which give accurate result up to taking 4 atoms of carbon and replaced it by silicon atoms. Figure 4-8 shows the configuration of 6H structure of $4Si_C$:SiC where figure (a) presents the structure when we take off four carbon atoms which are near each other, and figure (b) shows when we replaced two atoms of silicon which are near each other and the other two are near each other. Figure 4-9 demonstrates different configuration of the extra four silicon atoms in diamond structure.

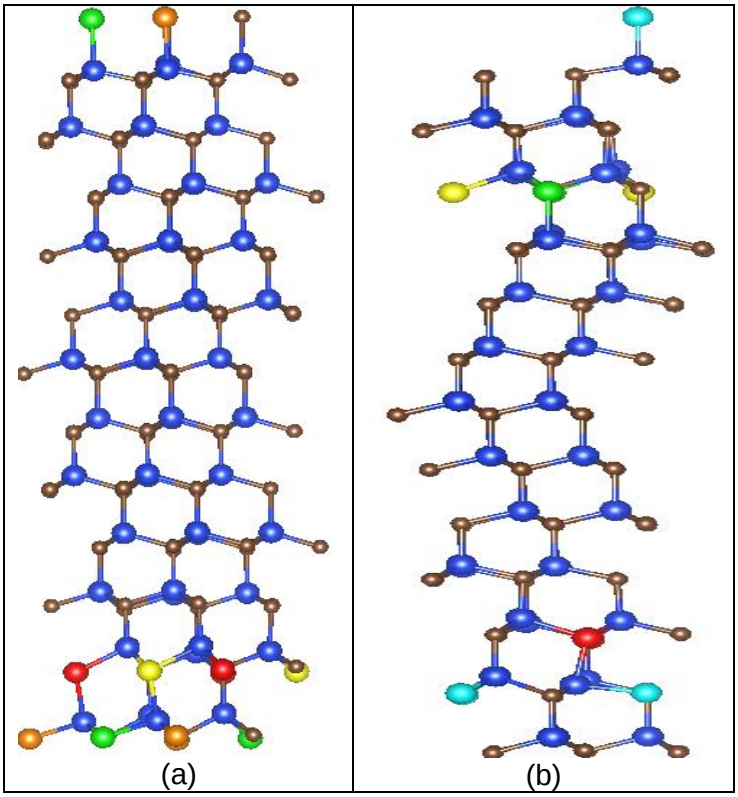

Figure 4-8 6H structure of $4Si_C$:SiC (a) (4 extra silicon atoms near each other. (b) (2 extra silicon atoms near each other and the other two near each other)

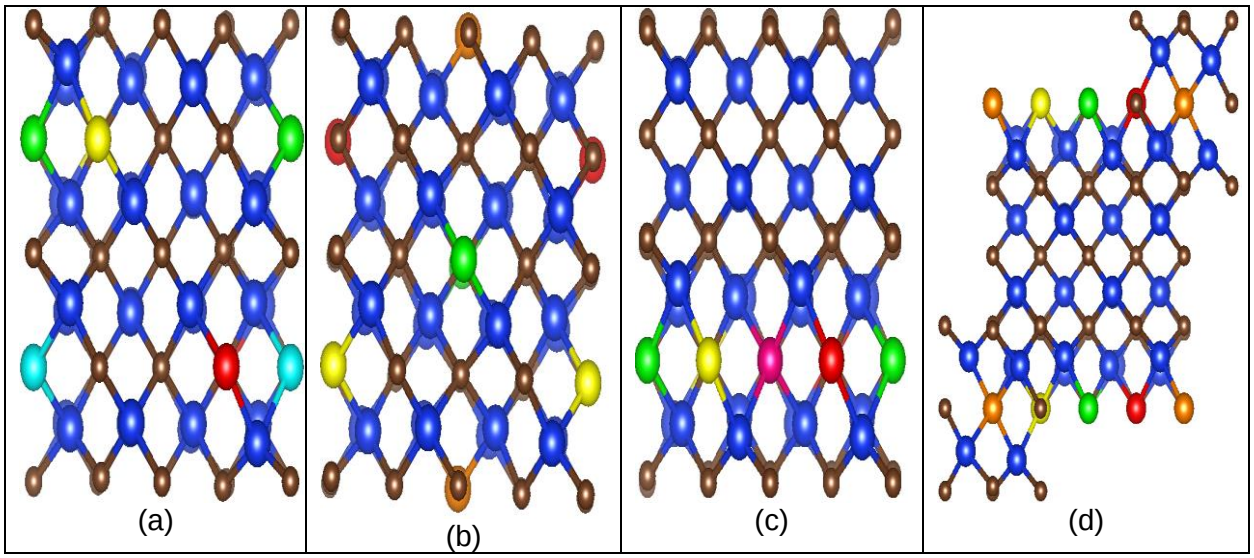
(a)
(b)
(c)
(d)

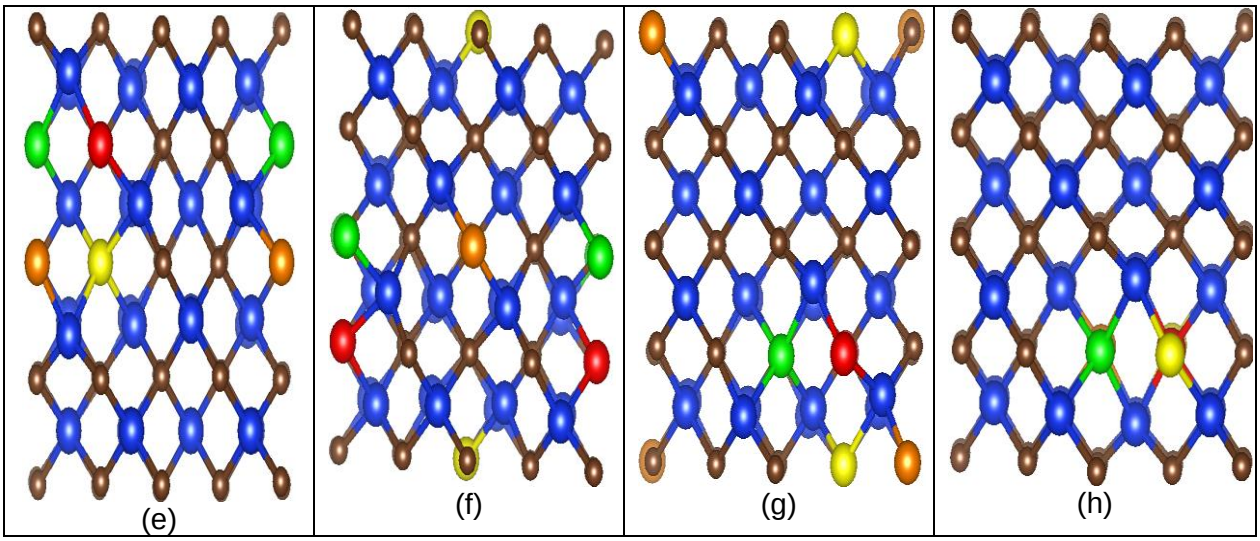
(e)
(f)
(g)
(h)

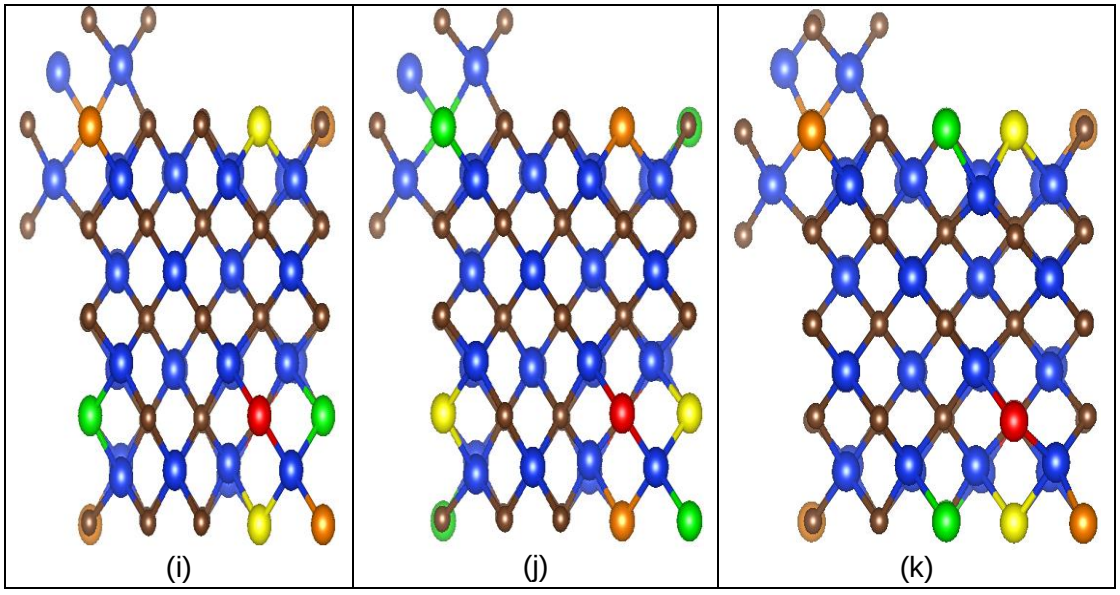

Figure 4-9 Diamond structure of $4Si_C$:SiC (a) (2 extra silicon near each other, and the other two are near each other), (b) (4 extra silicon atoms far from each other), (c) (4 in the middle of the structure), (d) (4 C atoms near each other at the same level), (e) (2 extra silicon atoms in one layer and the other 2 at the next layer), (f) (2 extra silicon atoms near each other and the other two spread far from each other), (g) (spread in two layers near each other),(h) (two extra silicon atoms behind each other and the other two behind each other), (i) (lattice parameter large to small), (j) (lattice parameter small to large), and (k) (3 extra silicon at the same layer and the forth one at the second layer and near to the other three).

Figure 4-10 shows the structure of FeSi and wurtzite structure of $4Si_C$:SiC where it can be clearly seen that in FeSi structure, the symmetry of the structure is broken by increasing the number of silicon atoms in it.

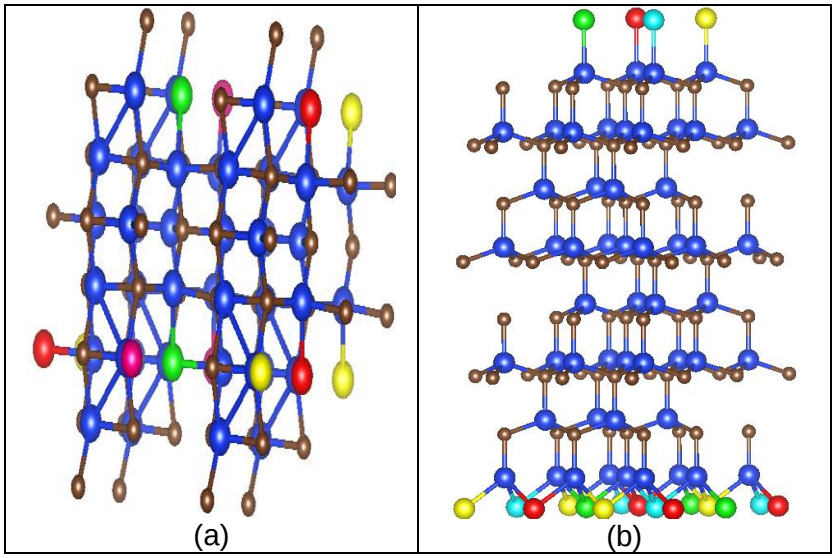

Figure 4-10 FeSi structure and wurtzite structure of $4Si_C$:SiC (a) FeSi structure of $4Si_C$:SiC when the four extra silicon atoms are near each other, and (b) is wurtzite structure of $4Si_C$:SiC when the four extra silicon atoms are near each other.

Table 4-19 demonstrates the volume after relaxation of diamond, FeSi, wurtzite, and 6H structure of $4Si_C$:SiC supercell 2x2x2 when the extra silicon atoms near each other using DFT. It can be clearly seen that 6H structure has the lowest relaxed volume which means it is the most stable structure among the other structure because the atoms in it are close to each other which make them interact

in proper way with each other. Wurtzite structure has the second lowest relaxed volume with different about 0.414 $A^{\circ 3}$ lower comparing to diamond structure. It is visible that FeSi structure has the highest relaxed volume which shows that it is unstable structure as will be shown in determining the lowest energy section. Also, from the lattice parameters of feSi structure shown in table 4.20, we can see how the lattice constant b has very large different about 5.444 A° comparing to the lattice parameter a while in wurtzite structure, the lattice parameters and the angels are ideal numbers.

Table 4-19 The volume after relaxation of diamond, FeSi, wurtzite, and 6H structure of $4Si_C$:SiC supercell 2x2x2 when the extra silicon atoms near each other using DFT

structure of $4Si_C$:SiC	Volume ($A^{\circ 3}$)	Volume per pair ($A^{\circ 3}$)
diamond	734.590	22.955
FeSi	833.510	26.047
wurtzite	721.330	22.541
6H	1061.810	22.121

Table 4-20 The lattice parameters and the angels of diamond, FeSi, wurtzite, and 6H structure of $4Si_C$:SiC supercell 2x2x2 when the extra silicon atoms near each other

Structure of $4Si_C$:SiC	Lattice parameters			The angels		
	a (A°)	b (A°)	c (A°)	α (°)	β (°)	γ (°)
Diamond	8.999	9.045	8.987	90	90	90
FeSi	11.916	6.472	10.812	90	88.027	90
Wurtzite	6.252	6.252	21.305	90	90	120
6H	6.304	6.237	31.070	90	90.431	119.649

Reputing the same procedure of all structures with replacing five atoms of carbon with five silicon atoms shown in figure 4-11 to see which structure would give stable structure with lower energy.

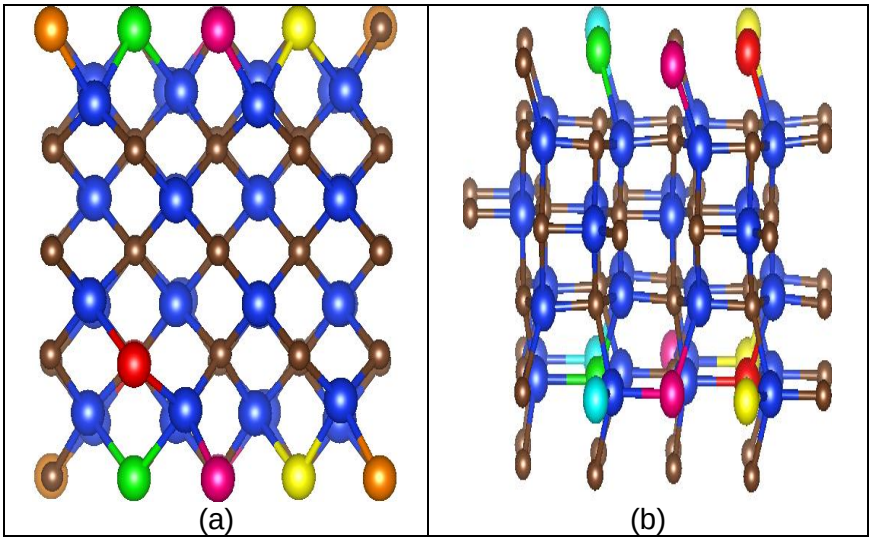

(a) (b)

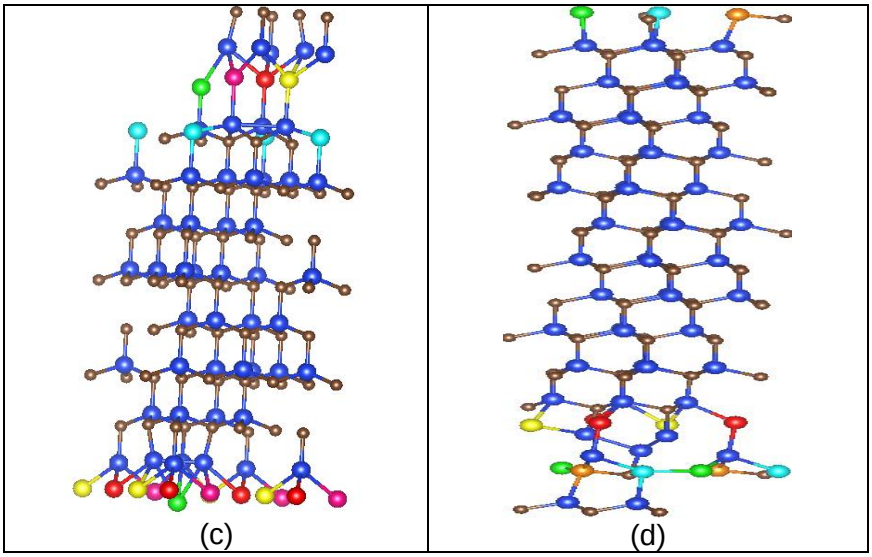

Figure 4-11 $5Si_C$:SiC structure of (a) diamond structure, (b) FeSi structure, (c) wurtzite structure, and (d) 6H structure when all five extra atoms of silicon are near each other.

Table 4-21 demonstrates the volume after relaxation of diamond, FeSi, wurtzite, and 6H structure of $5Si_C$:SiC supercell 2x2x2 when we replaced the extra silicon atoms taking the position near each other. The results indicate that 6H structure is the most stable structure comparing to the other where the relaxed volume is the lowest while FeSi structure is unstable structure with high relaxed volume about 2.277 $A^{\circ 3}$ comparing to 6H structure. Also, we can see that diamond structure has the second higher relaxed volume with different about 0.982 $A^{\circ 3}$ comparing to 6H structure. Table 4-22 shows how the wurtzite structure kept the ideal numbers of the lattice parameters and the angels, and how the changes in the lattice parameters of FeSi structure.

Table 4-21 The volume after relaxation of diamond, FeSi, wurtzite, and 6H structure of $5Si_C$:SiC supercell 2x2x2 when the extra silicon atoms near each other using DFT

structure of $5Si_C$:SiC	Volume ($A^{\circ 3}$)	Volume per pair ($A^{\circ 3}$)
Diamond	747.820	23.369
FeSi	791.280	24.727
Wurtzite	736.580	23.018
6H	1077.62	22.450

Table 4-22 the lattice parameters and the angels of diamond, FeSi, wurtzite, and 6H structure of $5Si_C$:SiC supercell 2x2x2 when the extra silicon atoms near each other

Structure of $5Si_C$:SiC	Lattice parameters			The angels		
	a (A°)	b (A°)	c (A°)	α (°)	β (°)	γ (°)
Diamond	9.065	9.099	9.065	90.266	90.032	89.955
FeSi	11.138	6.422	11.061	90	90.143	90
Wurtzite	6.220	6.220	21.979	90	90	120
6H	6.195	6.194	32.420	90	90.738	119.993

In diamond structure of $5Si_C$:SiC, we considered another configuration of the extra five silicon shown in figure 4-12, but it did not provide proper result.

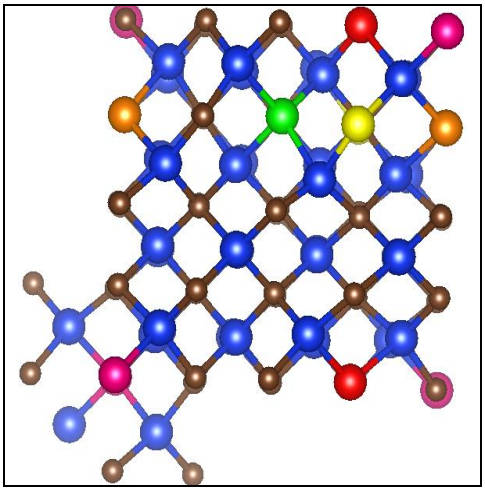

Figure 4-12 Diamond structure of $5Si_C$:SiC (5 extra silicon atoms near each other but not at same layers)

We did the same steps, and replaced 6 carbon atoms by 6 atoms of silicon shown in figure 4-13 where we considered all extra silicon near each other. It shows how the structure arranged after the relaxation. Table 4-23 shows the volume after relaxation of diamond, FeSi, wurtzite, and 6H structures of $6Si_C$:SiC supercell 2x2x2 when all extra silicon atoms near each other. We can see that the relaxed volume of FeSi structure increases highly while the relaxation volume of 6H structure increase with very small amount comparing to $5Si_C$:SiC which is the situation of diamond and the wurtzite structures.

Looking to the lattice parameters shown in table 4-24, it can be noticeable that the angel β in the wurtzite structure has a big change with different about 4.283° comparing to the ideal angel which is 90° while in 6H structure the angels changed with very slight different.

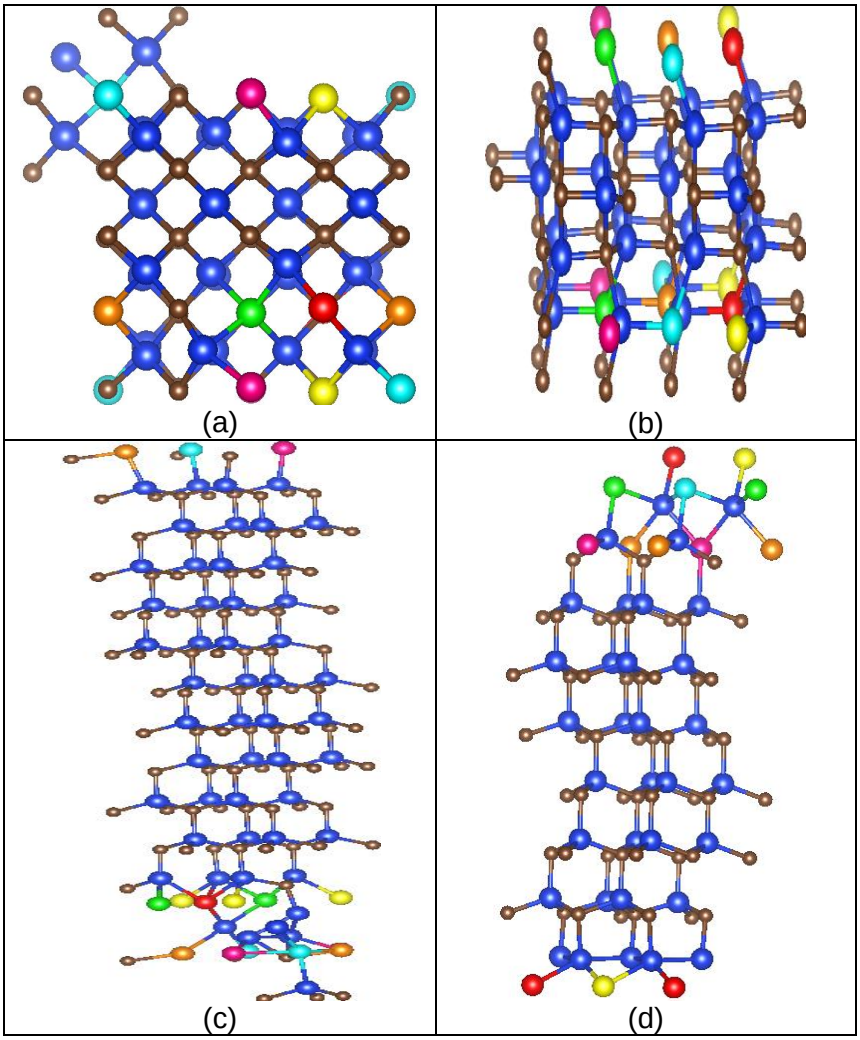

Figure 4-13 $6Si_C$:SiC structure of (a) diamond structure, (b) FeSi structure, (c) 6H structure, and (d) wurtzite structure, when all 6 extra silicon atoms near each other.

Table 4-23 The volume after relaxation of diamond, FeSi, wurtzite, and 6H structure of $6Si_C$:SiC supercell 2x2x2 when the extra silicon atoms near each other using DFT

structure of $6Si_C$:SiC	Volume ($A^{\circ 3}$)	Volume per pair ($A^{\circ 3}$)
Diamond	765.660	23.926
FeSi	809.190	25.287
Wurtzite	754.200	23.568
6H	1079.690	22.493

Table 4-24 The lattice parameters and the angels of diamond, FeSi, wurtzite, and 6H structure of $6Si_C$:SiC supercell 2x2x2 when the extra silicon atoms near each other

Structure of $6Si_C$:SiC	Lattice parameters			The angels		
	a (A°)	b (A°)	c (A°)	α (°)	β (°)	γ (°)
Diamond	9.145	9.149	9.149	89.734	90	90
FeSi	11.251	6.467	11.119	90	90.096	90
Wurtzite	6.196	6.196	22.767	90	85.717	119.999
6H	6.21960	6.195	32.417	91.799	90	120.128

As we mentioned above, all diamond, FeSi and wurtzite structures tend to give unstable structure and higher energy after 4 atoms of silicon taking the position of 4 carbon atoms, but it was not the situation with 6H structure until we

worked with 6H structure with replacing 7 atoms of carbon by silicon atoms. The seven atoms in 6H structure were near each other, but we got on higher energy which lead us to try different configuration. The seven carbon atoms were replaced in all structure by seven atoms of silicon, and in all it did not give accurate result. We focused on diamond and 6H structure, and examined them with spreading the seven atoms in different ways shown in figure 4-14 for 6H structure, and figure 4-15 for diamond structure. We have noticed that we should replace the carbon atoms which are at same layers by silicon atoms to get on stable structure and got on lower energy. Figure 4-16 shows how we distributed the extra silicon atoms in FeSi structure and wurtzite structure.

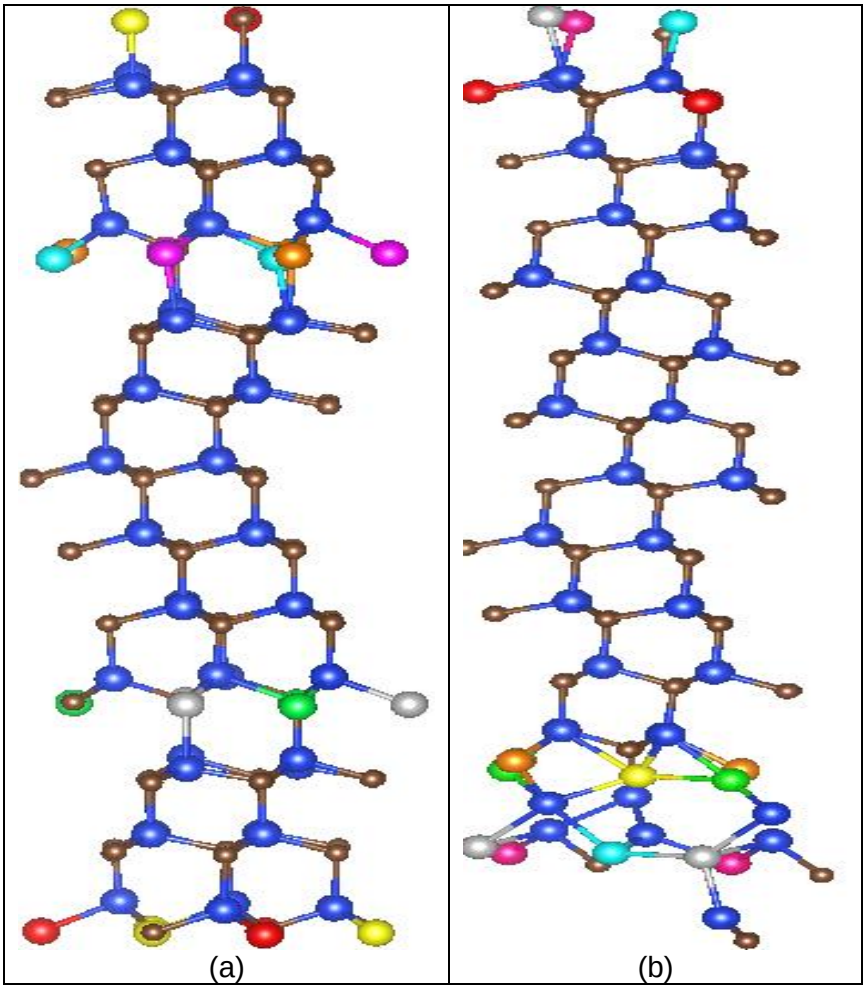

(a) (b)

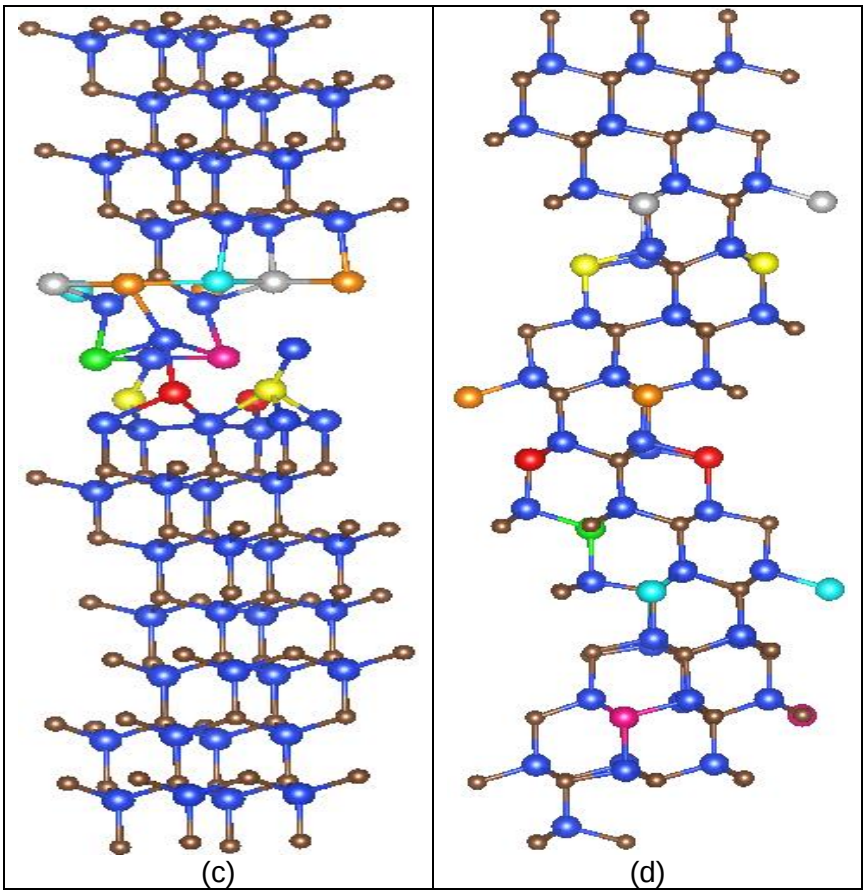

Figure 4-14 6H structure of $7Si_C$:SiC,(a) is (2 extra silicon atoms near each other,2 extra silicon atoms near each other and the last 3 extra silicon atoms near each other), (b) is (7 extra silicon atoms near each other but not at same levels), (c) is (7 silicon atoms near each other at same layers, and (d) 7 silicon atoms spread randomly.

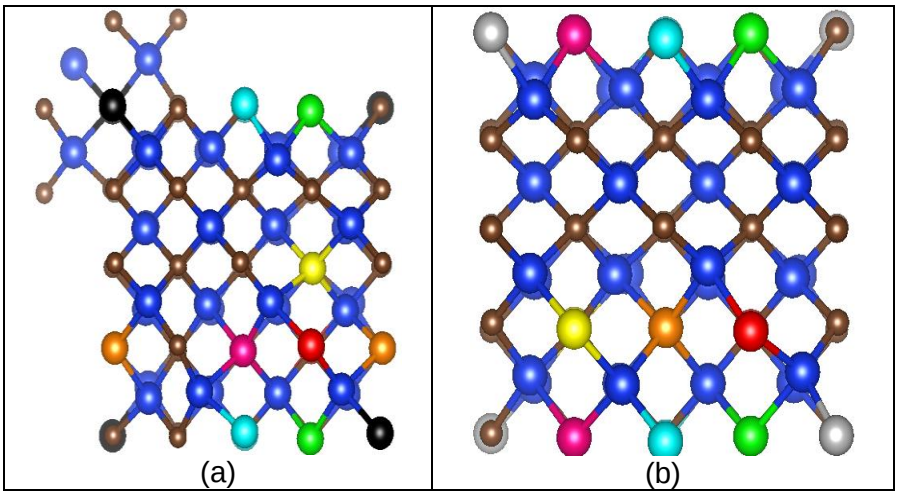

Figure 4-15 (a) diamond structure of $7Si_C$:SiC (7 extra silicon near each other but not same layers), and (b) is diamond structure of $7Si_C$:SiC (7 extra silicon atoms near each other at same layers)

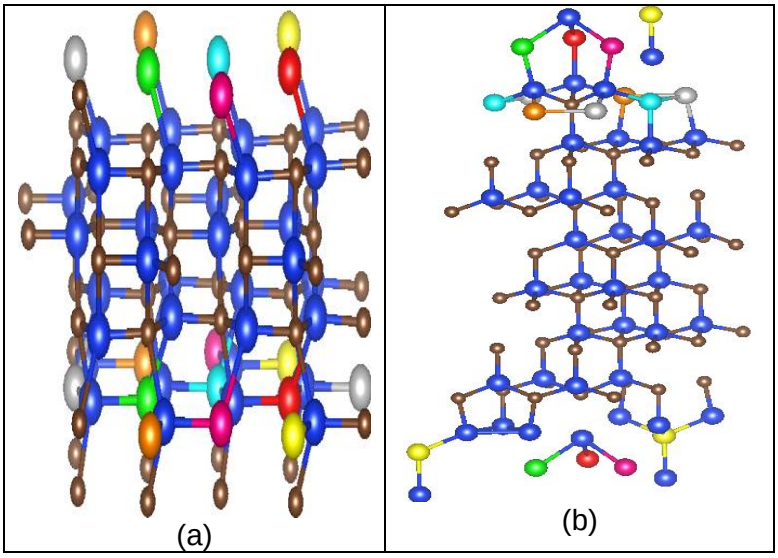

Figure 4-16 $7Si_C$:SiC structure (a) is FeSi structure, and (b) is wurtzite structure

Table 4-25 demonstrates the relaxed volume of 6H $7Si_C$:SiC structure supercell where it can be clearly seen that the relaxed volume when the extra silicon atoms near each other and at same layers, and when they are not at same layers but near each other have the lowest relaxed volume. On the other side, table 4-26 shows the relaxed volume of diamond $7Si_C$:SiC where it can be noticeable both configurations have similar relaxed volume with very slight different about 0.23 $A^{\circ 3}$.

Table 4-25 The relaxed volume of 6H $7Si_C$:SiC structure supercell 2x2x2 using DFT

6H structure of $7Si_C$:SiC	Volume ($A^{\circ 3}$)	Volume per pair ($A^{\circ 3}$)
(2 extra silicon atoms near each other, 2 near each other, and the other 3 near each other)	1106.800	23.058
(7 extra silicon atoms near each but not at same layers)	1095.44	22.82
(7 extra silicon atoms spread randomly)	1121.190	23.358
(7 extra silicon atoms near each other and at same layers sequentially)	1101.410	22.946

Table 4-26 The relaxed volume of diamond $7Si_C$:SiC structure supercell 2x2x2

Diamond structure of $7Si_C$:SiC	Volume (A°)	Volume per pair (A°)
(7 extra silicon atoms near each other but not at same level)	781.688	24.427
(7 extra silicon atoms near each other and at same layers sequentially)	782.422	24.450

Table 4-27, and 4-28 show the volume after relaxation, the lattice parameters and the angels of diamond, FeSi, wurtzite, and 6H structure of $7Si_C$:SiC supercell when the extra silicon atoms near each other where it is visible that still 6H structure kept the smallest relaxed volume and the FeSi structure has the highest relaxed volume, and the wurtzite structure kept the ideal angels and the lattice parameter $a = b$.

Table 4-27 The volume after relaxation of diamond, FeSi, wurtzite, and 6H structure of $7Si_C$:SiC supercell 2x2x2 when the extra silicon atoms near each other using DFT

structure of $7Si_C$:SiC	Volume ($A^{\circ 3}$)	Volume per pair ($A^{\circ 3}$)
diamond	781.690	24.427
FeSi	827.720	25.866
wurtzite	763.540	23.860
6H	1095.440	22.821

Table 4-28 The lattice parameters and the angels of diamond, FeSi, wurtzite, and 6H structure of $7Si_C$:SiC supercell 2x2x2 when the extra silicon atoms near each other

Structure of $7Si_C$:SiC	Lattice parameters			The angels		
	a (A°)	b (A°)	c (A°)	α (°)	β (°)	γ (°)
Diamond	9.203	9.220	9.220	90.263	90.037	89.962
FeSi	11.363	6.506	11.195	90	90.072	90
Wurtzite	6.238	6.238	22.653	90	90	120
6H	6.185	6.175	33.277	89.409	89.938	119.939

We faced the same problem in 6H structure when we replaced eight carbon atoms, which are near each other but not at same layers, by eight atoms of silicon. We examined different configurations of 6H structures and diamond structure shown in figure 4-17 and figure 4-18 respectively. When the eight atoms of extra silicon were near each other and at the same layers, we got on accurate result for 6H structure, but the result in diamond structure shows unstable structure. We did the same with wurtzite structure and FeSi structure with replacing eight carbon atoms by silicon shown in figure 4-19, but it gave unstable structures.

We got on the relaxed volume for the different configurations of 6H structures, and diamond structures shown in table 4-29 and table 4-30 respectively. 6H structure gave the same relaxed volume when the eight extra silicon atoms are near each other in both when they are at the same layers and

when they are near each other but not at same layers, which is the same situation in diamond structure.

Comparing the relaxed volume, the lattice parameters, and the angels of 6H structure and diamond structure with FeSi structure and the wurtzite structure shown in table 4-31 and 4-32, it can be clearly seen that all structures kept the ideal angels except in FeSi structure where it shows also huge different in the lattice parameters.

The results indicate that 6H structure is the most favorable structure comparing to the wurtzite structure, which lose its stability with replacing five atoms of carbon by silicon, diamond structure and FeSi structures which lose their stability when we replaced 4 atoms of carbon by silicon.

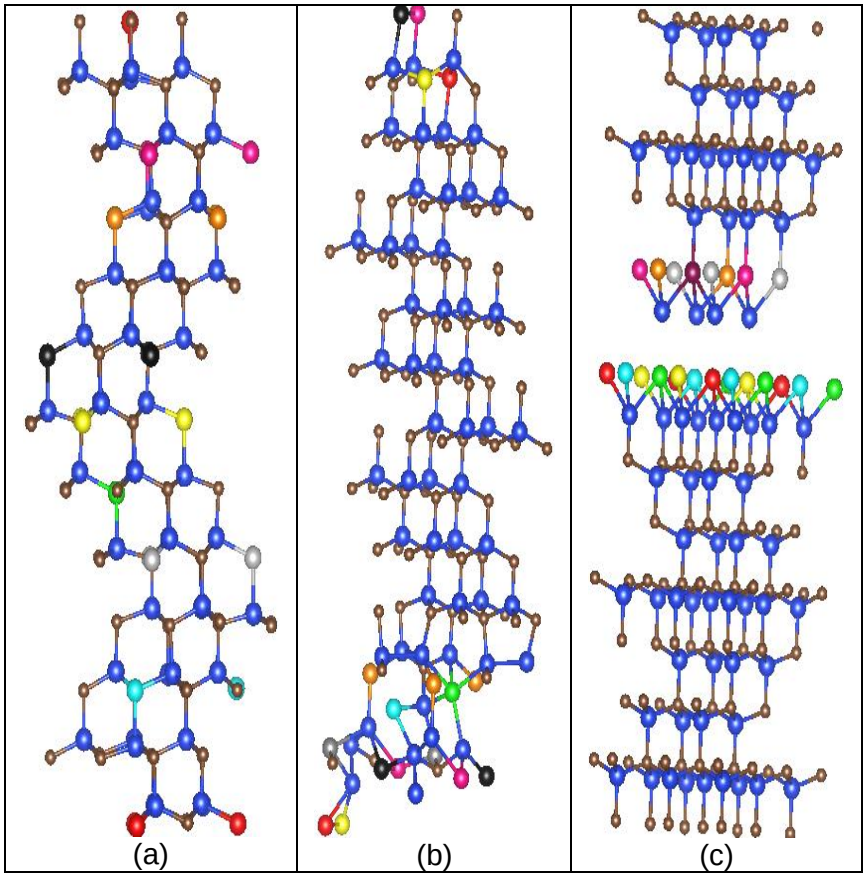

Figure 4-17 6H structure of $8Si_C$:SiC. (a) is (8 extra silicon atoms spread randomly), (b) (8 extra silicon atoms near each other but not at same layers), and (c) (8 extra silicon atoms near each other and at same layers)

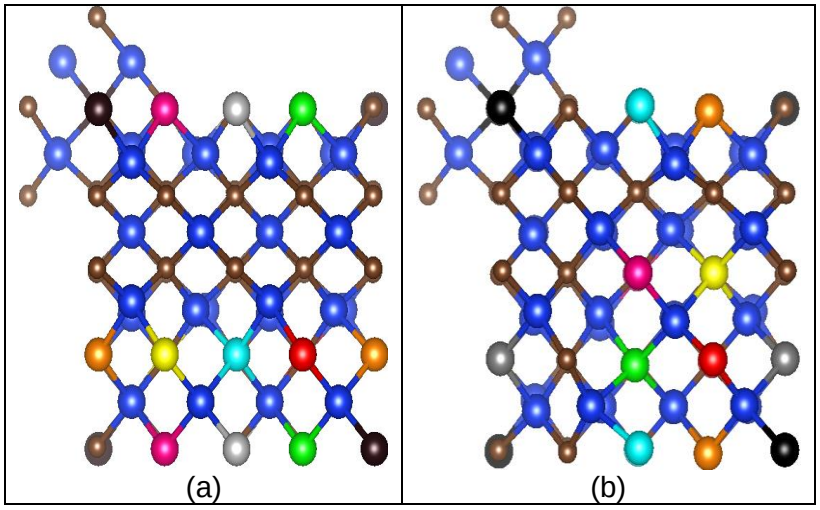

Figure 4-18 (a) diamond structure of $8Si_C$:SiC (8 extra silicon atoms near each other at same layers), and (b) is Diamond structure of $8Si_C$:SiC (8 extra silicon atoms near each other but not same layers)

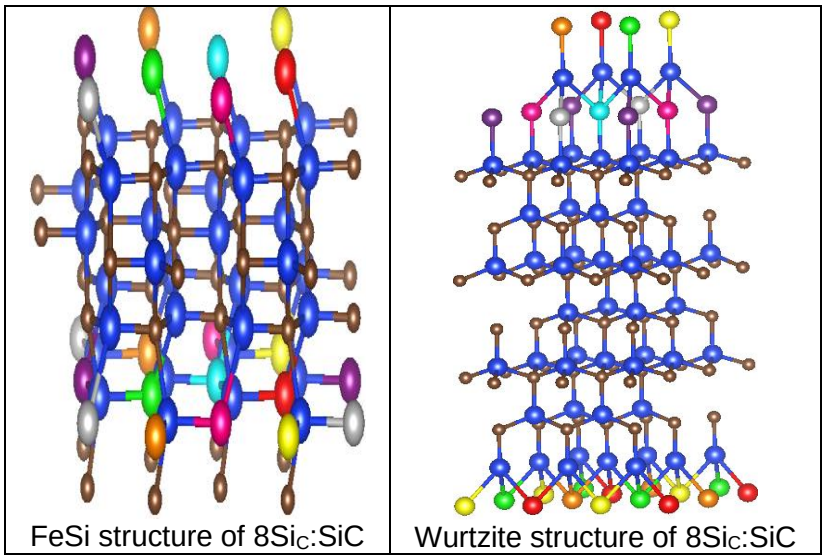

Figure 4-19 (a) FeSi structure of $8Si_C$:SiC, and (b) is wurtzite structure of $8Si_C$:SiC.

Table 4-29 The relaxed volume of 6H $8Si_C$:SiC structure supercell 2x2x2 using DFT

6H structure	Volume ($A^{\circ 3}$)	Volume per pair ($A^{\circ 3}$)
$8Si_C$:SiC (8 extra silicon atoms near each other but not at same levels)	1106.730	23.056
$8Si_C$:SiC (8 extra silicon atoms spread randomly)	1139.100	23.731
$8Si_C$:SiC (8 extra silicon atoms near each other and at same layers sequentially)	1113.150	23.190

Table 4-30 The relaxed volume of diamond $8Si_C$:SiC structure supercell 2x2x2

Diamond structure	Volume (A°)	Volume per pair(A°)
$8Si_C$:SiC (8 extra silicon atoms near each other but not at same level)	801.18	25.036
$8Si_C$:SiC (8 extra silicon atoms near each other and at same layers sequentially)	800.11	25.003

Table 4-31 The volume after relaxation of diamond, FeSi, wurtzite, and 6H structures of $8Si_C$:SiC supercell 2x2x2 when the extra silicon atoms near each other using DFT

structure of $8Si_C$:SiC	Volume ($A^{\circ 3}$)	Volume per pair ($A^{\circ 3}$)
diamond	800.11	25.003
FeSi	845.66	26.426
wurtzite	775.35	24.229
6H	1113.150	23.190

Table 4-32 The lattice parameters and the angels of diamond, FeSi, wurtzite, and 6H structures of $8Si_C$:SiC supercell 2x2x2 when the extra silicon atoms near each other

Structure of $8Si_C$:SiC	Lattice parameters			The angels		
	a (A°)	b (A°)	c (A°)	α (°)	β (°)	γ (°)
Diamond	9.280	9.291	9.291	90	90	90
FeSi	11.467	6.550	11.257	89.999	90	90
Wurtzite	6.135	6.135	23.780	90	90	120
6H	6.165	6.165	33.812	90	90	120

4.2 Calculating the Lowest Energies of Structures and the Formation Enthalpies of Silicon Rich Silicon Carbide Structures

When all structures which are discussed above are fully relaxed, we determined the lowest energies, and calculated the formation enthalpies. We started with calculating the energies and the formation enthalpies when just one carbon atom replaced by one atom of silicon in diamond, FeSi, wurtzite and 6H structures. Table 4-33 demonstrates the total energies, and the formation enthalpies of diamond, FeSi, wurtzite, and 6H structure of Si_C:SiC supercell. In diamond, FeSi, and wurtzite structures, we have total number of 33 silicon atoms, and 31 atoms of carbon while in 6H structure we have 49 atoms of silicon and 47 atoms of carbon. It can be clearly seen that 6H structure has the lowest formation enthalpy with different about 0.012 eV comparing to diamond structure and FeSi structure which have exactly same formation enthalpies. On the other side, we can see that wurtzite structure has the highest formation enthalpy with different around 0.021 eV comparing to the lowest energy which belongs to 6H structure. It indicates that 6H structure is the most favorable structure of Si_C:SiC comparing to the other three structures.

Table 4-33 The total energies, and the formation enthalpies of diamond, FeSi, wurtzite, and 6H structure of Si_C:SiC supercell 2x2x2 using DFT

Structure of Si_C:SiC 2x2x2	Total energy (eV)	Formation enthalpy (eV)	Formation enthalpy per atom (eV)
Diamond (33Si31C)	-474.514	-6.974	-0.108
FeSi (33Si31C)	-474.514	-6.974	-0.108
Wurtzite (33Si31C)	-473.868	-6.328	-0.098
6H (49Si47C)	-714.793	-11.541	-0.120

Also, we calculated the energies and the formation enthalpies when we replaced two atoms of carbon by silicon atoms in the two structures. We examined two situations of arranging the extra two silicon in 6H structure, and diamond structure when they are near each other and far from each other. Table 4-34, and 4-35 show the total energies and the formation enthalpies of 6H, and diamond structures of $2Si_C$:SiC supercell respectively. It can be clearly seen that in both 6H and diamond structures, the formation enthalpies decreased when the extra two silicon are near each other about 0.003 eV in 6H structure, and around 0.001 eV in diamond structure. It indicates that when the extra silicon atoms near each other,

the atoms in that structure will interact with each other more in proper way than when they far from each other.

Table 4-34 The total energies and the formation enthalpies of 6H structure of $2Si_C$:SiC supercell 2x2x2 using DFT

6H of $2Si_C$:SiC (50Si46C)	Total Energy (eV)	Formation enthalpy (eV)
2 extra silicon atoms near each other	-707.217	-7.849 (-0.081 per atom)
2 extra silicon atoms far from each other	-706.925	-7.557 (-0.078 per atom)

Table 4-35 The total energies and the formation enthalpies of diamond structure of $2Si_C$:SiC supercell 2x2x2 using DFT

Diamond structure of $2Si_C$:SiC (34Si30C)	Total Energy (eV)	Formation energy (eV)
2 extra silicon atoms near each other	-467.521	-3.865 (-0.060 per atom)
2 extra silicon atoms far from each other	-467.489	-3.833 (-0.059 per atom)

Comparing the formation enthalpies of diamond, FeSi, wurtzite, and 6H structure of $2Si_C$:SiC supercell shown in table 4-26, we can see that still 6H

structure has the lowest formation enthalpy with different about 0.021 eV comparing to diamond structure which has the second lowest formation energy. It is noticeable that diamond structure has formation enthalpy which is almost same comparing to FeSi structure with different around 0.001 eV, and wurtzite structure has the highest formation enthalpy with different about 0.029 eV comparing to 6H structure. It means that wurtzite structure is less stable than 6H, diamond and FeSi structures.

Table 4-36 The total energies, and the formation enthalpies of diamond, FeSi, wurtzite, and 6H structure of $2Si_C$:SiC supercell 2x2x2 using DFT

Structure of $2Si_C$:SiC 2x2x2	Total energy (eV)	Formation enthalpy (eV)	Formation enthalpy per atom (eV)
Diamond (34Si30C)	-467.521	-3.865	-0.060
FeSi (34Si30C)	-467.489	-3.833	-0.059
Wurtzite (34Si30C)	-467.012	-3.356	-0.052
6H (50Si46C)	-707.217	-7.849	-0.081

In addition, we thought about different arrangement of the extra three silicon atoms in our structure when they are near each other, far from each other and 2 of them are near each other, and the third one is far from them. We determined the energies and calculated the formation enthalpies off all three situations in 6H structure, and diamond structure shown in table 4-37 and 4-38 respectively. The results show that when the extra silicon atoms near each other,

it tends to give more accurate results than when they are far from each other, or some of them are near each other and the rest are far. It is visible that the formation enthalpy of 6H structure when the extra silicon atoms are near each other lower than when they are far around 0.012 eV, and about 0.01 eV when two of them near and the third one far, and in diamond structure, the formation enthalpy is lower about 0.01 eV comparing when two of them are near and the third one is far.

Table 4-37 The total energies and the formation enthalpies of 6H structure of $3Si_C$:SiC supercell 2x2x2 using DFT

6H of $3Si_C$:SiC (51Si45C)	Total Energy (eV)	Formation energy (eV)
3 extra silicon atoms near each other	-700.548	-5.064 (-0.052 per atom)
3 extra silicon atoms far from each other	-699.344	-3.86 (-0.040 per atom)
2 extra silicon atoms near each other and one extra far from them	-699.517	-4.033 (-0.042 per atom)

Table 4-38 The total energies and the formation enthalpies of diamond structure of $3Si_C$:SiC supercell 2x2x2 using DFT

Diamond of $3Si_C$:SiC (35Si29C)	Total Energy (eV)	The formation energy (eV)
3 extra silicon atoms near each other	-460.683	-0.911 (-0.014 per atom)
3 extra silicon atoms far from each other	-460.094	-0.322 (-0.005 per atom)
2 extra silicon atoms near each other and one extra far from them	- 460.052	-0.280 (-0.004 per atom)

Thus, we decided to calculate for wurtzite structure, and FeSi structure when the extra silicon atoms are near each other. Table 4-39 shows the comparison of the four structures we have. It can be clearly seen that the formation enthalpies for all structures increased specially in FeSi structure where the formation increased rapidly. Although the formation enethalpy of 6H structure increased, it is still the most favorable comparing to the other structures. Diamond structure and wurtzite structure have very close formation enthalpies with different about 0.002 eV while the difference between wurtzite structure and 6H structure is about 0.036 eV.

Table 4-39 The total energies, and the formation enthalpies of diamond, FeSi, wurtzite, and 6H structure of $3Si_C$:SiC supercell 2x2x2 using DFT

Structure of $3Si_C$:SiC 2x2x2	Total energy (eV)	Formation enthalpy (eV)	Formation enthalpy per atom (eV)
Diamond (35Si29C)	-460.683	-0.911	-0.014
FeSi (35Si29C)	-460.093	-0.321	-0.005
Wurtzite (35Si29C)	-460.855	-1.083	-0.016
6H (51Si45C)	-700.548	-5.064	-0.052

We considered different configurations of distributing the extra silicon atoms in $4Si_C$:SiC to see the validity of our expectation about choosing the extra silicon atoms to be near each other. We examined two different configurations of 6H structure where we choose the extra four silicon to be spread into two sets, each set has two silicon atoms near each other shown in table 4-40, and it concluded that when the extra silicon atoms near each other, we will obtain more accurate result. However, in diamond structure, we considered numerous configurations shown in table 4-41 because the formation enthalpies become above zero which means that the structures are unstable any more. It can be clear that when the extra silicon atoms are far from each other, we got on the highest

formation enthalpy, while we got on lowest formation enthalpy when the four extra silicon atoms at same plane and near each other, and when the four extra silicon atoms are at the same plane in the middle.

We considered the situations where the first one when two extra silicon atoms are near each other, the third one, and the forth one far from each other, and the second one is when two extra silicon are near each other and the other two are near each other, we obtained on the same results which is lower than when they are far from each other, but still not stable as 6H structure. Also, we considered the situations where the lattice parameters a,b, and c are small, and relaxed the system, then calculate the energy, and the other one when we started with large lattice parameters, and we ended with exactly same results for both configuration.

Then, we calculated also the formation enthalpies for FeSi structure and wurtzite structure, and compare their result with 6H structure and diamond structure shown in table 4-42. The results show how Fei structure lose its stability with high formation enthalpy with different about 0.198 eV comparing to diamond structure which also lose its stability which shows that it is larger than diamond structure almost 12 times. Comparing the other two stable structures, 6H and wurtzite structures, we can see that 6H structure has lower formation enthalpy with different about 0.016 comparing to wurtzite structure which leads us to know that 6H structure is the most stable structure among all our structures.

Table 4-40 The total energies and the formation enthalpies of 6H structure of $4Si_C$:SiC supercell 2x2x2 using DFT

6H of $4Si_C$:SiC (52Si44C)	Total Energy (eV)	Formation enthalpy (eV)
2 extra silicon atoms near each other and the other 2 extra silicon near each other	-692.890	-1.29 (-0.013 per atom)
4 extra silicon atoms near each other	-693.784	-2.184 (-0.022 per atom)

Table 4-41 The total energies and the formation enthalpies of diamond structure of $4Si_C$:SiC supercell 2x2x2 using DFT

Diamond structure of $4Si_C$:SiC 2x2x2 (36Si28C)	Total Energy (eV)	The formation enthalpy (eV)
4 extra silicon far from each other	-452.930	2.958 (0.046 per atom)
2 extra silicon near, the third far, and the forth far	-453.847	2.041 (0.031 per atom)
- 4 extra silicon at same layer - 4 extra silicon same layer in middle	-454.757	1.131 (0.017 per atom)
4 extra silicon near each other but not at the same layer (the lattice small)	-453.525	2.363 (0.036 per atom)
2 extra silicon near each other and the 2 near each other	-453.896	1.992 (0.031 per atom)
4 extra silicon near each other but not at the same layer with (a=b=c=11)	-453.525	2.363 (0.036 per atom)

Table 4-42 The total energies, and the formation enthalpies of diamond, FeSi, wurtzite, and 6H structure of $4Si_C$:SiC supercell 2x2x2 using DFT

Structure of $4Si_C$:SiC 2x2x2	Total energy (eV)	Formation enthalpy (eV)	Formation enthalpy per atom (eV)
Diamond (36Si28C)	-454.757	+1.131	+0.017
FeSi (36Si28C)	-442.110	+13.778	+0.215
Wurtzite (36Si28C)	-456.272	-0.384	-0.006
6H (52Si44C)	-693.784	-2.184	-0.022

We determined the energies and the formation enthalpies of $5Si_C$:SiC of 6H, diamond, FeSi, and wurtzite structures shown in table 4-43. The results show how the wurtzite structure lose its stability with replacing five atoms of carbon with five silicon atoms. It can be clearly seen that the formation enthalpies of 6H decreased when we compare it with $4Si_C$:SiC of 6H, which is also the situation of FeSi structure. However, in FeSi, it is still unstable structure, but in 6H structure, $5Si_C$:SiC is more stable than $4Si_C$:SiC.

Table 4-43 The total energies, and the formation enthalpies of diamond, FeSi, wurtzite, and 6H structure of $5Si_C$:SiC supercell 2x2x2 using DFT

Structure of $5Si_C$:SiC 2x2x2	Total energy (eV)	Formation enthalpy (eV)	Formation enthalpy per atom (eV)
Diamond (37Si27C)	-448.583	+3.421	+0.053
FeSi (37Si27C)	-444.449	+7.555	+0.118
Wurtzite (37Si27C)	-450.536	+1.468	+0.022
6H (53Si43C)	-692.516	-4.8	-0.05

repeating the procedure with taking off 6 atoms of carbon and replaced them by silicon atoms in all structures shown in table 4-44, we can see that the formation enthalpies has increased in all structures, but it is still below zero in 6H structure which make it the most stable structure comparing with the others.

Table 4-44 The total energies, and the formation enthalpies of diamond, FeSi, wurtzite, and 6H structure of $6Si_C$:SiC supercell 2x2x2 using DFT

Structure of $6Si_C$:SiC 2x2x2	Total energy (eV)	Formation enthalpy (eV)	Formation enthalpy per atom (eV)
Diamond (38Si26C)	-441.809	+6.311	+0.098
FeSi (38Si26C)	-439.760	+8.36	+0.130
Wurtzite (38Si26C)	-446.860	+1.26	+0.019
6H (54Si42C)	-687.673	-3.841	-0.040

Replacing seven atoms of carbon by silicon atoms in 6H structure when the seven extra silicon atoms are near each other but not at same layers made the structure unstable. We tried different configurations shown in table 4-45 to determine stable structure of 6H. We have found that we should choose the carbon atoms which will be replaced by silicon atoms at the same layers to get on accurate structure. It is visible that in 6H structure, the second lowest formation enthalpy belongs to the configuration where the seven extra silicon atoms are near each other, and the following is when three extra silicon atoms are near each other and the other four are near each other. However, when we spread the extra seven atoms of silicon randomly, it gives positive formation enthalpy.

Table 4-45 The total energies and the formation enthalpies of 6H structure of $7Si_C$:SiC supercell 2x2x2 using DFT

6H structure $7Si_C$:SiC (2x2x2)	Total Energy (eV)	Formation enthalpy (eV)
(2near-2near-3near) (55Si41C)	-673.394	6.554 (0.068 per atom)
(3near-4near) (55Si41C)	-676.655	3.293 (0.034 per atom)
(dif con) (55Si41C)	-671.100	8.848 (0.092 per atom)
(near and at the same layers) (55Si41C)	-683.691	-3.742 (-0.0389 per atom)
(near but not on same layers) (55Si41C)	-679.620	+ 0.328 (+0.003 per atom)

We also examined the other structures with replacing seven atoms of carbon by seven atoms of silicon shown in table 4-46, but all of them tent to give unstable structures. It can be clearly seen that FeSi structure has the highest formation enthalpy with different about 0.097 eV comparing with 6H structure, and diamond structure has the second highest formation enthalpy with different about 0.0811 comparing to 6H structure. Although wurtzite structure is smaller than diamond and FeSi structures, it is larger than 6H structure around 0.0361 eV.

Table 4-46 The total energies, and the formation enthalpies of diamond, FeSi, wurtzite, and 6H structure of $7Si_C$:SiC supercell 2x2x2 using DFT

Structure of $7Si_C$:SiC 2x2x2	Total energy (eV)	Formation energy (eV)	Formation enthalpy per atom (eV)
Diamond (39Si25C)	-436.519	+7.717	+0.120
FeSi (39Si25C)	-435.473	+8.766	+0.136
Wurtzite (39Si25C)	-439.401	+4.835	+0.075
6H (55Si41C)	-683.690	-3.742	-0.0389

We faced the same problem in 6H structure when we replaced the carbon atoms by silicon atoms, which are near each other but not at the same layers, with getting higher formation energy, so we tried for different configurations shown in table 4-47. It is clear that when the extra silicon atoms near each other and at same layers, it gives stable structure of 6H.

Table 4-47 The total energies and the formation enthalpies of 6H structure of $8Si_C$:SiC supercell 2x2x2 using DFT

6H structure $8Si_C$:SiC (2x2x2)	Total Energy (eV)	Formation enthalpy (eV)
(near but not on same layers) (56Si40C)	-674.950	+ 1.114 (+0.011 per atom)
(dif con) (56Si40C)	-664.461	11.454 (+0.119 per atom)
(near and at the same layers) (56Si40C)	-676.604	-0.54 (-0.005 per atom)

We determined the energies and calculated the formation enthalpies of diamond, FeSi and wurtzite structures shown in table 4-48 to see how they change with high number of silicon. It is noticeable that all structures lose their stability except 6H structure which has the lowest formation enthalpy. It shows slight different in FeSi structure comparing to $7Si_C$:SiC of FeSi structure.

Table 4-48 The total energies, and the formation enthalpies of diamond, FeSi, wurtzite, and 6H structure of $8Si_C$:SiC supercell 2x2x2 using DFT

Structure of $8Si_C$:SiC 2x2x2	Total energy (eV)	Formation enthalpy (eV)	Formation enthalpy per atom (eV)
Diamond (40Si26C)	-430.571	+9.781	+0.152
FeSi (40Si26C)	-431.569	+8.783	+0.137
Wurtzite (40Si26C)	-435.949	+4.403	+0.068
6H (56Si40C)	-676.604	-0.537	-0.005

Figure 4-20 shows how the formation energies change with different numbers of extra silicon atoms of 6H, diamond, wurtzite, and FeSi structures. It can be clearly seen that all four structures start with the same point, then 6H structure and wurtzite structure take different paths while diamond structure and FeSi structure have strong hybridization up to 3.

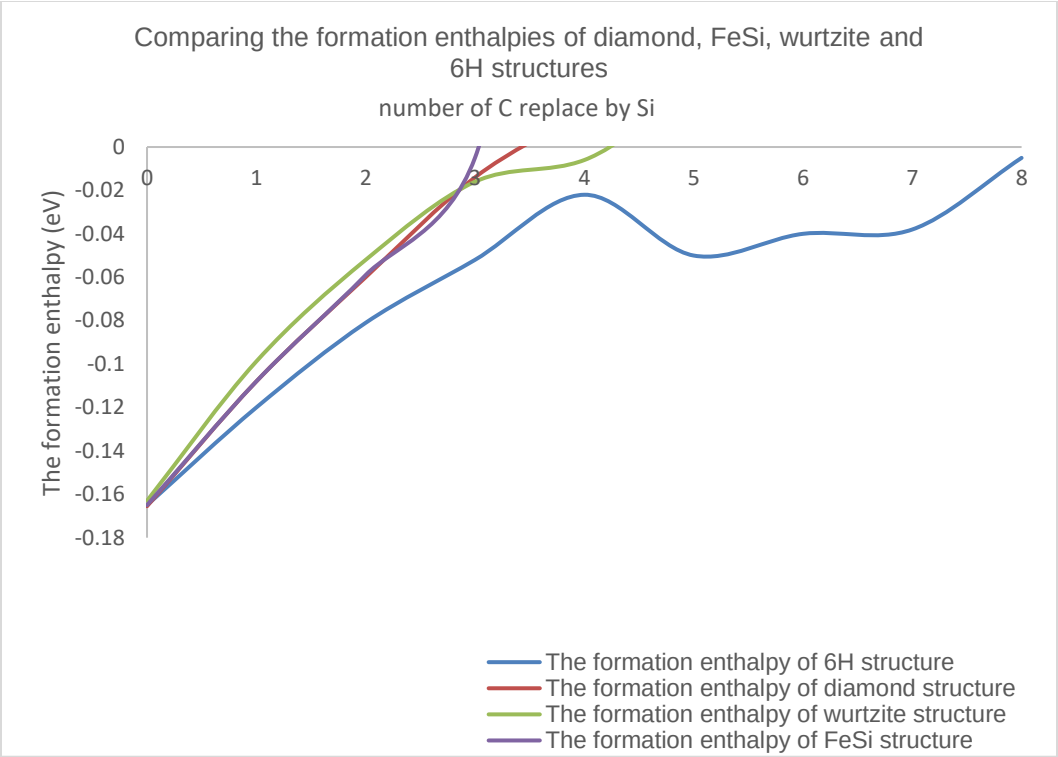

Figure 4-20 Comparing the formation enthalpies of 6H, diamond, wurtzite, and FeSi structures of silicon rich silicon carbide

Chapter 5

Electronic Properties of Silicon Rich Silicon Carbide and the Electrostatic Energies of Pristine and Silicon Rich Silicon carbide

5.1 DOS plots of silicon rich silicon carbide

In the first part of this chapter, we have mainly focused on how the extra silicon atoms contribute to the density of state (DOS), and comparing the partial DOS of extra silicon atoms with the host silicon atom. Figure 5-1 shows the partial DOS plot of diamond structure of Si_C:SiC for the host Si, where it can be clearly seen that there is a gap between the fermi level and the bottom of the conduction band about 0.68 eV, where this gap showed up in the extra silicon plot shown in figure 5-2. Figure 5-1 demonstrates how s orbital and p orbital has strongly coupled with each other in the conduction band, and p orbital takes a while to go up which is the opposite in the extra silicon plot which shows that p orbital goes very quickly in the valance band. Figure 5-2 shows how s orbital and p orbital contribution from extra silicon atom in conduction band was not as large as the host silicon atoms. Overall, the extra Si-p band act like a localized band at the top of the valence band.

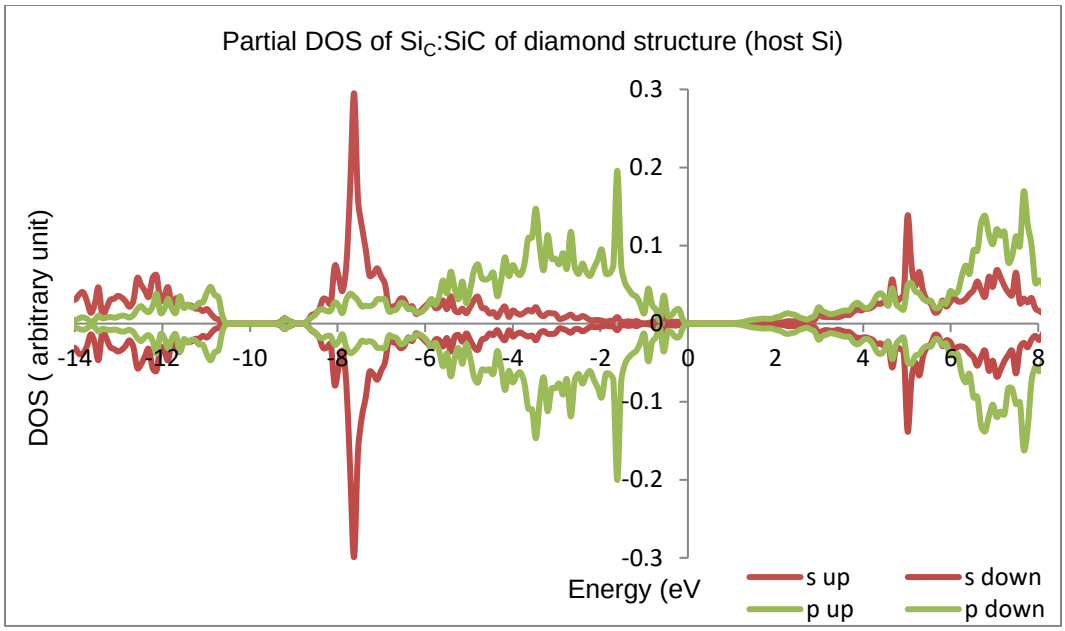

Figure 5-1The partial DOS plot of diamond structure of Si$_C$:SiC (host Si)

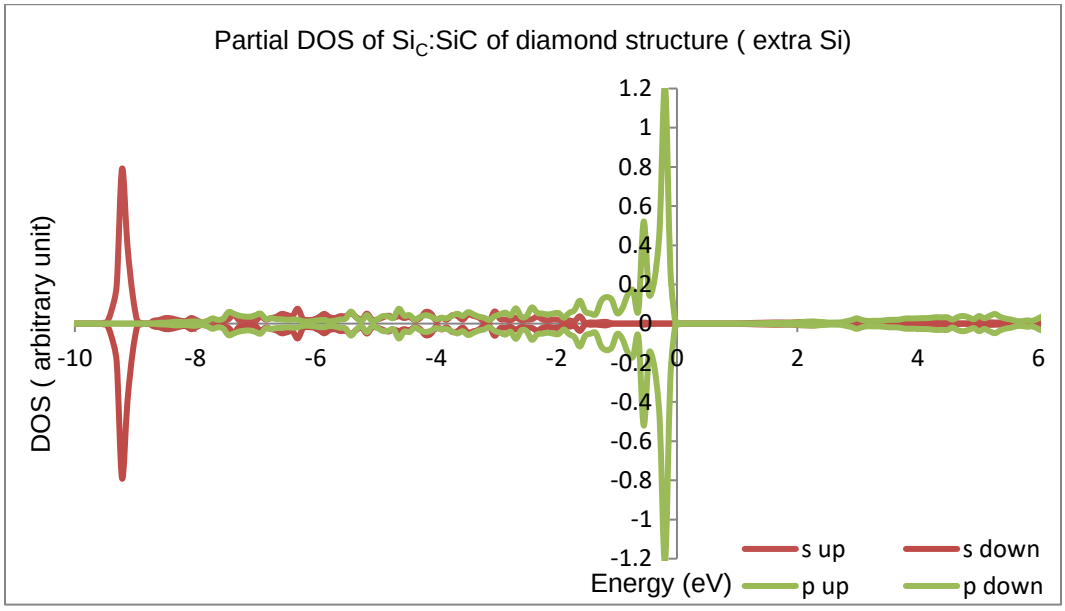

Figure 5-2 The partial DOS plot of diamond structure of Si$_C$:SiC (extra Si)

Figure 5-3 shows the partial DOS of host silicon of wurtzite structure and it shows that there is gap from fermi level up to the bottom of conduction band about 0.59 eV which is smaller than the gap in the partial DOS of host silicon in diamond structure around 0.09 eV. Figure 5-4 shows the extra silicon plot in wurtzite structure. It can be clearly seen that the host silicon has contribution from both s orbital and p orbital with high hybridization in the valance band as in diamond structure, and the extra silicon behave similarly in the plot of diamond and wurtzite structure except that p orbital goes very quickly in diamond structure, but it takes a while to increase and reach to the highest peak in wurtzite structure. On the other side, we can see that in the host silicon plot of wurtzite structure, in the valance band, p orbital goes very quickly

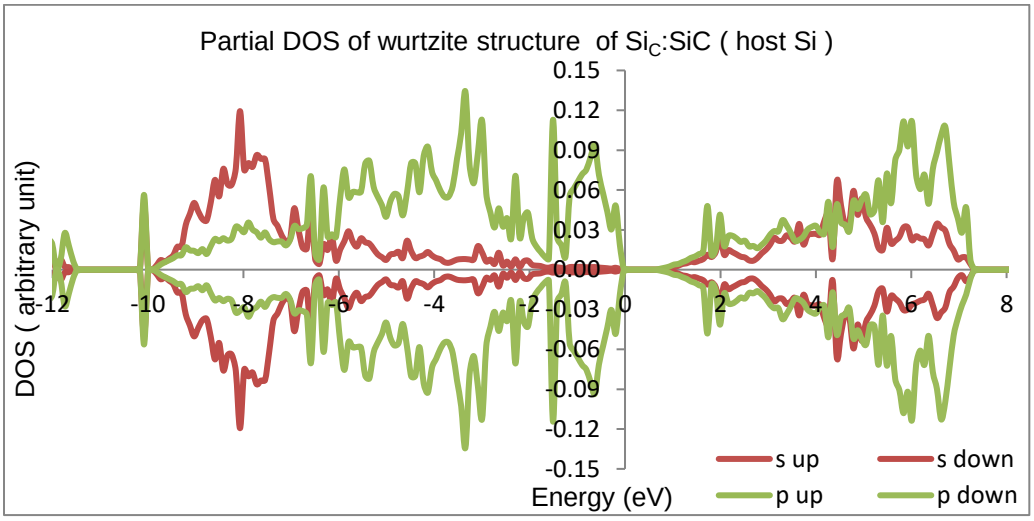

Figure 5-3 The partial DOS plot of wurtzite structure of Si$_C$:SiC (host Si)

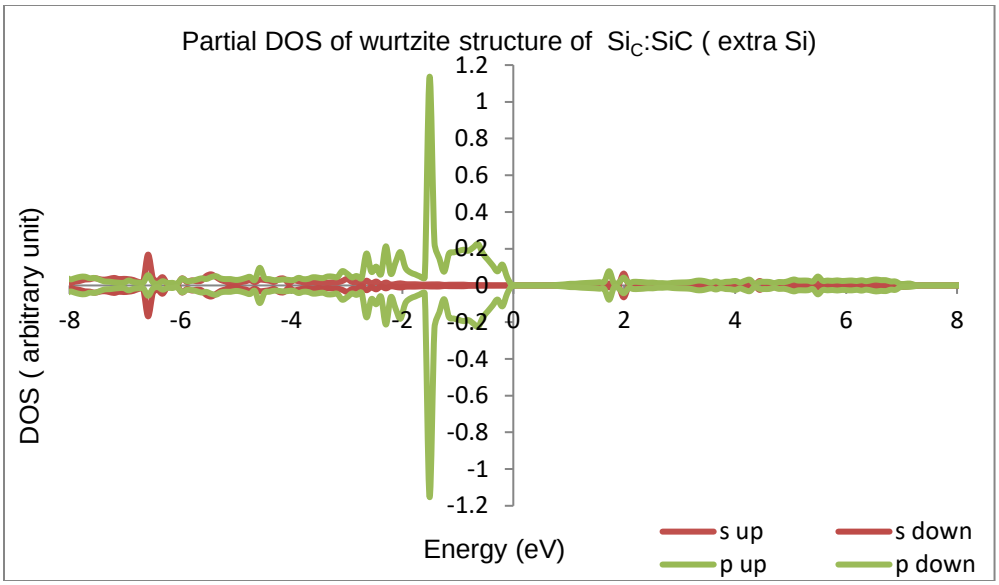

Figure 5-4 The partial DOS plot of wurtzite structure of Si_C:SiC (extra Si)

Figure 5-5 and 5-6 show the partial DOS plot of host silicon and extra silicon of FeSi structure. It can be clearly seen that there is a gap around 0.77 eV in the host silicon plot which is larger than the band gap which we had in wurtzite structure with difference around 0.18 eV. The contribution in the host silicon plot comes from s orbital and p orbital as in diamond structure and wurtzite structure. Also, it is visible to see that in the host silicon plot of FeSi structure, p orbital takes a while to increase, but it increases quicker than s orbital in the valance band which is the same situation in the extra silicon plot of diamond structure. On the other side, in the extra silicon plot of FeSi structure, p orbital has a very large contribution in the valance band and the most contribution is from p orbital in the valance band which is the same situation in diamond structure.

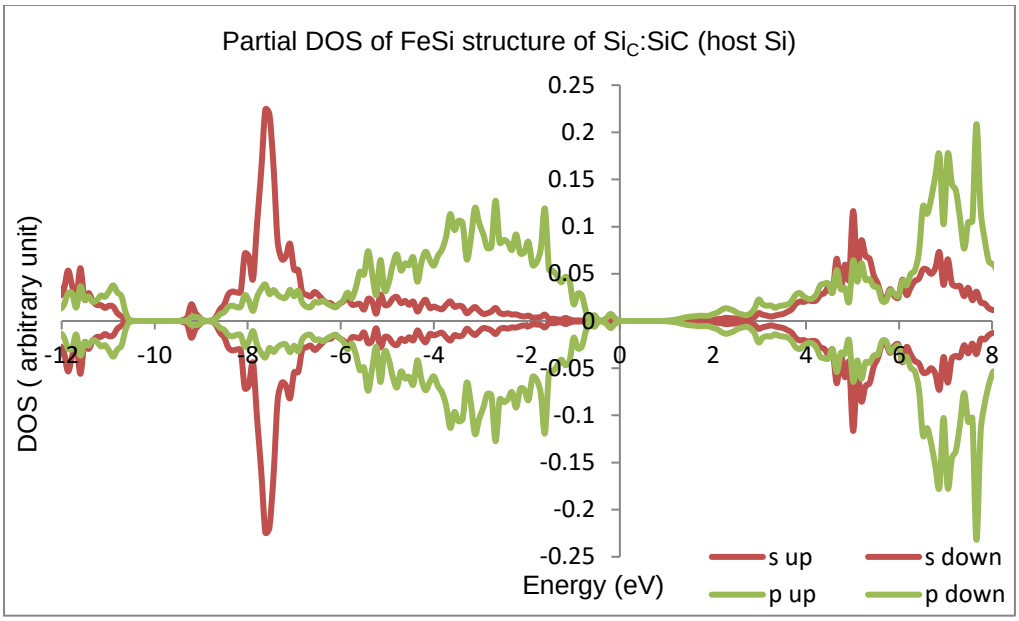

Figure 5-5 The partial DOS plot of FeSi structure of Si$_C$:SiC (host Si)

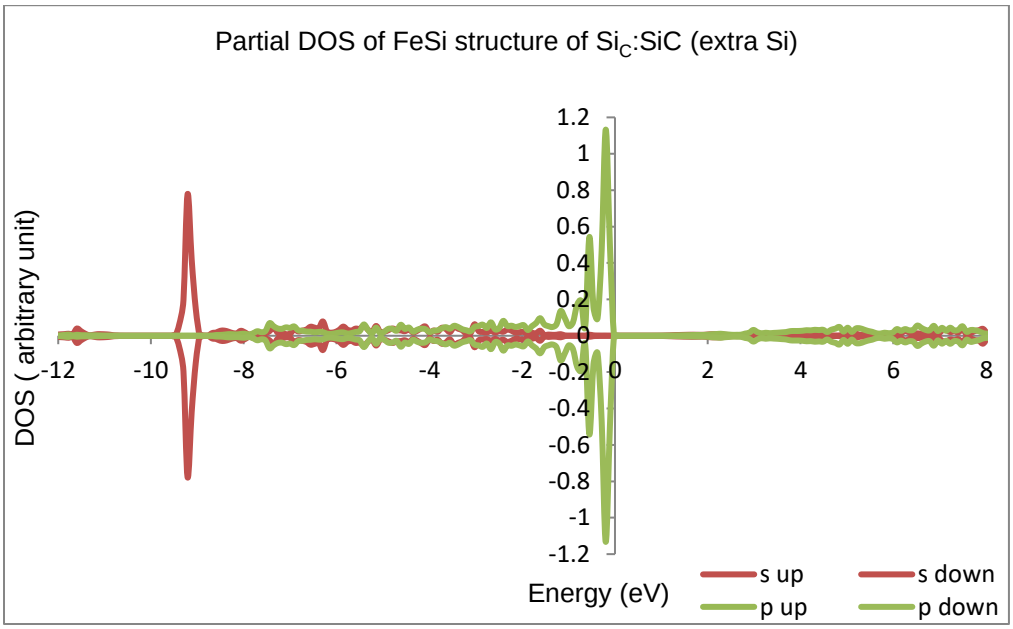

Figure 5-6 The partial DOS plot of FeSi structure of Si$_C$:SiC (extra Si)

Lastly, we can see in the partial DOS plot of the host silicon of 6H structure shown in figure 5-7 that there is a gap about 0.77 eV which is the same gap in FeSi structure. Also, it is noticeable that the contribution in the host silicon of 6H structure comes from s orbital and p orbital in the conduction band and the valance band, and p orbital in the valance band goes very quickly near the fermi level which is the same situation in the partial dos of extra silicon shown in figure 5-8 and the same as the extra silicon plot in diamond structure. It can be clearly seen that the orbitals behave differently in the extra silicon such that the contribution in the conduction band is from p orbital, but it is very small comparing with the host silicon while s orbital is almost zero in the conduction band. Also, it can be clearly seen that in the extra silicon plot the most contribution comes from p orbital, but the highest peak comes from s orbital around -10.136 eV.

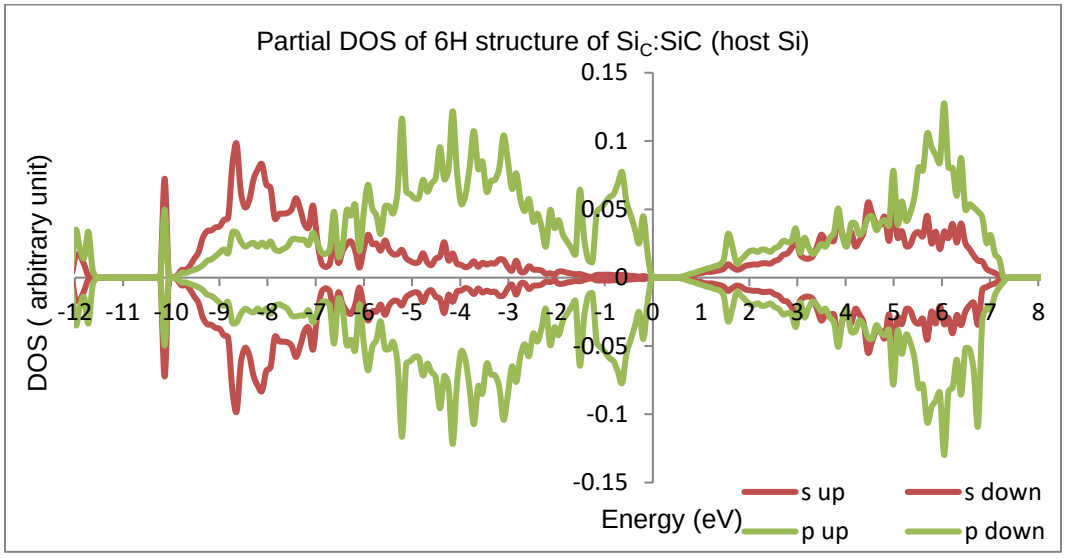

Figure 5-7 The partial DOS plot of 6H structure of Si$_C$:SiC (host Si)

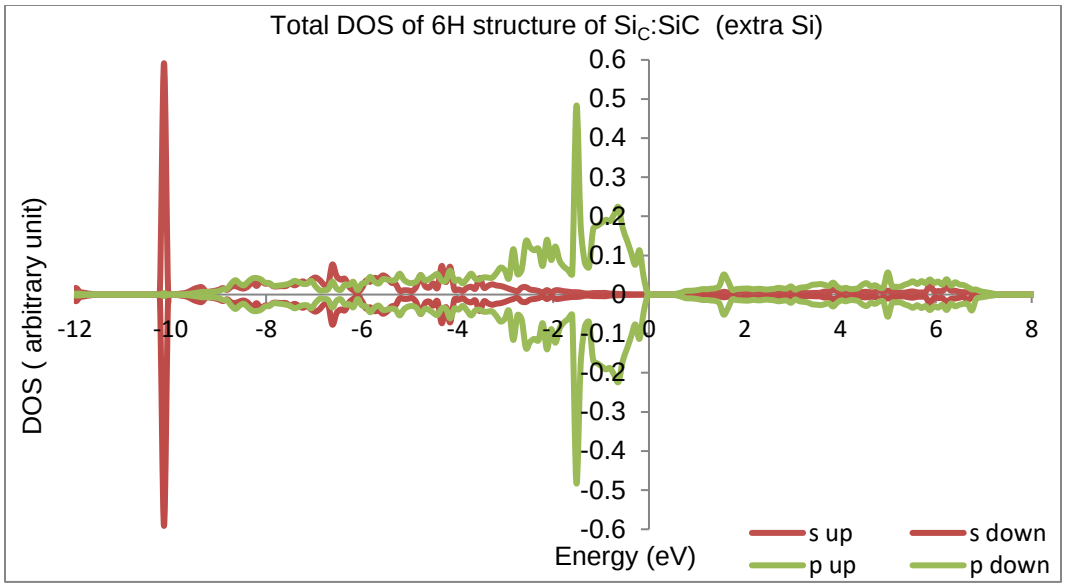

Figure 5-8 The partial DOS plot of 6H structure of Si_C:SiC (extra Si)

Then, we plot the partial DOS of extra silicon and the host silicon in silicon rich silicon carbide $2Si_C$:SiC of diamond, wurtzite, FeSi and 6H structure. Figure 5-9 shows the partial DOS plot of host silicon in diamond structure of $2Si_C$:SiC which shows that there is a gap from fermi level to the bottom of conduction band about 0.24 eV, and 5-10 and 5-11 demonstrate the partial DOS of the extra two silicon respectively. It can be clearly seen that s orbital and p orbital have strong hybridization in the conduction band of regular silicon plot while in the valance band they are uncoupled and p orbital take time to go up in host silicon. On the other side, in the extra silicon plots, p orbital goes very quickly in the valance band and the most contribution comes from p orbital and in the valance band s orbital has no contribution and it is almost zero.

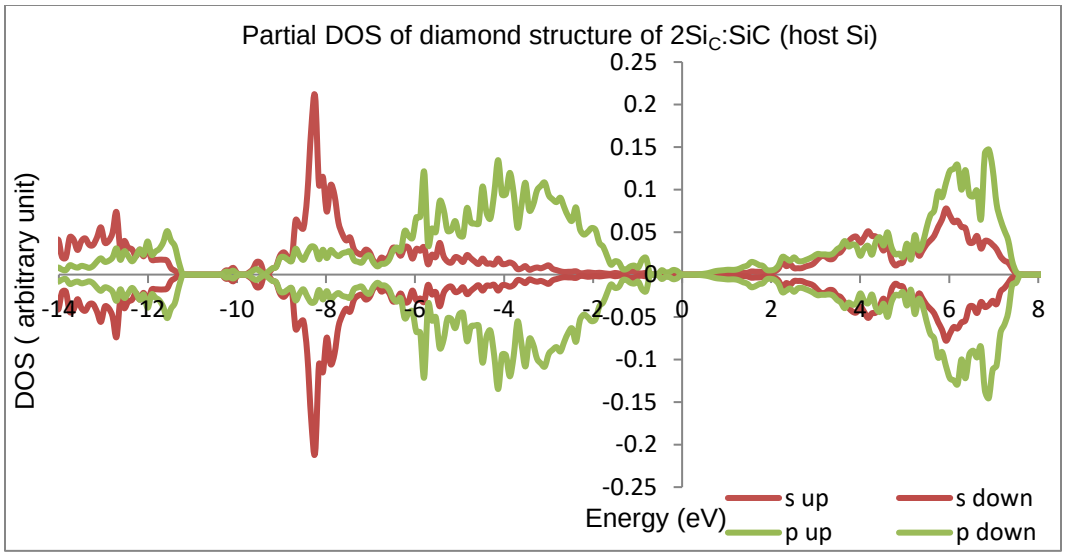

Figure 5-9 The partial DOS plot of diamond structure of 2Si$_C$:SiC (host Si)

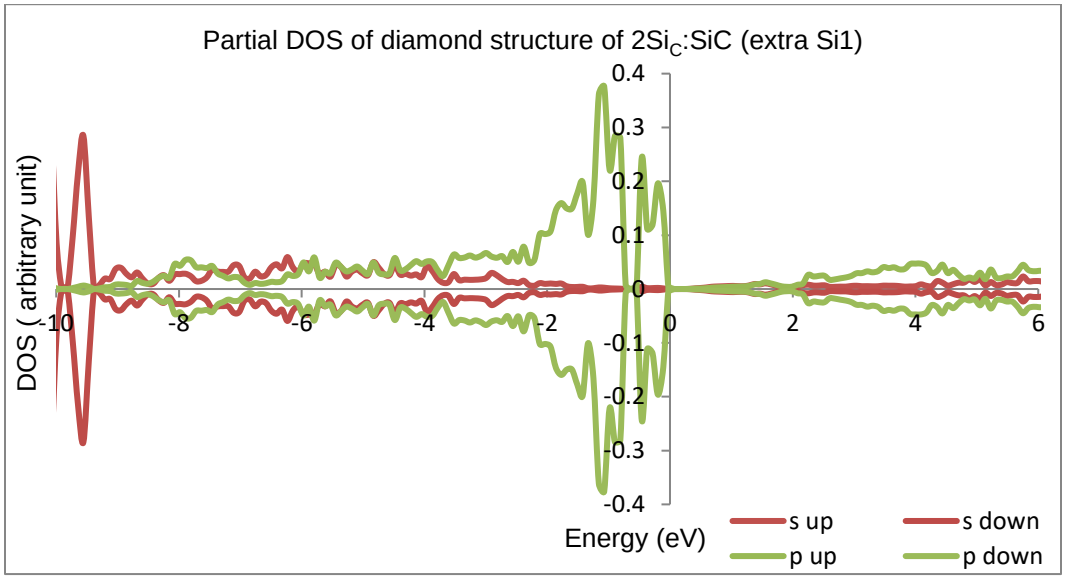

Figure 5-10 The partial DOS plot of diamond structure of 2Si$_C$:SiC (extra Si 1)

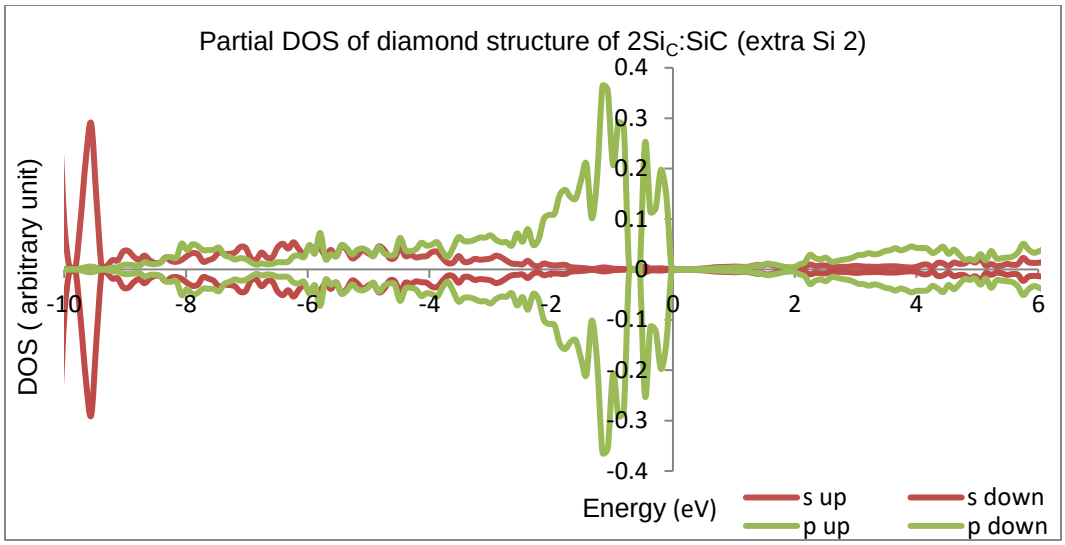

Figure 5-11 The partial DOS plot of diamond structure of $2Si_C$:SiC (extra Si 2)

Figure 5-12 shows the partial DOS plot of wurtzite structure of host silicon in $2Si_C$:SiC, figure 5-13, and 5-14 demonstrate the partial DOS plots of wurtzite structure of the extra two silicon respectively which are almost same. It is visible that there is no gap in wurtzite structure, and s orbital and p orbital have contribution in both valance band and conduction band in both host and extra silicon plots. It looks that both regular and extra silicon behave similar to each other.

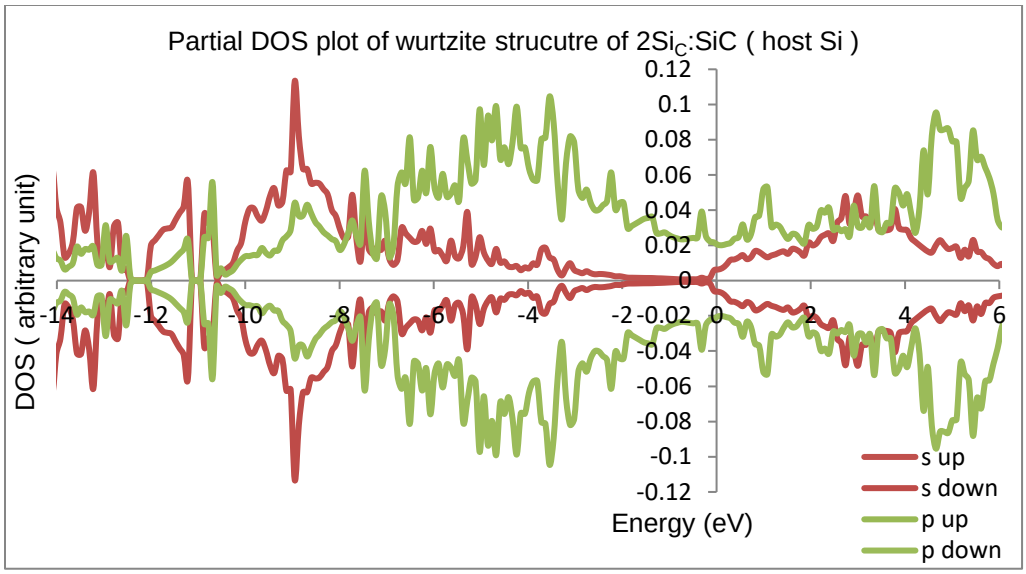

Figure 5-12 The partial DOS plot of wurtzite structure of 2Si$_C$:SiC (host Si)

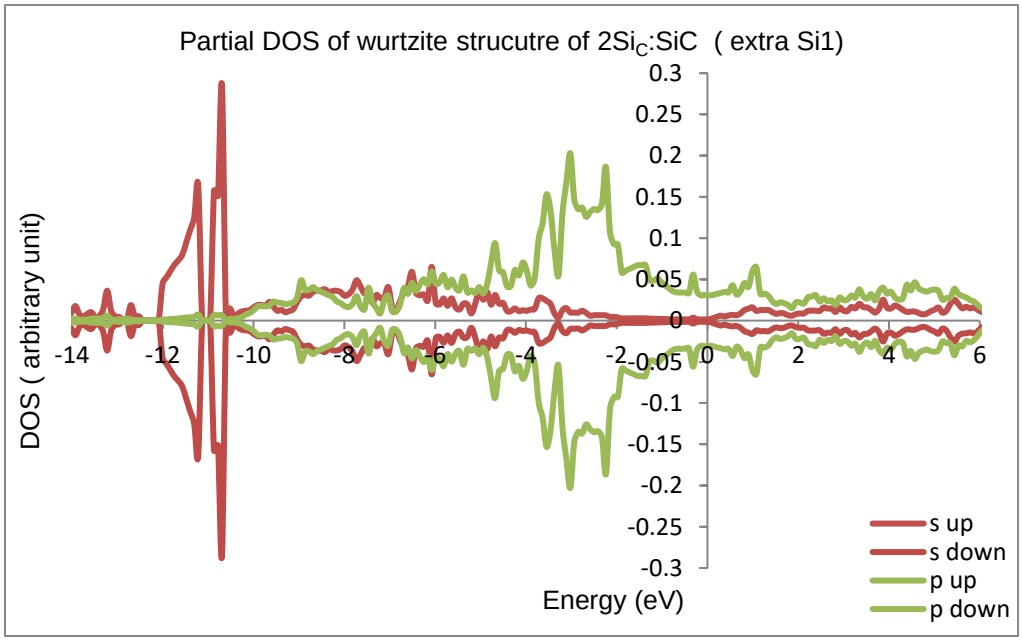

Figure 5-13 The partial DOS plot of wurtzite structure of 2Si$_C$:SiC (extra Si1)

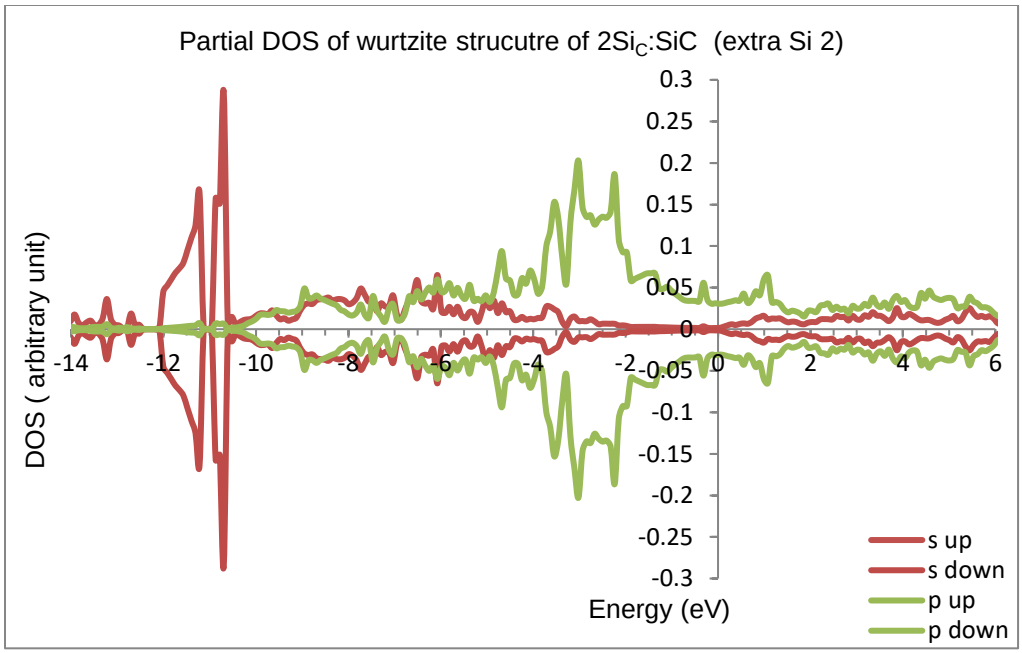

Figure 5-14 The partial DOS plot of wurtzite structure of 2Si$_C$:SiC (extra Si 2)

Comparing the partial DOS plots of regular silicon and extra silicon of FeSi shown in figure 5-15, 5-16, and 5-17 respectively with diamond structure, we can see that in host silicon of FeSi, p orbital takes time to go up, and s orbital and p orbital have high hybridization in the conduction band as in diamond structure. However, the partial DOS plots of the extra two silicon are same, and p orbital in the valance band goes up very quickly as in diamond structure and the contribution in the conduction band are almost zero from s orbital, and the contribution from p orbital is very small.

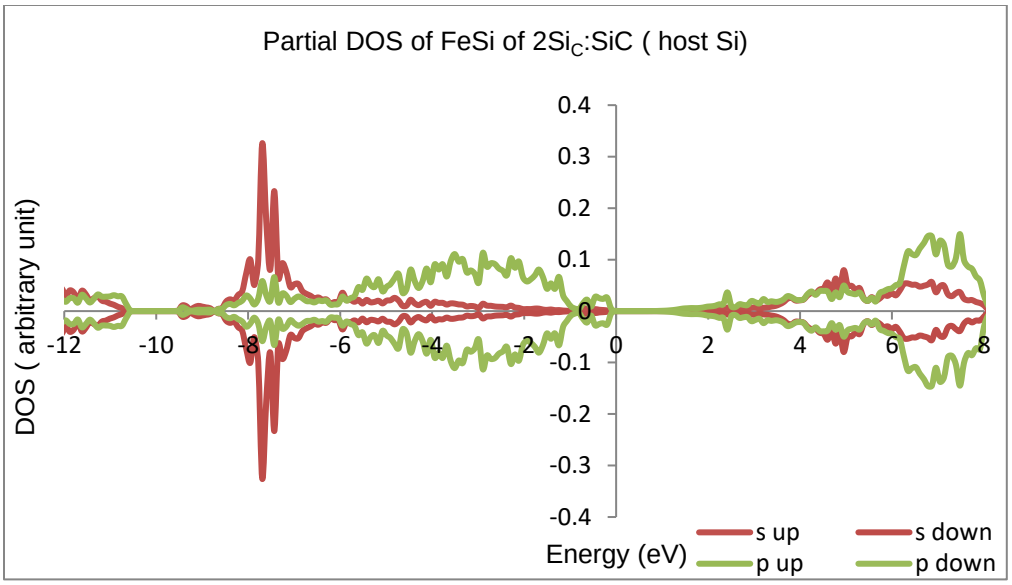

Figure 5-15 The partial DOS plot of FeSi structure 2Si$_C$:SiC (host Si)

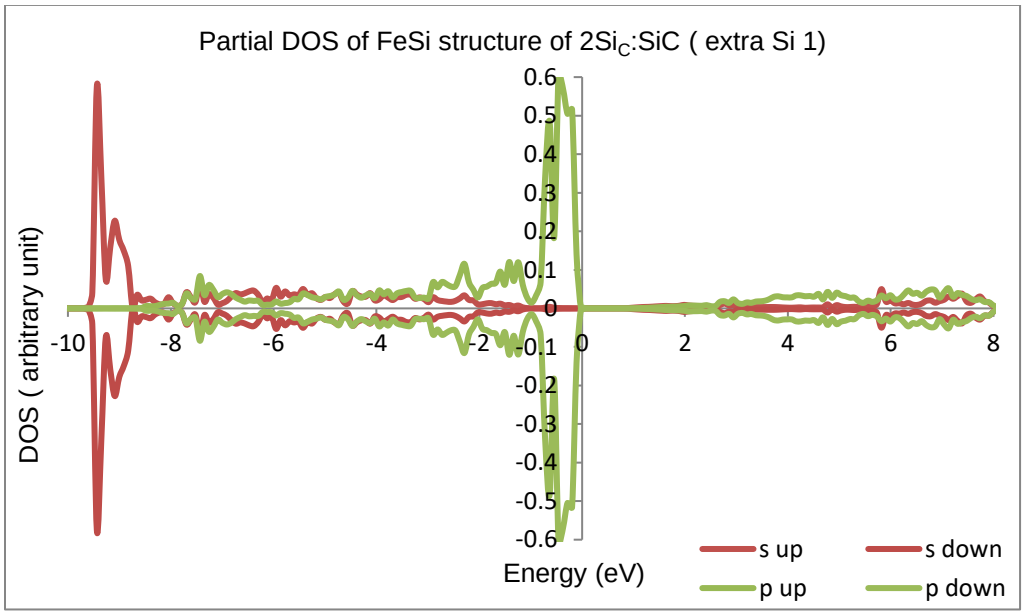

Figure 5-16 The partial DOS plot of FeSi structure of 2Si$_C$:SiC (extra Si 1)

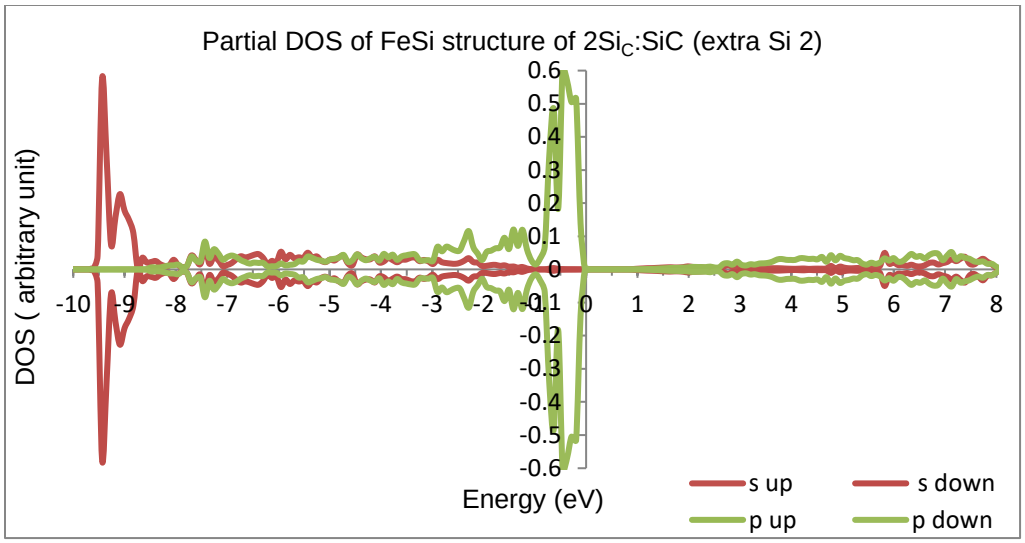

Figure 5-17 The partial DOS plot of FeSi structure of 2Si$_C$:SiC (extra Si 2)

Figure 5-18 shows the partial DOS plot of 6H structure of 2Si$_C$:SiC of host silicon, and figure 5-19, 5-20 demonstrate the partial DOS plot of 6H structure of 2Si$_C$:SiC of the extra two silicon atoms respectively. It can be clearly seen that there is a gap between fermi level and the bottom of conduction band about 0.15 eV which is different about 0.09 eV from the gap in host silicon in wurtzite structure. It is visible in figure 5-18 that p orbital goes up very quickly in the valance band, and the contribution comes from s, and p orbital. However, in figure 5-19, and 5-20 we can see that both extra two silicon plots have same DOS plots, and s orbital, and p orbital contribute more in the valance band than in the conduction band.

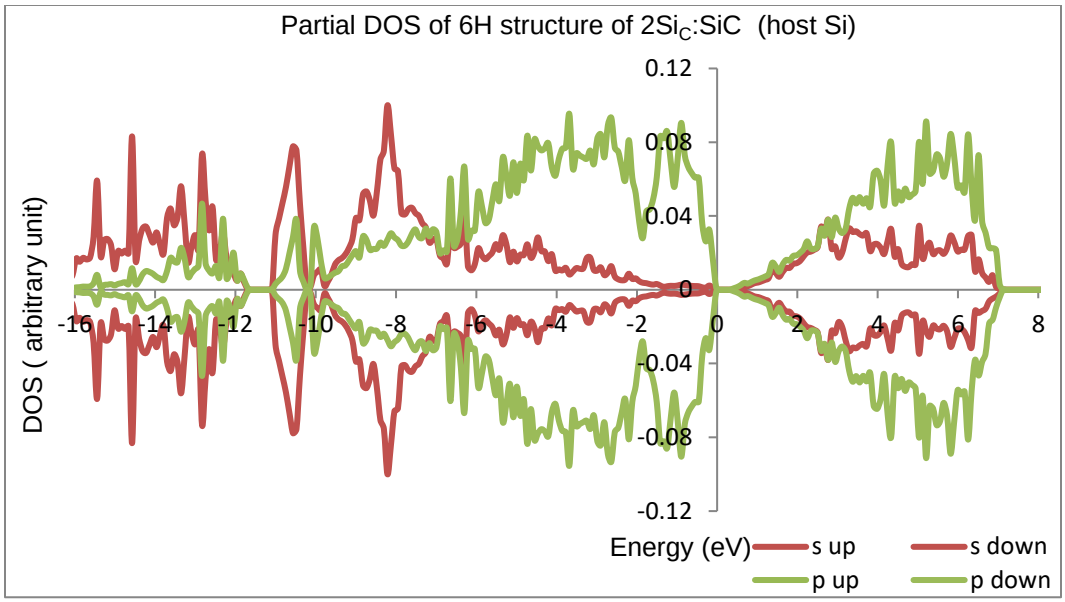

Figure 5-18 The partial DOS plot of 6H structure of 2Si$_C$:SiC (host Si)

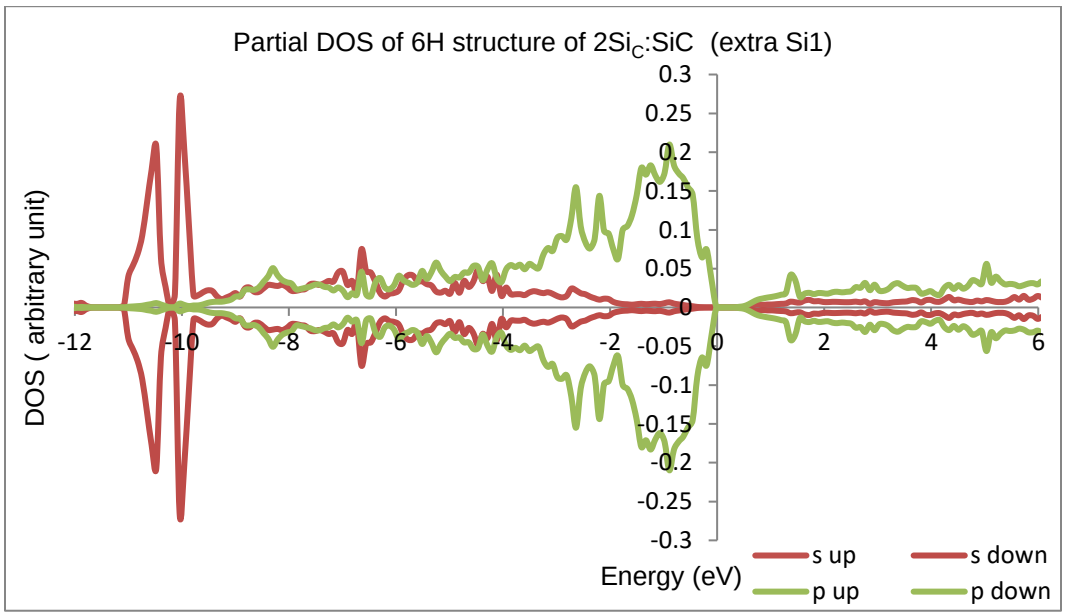

Figure 5-19 The partial DOS plot of 6H structure of 2Si$_C$:SiC (extra Si 1)

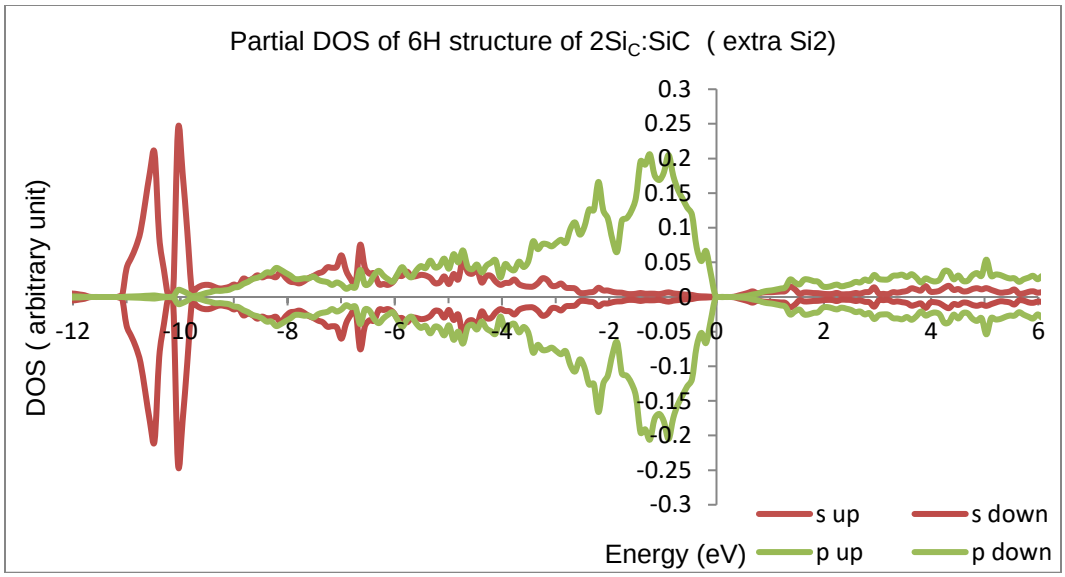

Figure 5-20 The partial DOS plot of 6H structure of 2Si$_C$:SiC (extra Si 2)

Moving to 3Si$_C$:SiC to see how the extra silicon DOS plots look like, and compare it with the host silicon. The figure 5-21 shows the partial DOS plot of diamond structure of 3Si$_C$:SiC of host silicon where it can be clearly seen that there is a gap around 0.16 eV between the fermi level and the bottom of the conduction band, and s, and p orbital contribute in both valance and conduction band, but stronger contribution in the valance band comes at a lower energy. However, p orbital contribution is higher in the valance band than s orbital. On the other side, the three extra silicon plots shown in figure 5-22, 5-23, 5-24 show how s and p orbitals act in the three plots like each other with slight different in the variation of s, and p orbital in both valance and conduction bands with very small contribution from the orbitals. Also, in the three plots, we can see that p orbital contribution is higher in the valance band.

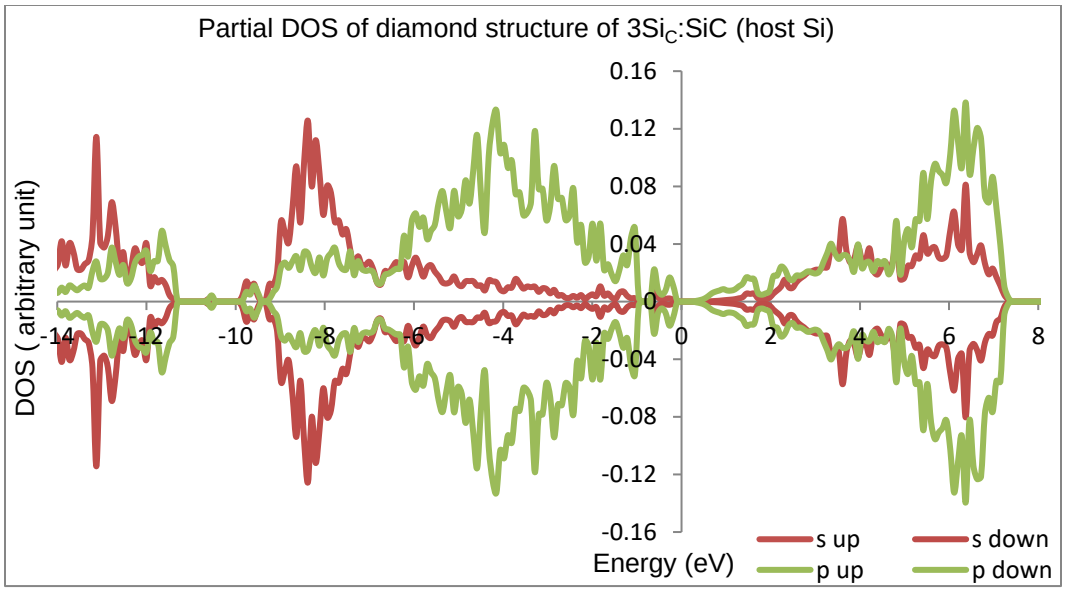

Figure 5-21 The partial DOS plot of diamond structure of 3Si$_C$:SiC (host Si)

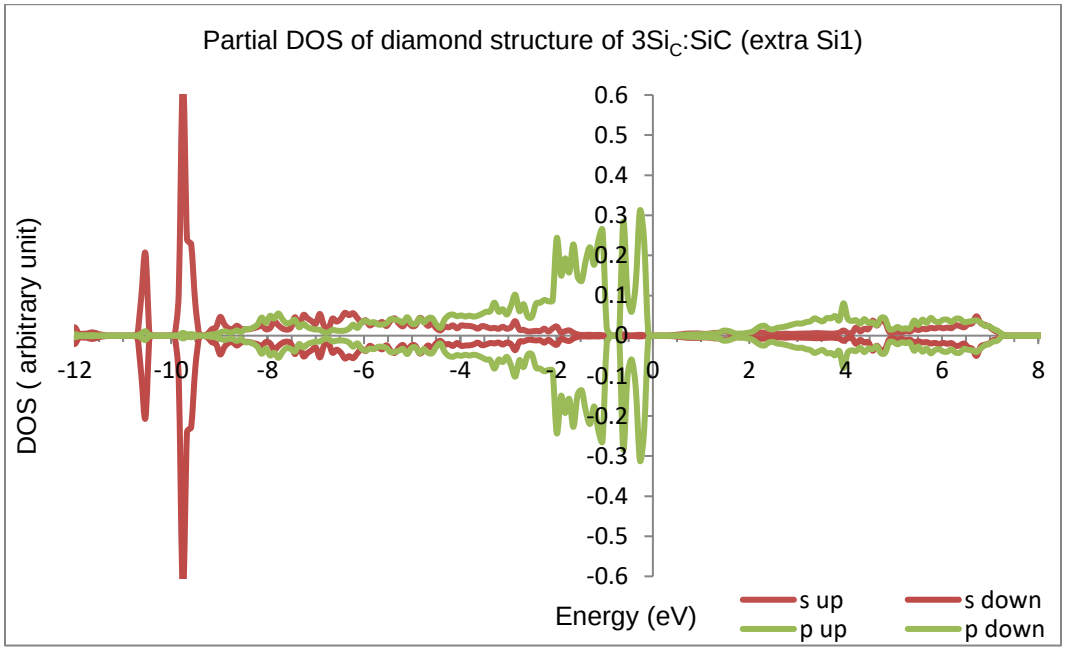

Figure 5-22 The partial DOS plot of diamond structure of 3Si$_C$:SiC (extra Si 1)

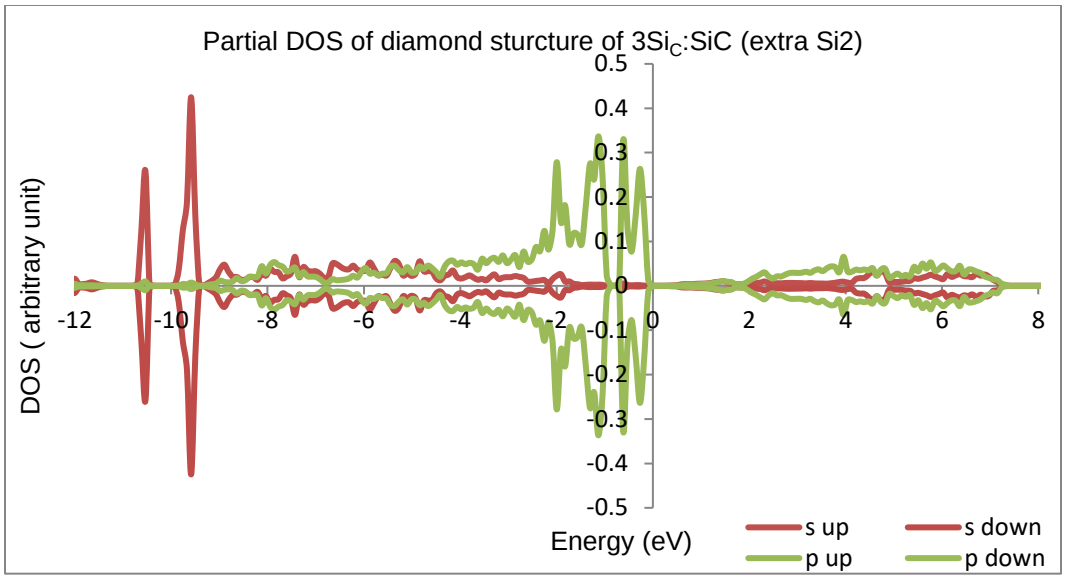

Figure 5-23 The partial DOS plot of diamond structure of 3Si$_C$:SiC (extra Si 2)

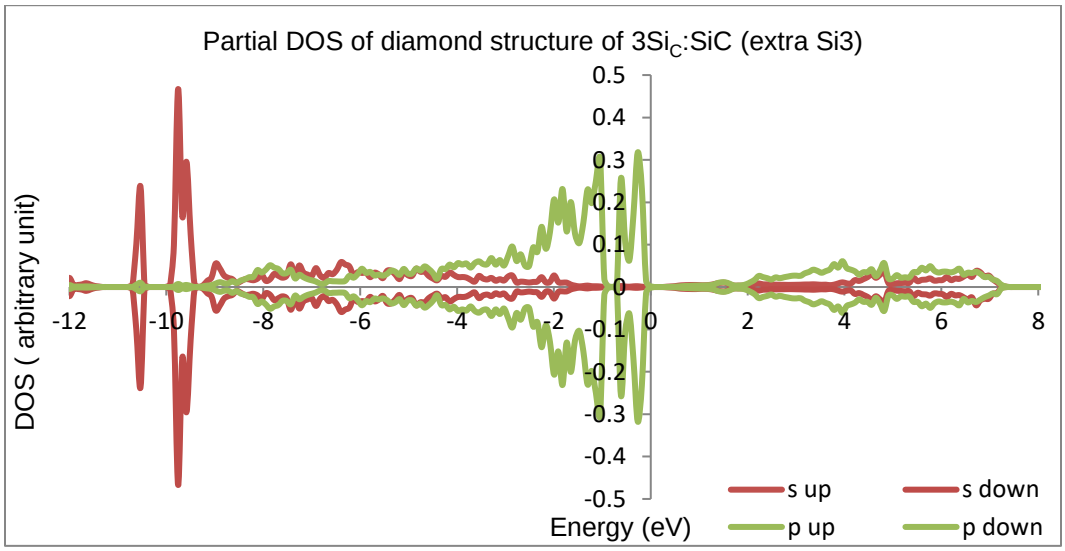

Figure 5-24 The partial DOS plot of diamond structure of 3Si$_C$:SiC (extra Si 3)

Figure 5-25, 5-26. 5-27, 5-28 show the partial DOS plots of host silicon and extra three silicon in the wurtzite structure of 3Si$_C$:SiC respectively. It can be clearly seen that s orbital and p orbital have very different contribution comparing to the

contribution in diamond structure of $3Si_C$:SiC. It can be noticeable that the spin up is not as the spin down where in the conduction band there is very long peak around 1.37 eV in the spin down which the spin up does not have. It is visible that the situation in the valance band as in the conduction band with peak around -5.05 eV. Also, we can see that there is no gap in the host silicon comparing to the diamond structure. On the other hand, the plots of the extra three silicon have similarity in the contribution of p orbital, but the contribution from s orbital in the three extra silicon plots in the valance band have more different than p orbital.

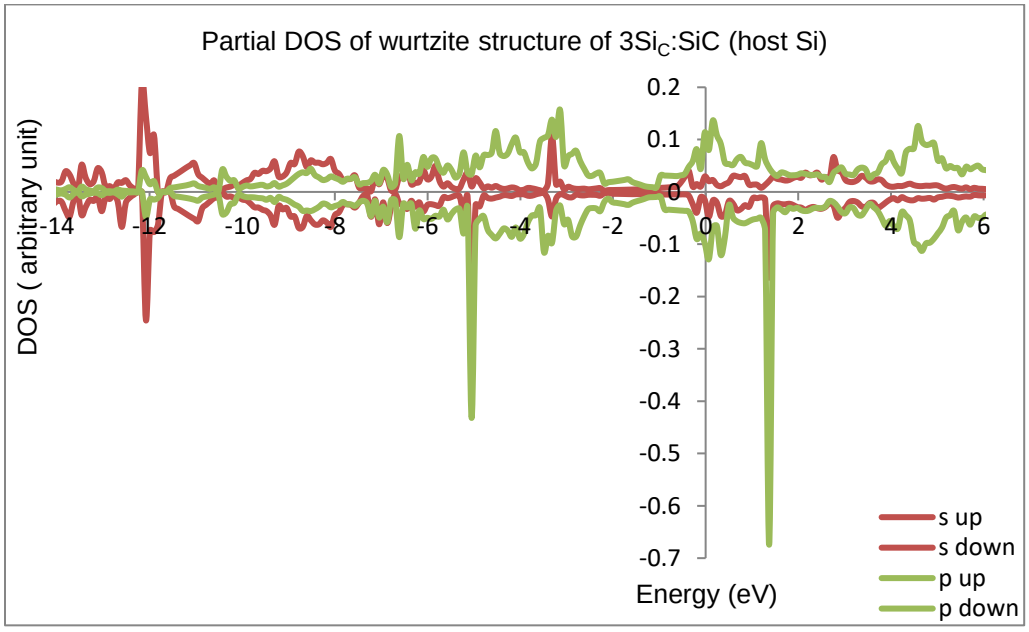

Figure 5-25 The partial DOS plot of wurtzite structure of $3Si_C$:SiC (host Si)

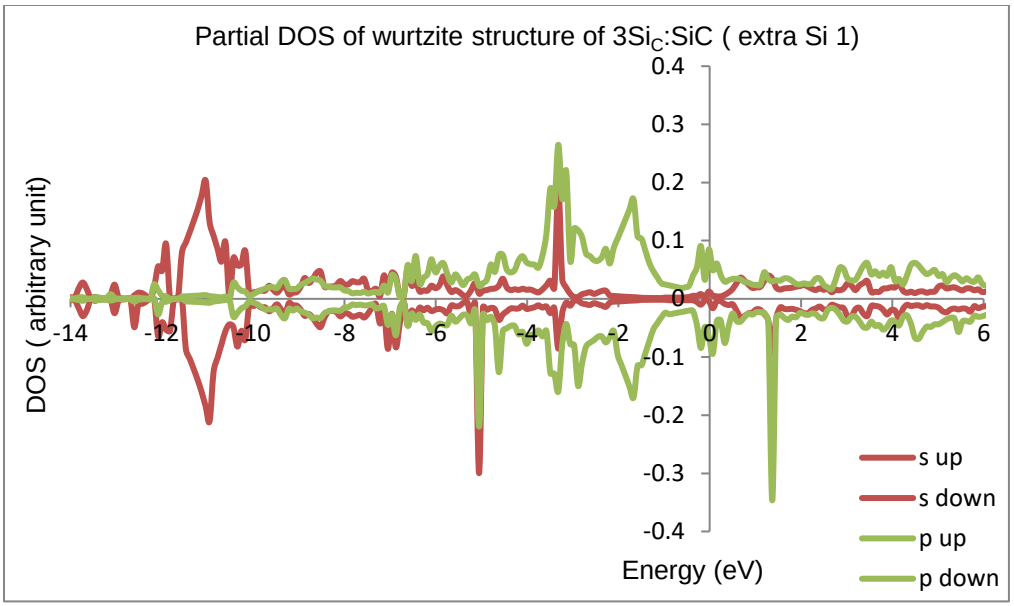

Figure 5-26 The partial DOS plot of wurtzite structure of 3Si$_C$:SiC (extra Si 1)

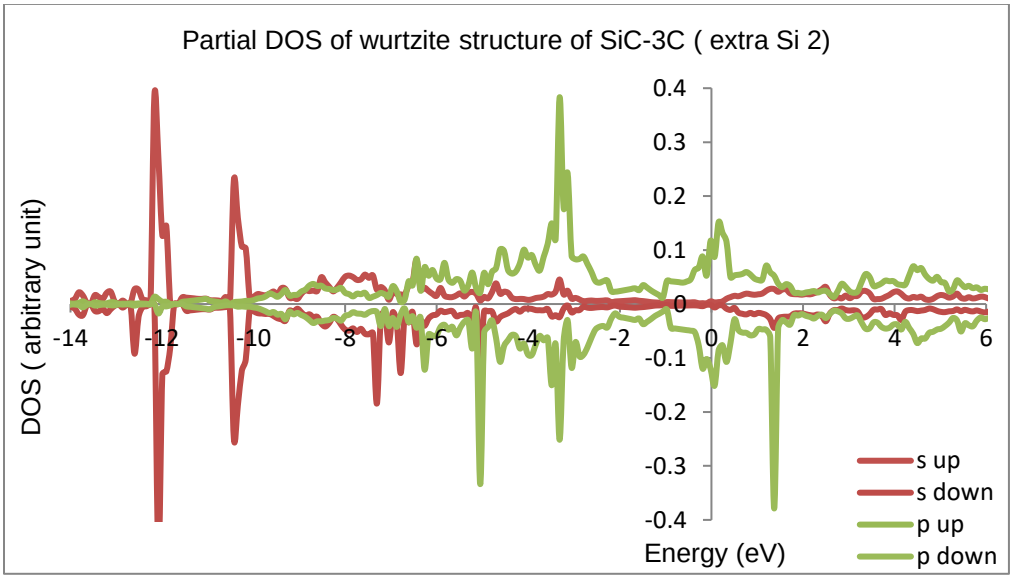

Figure 5-27 The partial DOS plot of wurtzite structure of 3Si$_C$:SiC (extra Si 2)

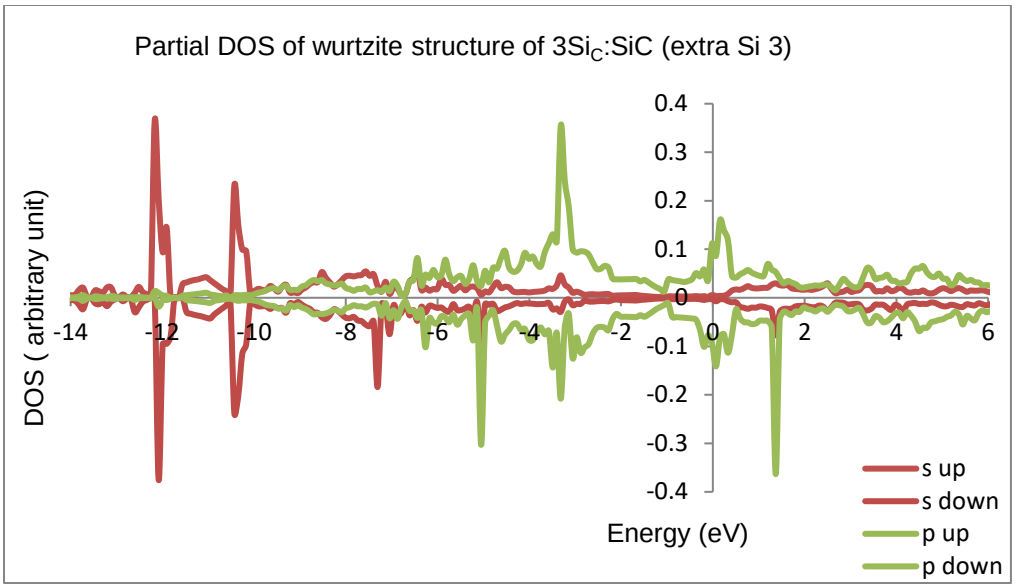

Figure 5-28 The partial DOS plot of wurtzite structure of 3Si$_C$:SiC (extra Si 3)

Figure 5-29, 5-30, 5-31, 5-32 show the partial DOS plots of FeSi structure of 3Si$_C$:SiC of host silicon and the extra three silicon respectively. It can be clearly seen that s orbital and p orbital coupled with each other in the beginning of the conduction band, but they are not in the valance band. P orbital goes very quickly near the fermi level in the valance band while s orbital takes a while to increase. On the other side, s orbital, and p orbital behave similarly in the conduction band, but in the valance band, the contribution from p orbital changed. We can see that in two extra silicon plots, p orbital has very high contribution near fermi level while the third one takes a while to increase.

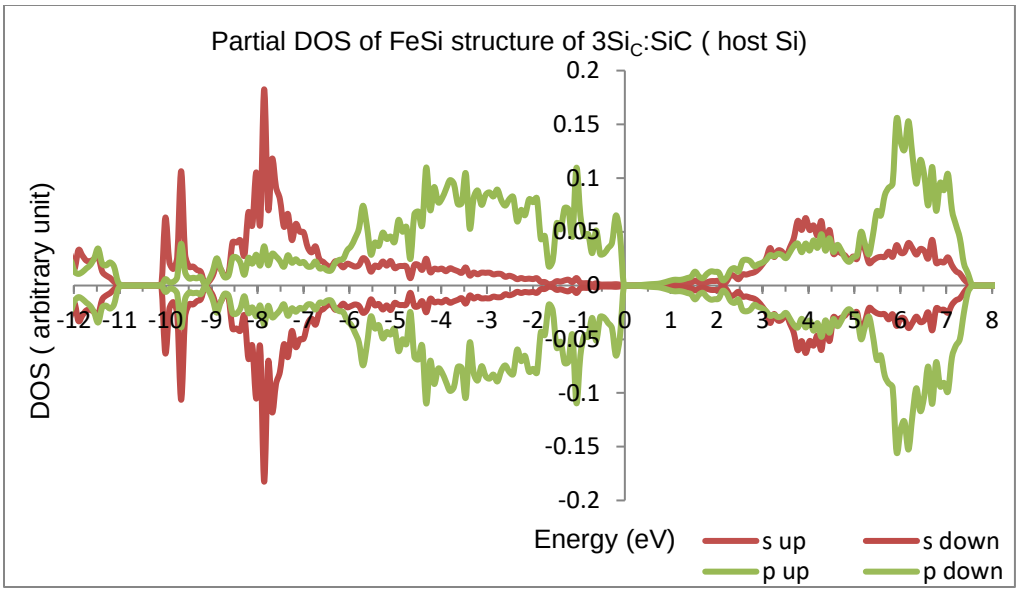

Figure 5-29 The partial DOS plot of FeSi structure of 3Si$_C$:SiC (host Si)

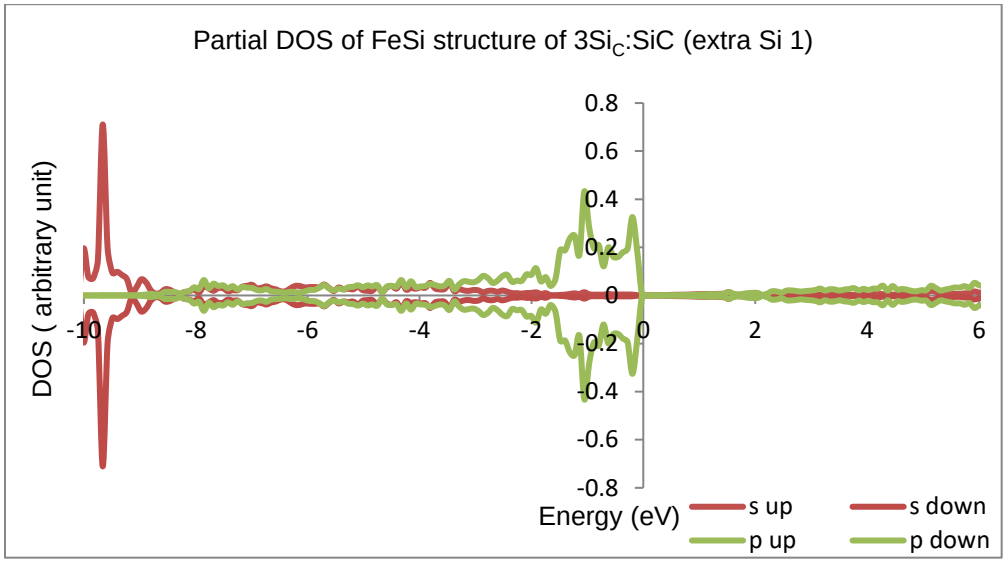

Figure 5-30 The partial DOS plot of FeSi structure of 3Si$_C$:SiC (extra Si 1)

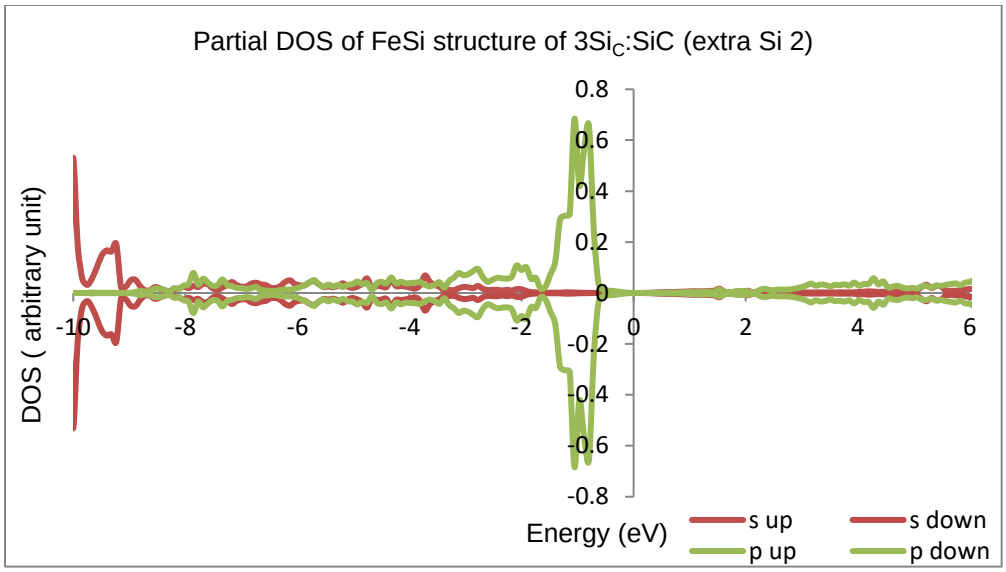

Figure 5-31 The partial DOS plot of FeSi structure of 3Si$_C$:SiC (extra Si 2)

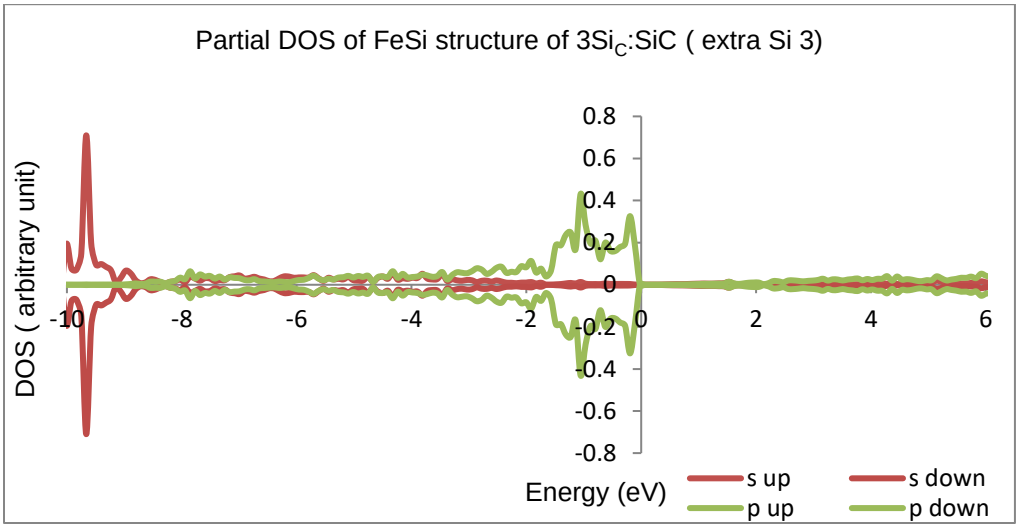

Figure 5-32 The partial DOS plot of FeSi structure of 3Si$_C$:SiC (extra Si 3)

Figure 5-33, 5-34, 5-35, 5-36 demonstrate the partial DOS of 6H structure of 3Si$_C$:SiC of host silicon and three extra silicon plots respectively. It can be clearly seen that in figure 5-33, the p orbital in the valance band goes very quickly as in

Fesi structure. Also, it is visible that in the conduction band in two extra silicon atoms, there is no contribution from s, and p orbital, but the third one has some contribution from p orbital in the conduction band. Also, it is noticeable that in the valance band of all the extra three silicon the most contribution comes from p orbital, but it takes a while to go up. We can conclude that the extra silicon atoms play different roles in the DOS plot from structure to other structure. In addition the band gap is zero at this level of calculation.

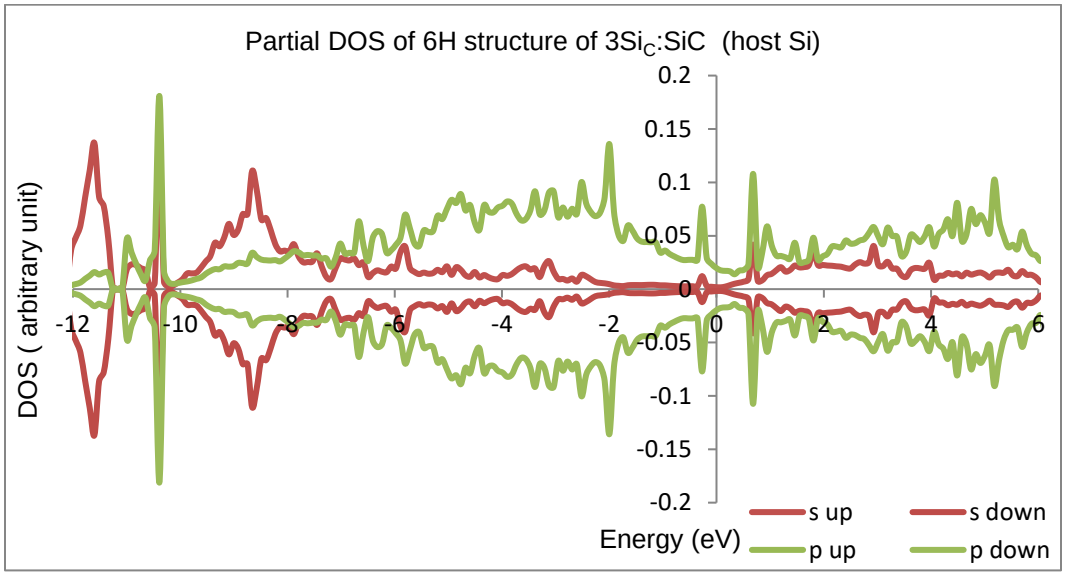

Figure 5-33 The partial DOS plot of 6H structure of 3Si$_C$:SiC (host Si)

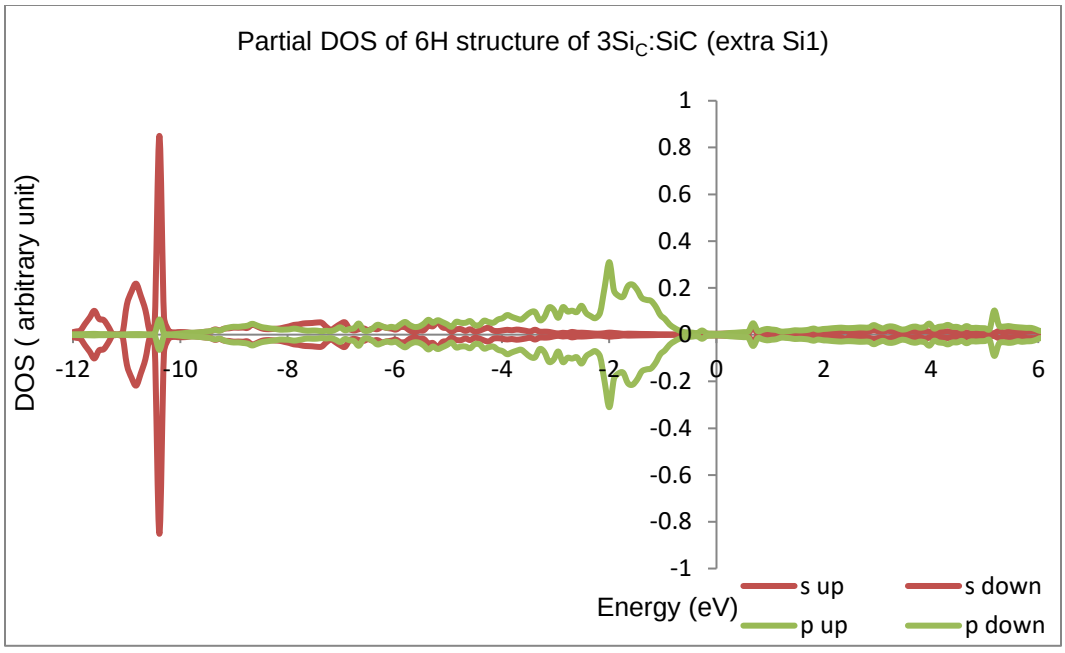

Figure 5-34 The partial DOS plot of 6H structure of 3Si$_C$:SiC (extra Si 1)

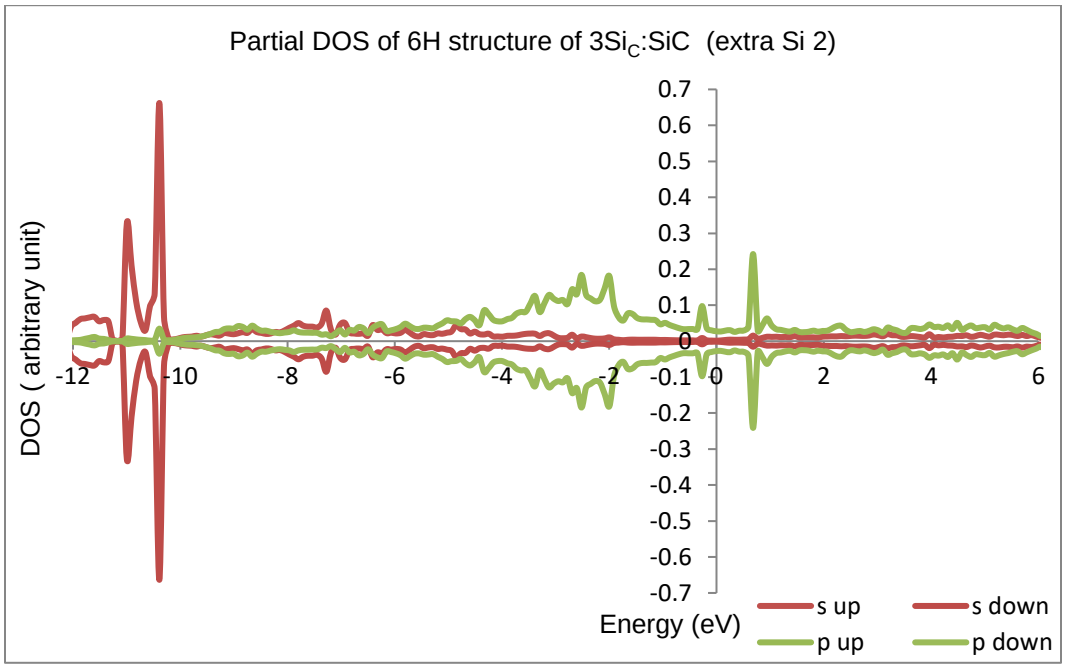

Figure 5-35 The partial DOS plot of 6H structure of 3Si$_C$:SiC (extra Si 2)

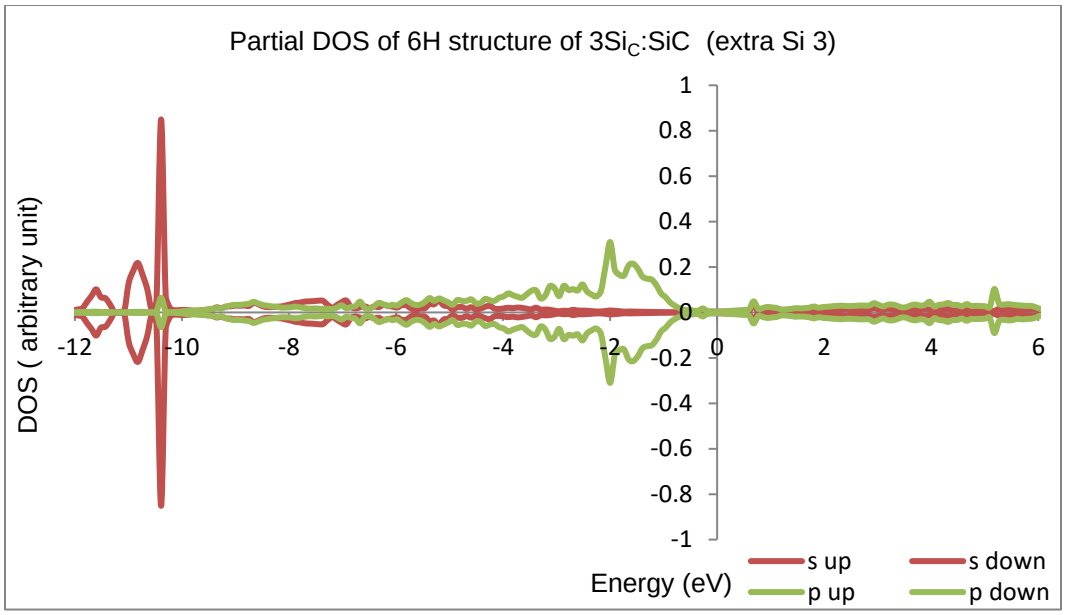

Figure 5-36 The partial DOS plot of 6H structure of 3Si$_C$:SiC (extra Si 3)

5.2 Calculating the Electrostatic Energies of Pristine Silicon Carbide and Silicon Rich Silicon Carbide structures

Electrostatic energy is the potential energy which comes from Coulomb forces due to ionic nature of the crystal structures. We calculated the electrostatic energy of 2H, 4H, 6H, diamond, FeSi, wurtzite structures of pristine silicon carbide 1x1x1 unit cell, and calculated for diamond, FeSi, wurtzite and 6H structures of silicon carbide 2x2x2 supercell, and silicon rich silicon carbide structures of these geometric.

Table 5-1 shows the electrostatic energy of pristine structures 1x1x1 unit cell for all six structures. It can be clearly seen that 2H structure has the lowest electrostatic energy gain among the pristine structures while FeSi structure has the highest electrostatic energy gain.

Table 5-2, 5-3, 5-4, and 5-5 show the electrostatic energies of 6H, diamond, FeSi, and wurtzite structures of pristine silicon carbide, and silicon rich silicon carbide 2x2x2 supercell respectively. It is visible that in pristine silicon carbide 2x2x2, the lowest electrostatic energy belongs to FeSi structure with different about 0.006 eV comparing to diamond structure which has the second lowest electrostatic energy while 6H has the highest electrostatic energy with different around 0.032 eV comparing to wurtzite structure.

Comparing the electrostatic energies of silicon rich silicon carbide Si_C:SiC of 6H, diamond, wurtzite, and FeSi structures, we can see that in Si_c:SiC, 6H structure has the lowest electrostatic energy with different about 0.194 eV comparing to diamond structure which has the second lowest electrostatic energy.

By increasing the numbers of silicon atoms, we can see that the electrostatic energy increases in all structures. However, it is noticeable that in diamond structures, the electrostatic energy remains high, and it has more energy gain from electrostatic energy. FeSi structure is maintaining the high electrostatic energy contribution, and it has the second lowest electrostatic energy comparing to 6H and wurtzite structures. On the other side, in wurtzite structure, and 6H structure, the electrostatic energies are fluctuating a lot, and it is increasing very quickly as the number of silicon atoms increases.

In conclusion, we can see that diamond structure is more favorable than the other structures electrostatically. There is a large electrostatic contribution which results in ionic bonding. In addition, the strong coupled and high hybridization between s orbital and p orbital in partial dos plot of silicon and carbon atoms in the conduction band, shown earlier in this chapter and in appendix A, B, C, and, D, will create strong covalent bonding.

Figure 5-37 shows how the electrostatic energies of 6H, diamond, FeSi, and wurtzite structures are changed with the increasing of silicon atoms. It can be clearly seen that in 6H structure, the electrostatic energy increases rapidly while in diamond structure, the electrostatic energy is increasing very slowly.

Table 5-1 Electrostatic energies of pristine structures 2H, 4H, 6H, wurtzite, FeSi, and diamond structures 1x1x1 unit cell

structure 1x1x1	Electrostatic energy (eV)	Electrostatic energy per atom (eV)

2H (2Si2C)	-566.905	-141.726
4H (4Si4C)	-1134.827	-141.853
6H (6Si6C)	-1702.606	-141.889
Wurtzite (4Si4C)	-1134.696	-141.837
Diamond (1Si1C)	-283.827	-141.913
FeSi (4Si4C)	-1135.565	-141.945

Table 5-2 Electrostatic energies of pristine SiC and silicon rich silicon carbide of 6H structures 2x2x2 supercell

6H structure 2x2x2	Electrostatic energy (eV)	Electrostatic energy per atom (eV)
SiC	-13620.788	-141.883
Si_c:SiC	-13502.131	-140.647
$2Si_c$:SiC	-13347.060	-139.031
$3Si_c$:SiC	-13063.271	-136.075
$4Si_c$:SiC	-12808.327	-133.42
$5Si_c$:SiC	-9765.791	-101.726
$6Si_c$:SiC	-10040.274	-104.586
$7Si_c$:SiC	-6922.872	-72.113
$8Si_c$:SiC	-4640.858	-48.342

Table 5.3 Electrostatic energies of pristine SiC and silicon rich silicon carbide of diamond structures 2x2x2 supercell

Diamond structure 2x2x2	Electrostatic energy (eV)	Electrostatic energy per atom (eV)
SiC	-9084.159	-141.939
Si_c:SiC	-8989.018	-140.453
2Si_c:SiC	-8892.307	-138.942
3Si_c:SiC	-8792.904	-137.389
4Si_c:SiC	-8690.439	-135.788
5Si_c:SiC	-8601.171	-134.393
6Si_c:SiC	-8513.628	-133.025
7Si_c:SiC	-8408.618	-131.384
8Si_c:SiC	-8303.765	-129.746

Table 5.4 Electrostatic energies of pristine SiC and silicon rich silicon carbide of FeSi structures 2x2x2 supercell

FeSi structure 2x2x2	Electrostatic energy (eV)	Electrostatic energy per atom (eV)
SiC	-9084.618	-141.947
Si_c:SiC	-8988.835	-140.45
2Si_c:SiC	-8893.010	-138.953

$3Si_c$:SiC	-8807.504	-137.617
$4Si_c$:SiC	-7755.299	-121.176
$5Si_c$:SiC	-8248.477	-128.882
$6Si_c$:SiC	-8153.699	-127.401
$7Si_c$:SiC	-8069.778	-126.09
$8Si_c$:SiC	-7995.453	-124.928

Table 5-5 Electrostatic energies of pristine SiC and silicon rich silicon carbide of wurtzite structures 2x2x2 supercell

Wurtzite structure 2x2x2	Electrostatic energy (eV)	Electrostatic energy per atom (eV)
SiC	-9078.486	-141.851
Si_c:SiC	-8973.132	-140.205
$2Si_c$:SiC	-8807.606	-137.618
$3Si_c$:SiC	-8493.740	-132.714
$4Si_c$:SiC	-8202.216	-128.159
$5Si_c$:SiC	-7326.227	-114.472
$6Si_c$:SiC	-6337.375	-99.021
$7Si_c$:SiC	-6464.688	-101.01
$8Si_c$:SiC	-4186.198	-65.409

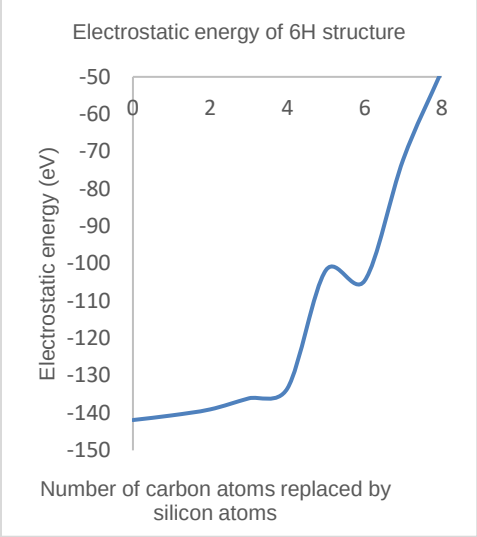

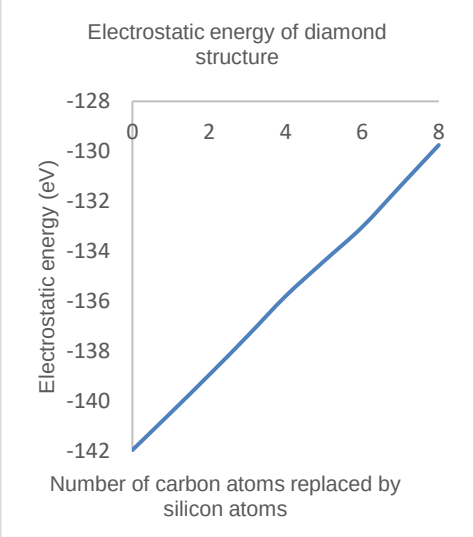

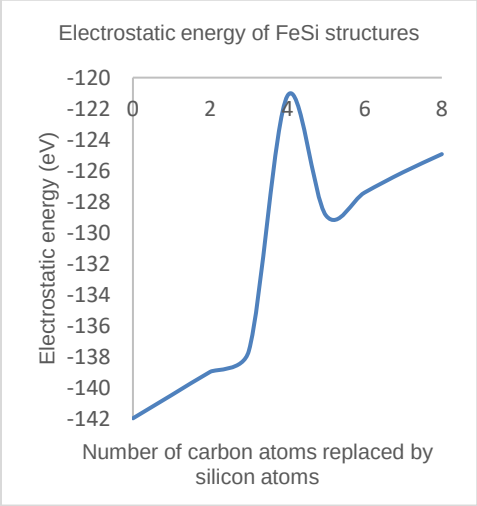

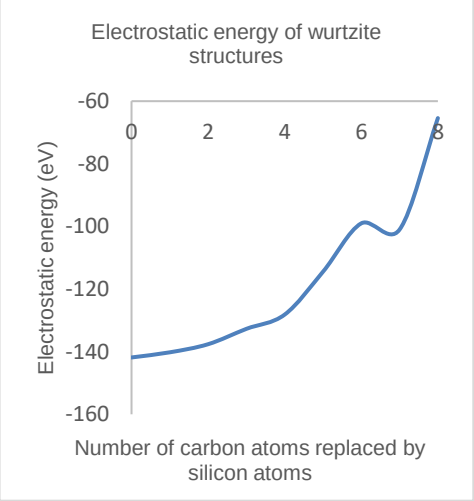

Figure 5-37 The electrostatic energies 6H, diamond, FeSi, and wurtzite structures with different number of carbon atoms replaced by silicon atoms

Chapter 6

Conclusion and Future Studies

6.1 Conclusion

The aim of this research was to examine the stability and the electronic properties of silicon rich silicon carbide materials with tunable bandgap which can be suitable for solar applications. Different structures were considered namely diamond structure, FeSi structure, wurtzite structure, and 6H structure. Within these structures, different numbers of carbon atoms were replaced by silicon atoms, density functional theory was used to study these structures.

We have seen that overall within the space of this thesis, with the increase of the number of silicon atoms and consequently decreasing the number of carbon atoms, the formation enthalpies increase, and the structures tend to lose its thermodynamic stability.

We found that 6H structures have the lowest energies comparing to the other structures. We noticed that substituted Si atoms preferred to be near each other than when they are far from each other, or spread randomly in the structures.

Also, we have found that it would be better to choose the extra silicon atoms to be at the same layers and near to each other simultaneously to get energetically favorable structures, we have found that near Fermi level, the most contributions came from p orbital in all partial dos of silicon and carbon, and the total dos in both valance band and conduction band. Also, we noticed that s orbital and p orbital in some structures have strong hybridization in the conduction bands.

Finally, we have predicted new structures of silicon rich silicon carbide, and studied their electronic properties such as the density of states. Although diamond structure, wurtzite structure, and FeSi structure have same number of atoms, they gave different energies and formation enthalpies, and we found that these differences are due to the configuration effect. We conclude that 6H structures of silicon rich silicon carbide, which have the lowest formation enthalpies up to 8 atoms of carbon that replaced by silicon atoms, are the most favorable structure among the other structures. Also, wurtzite structures of silicon rich silicon carbide gave thermodynamically stable results up to 4 atoms of carbon replaced by silicon, and then it lost its stability after 4 carbon atoms which are replaced by silicon atoms. Similarly, FeSi and diamond structures lost their stability when 4 atoms of carbon replaced by 4 atoms of silicon.

6.2 Future Studies

As the structures plays a significant role in calculating the energies and the formation enthalpies of silicon rich silicon carbide, amorphous silicon rich silicon carbide then should be examined as well. In addition, molecular dynamics calculations should be studied in detail to know more about silicon rich silicon carbide structures. Also, it will be important to study the structures with more different configurations of the extra carbon atoms, which can be replaced by silicon atoms, as it gave different results with different arrangement of the extra atoms. In addition, interstitial dopants need to be examined as well. Optical absorption study should be calculated as well to get an estimation of the results which will be utilized and useful in the photovoltaic application. Lastly, since we know that DFT

underestimate the band gap specially for materials such SiC, Si, and C, hybrid DFT should be used to calculate the band gap properly.

Appendix A

DOS plot of diamond Structures of Silicon Rich Silicon Carbide

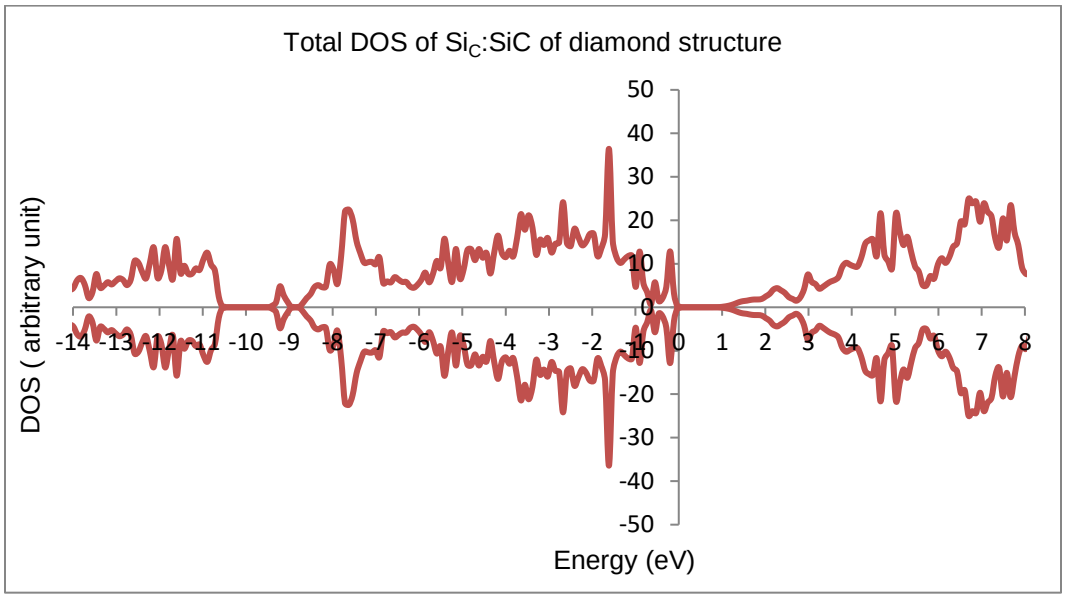

Figure A1 The total DOS plot of diamond structure of Si_C:SiC

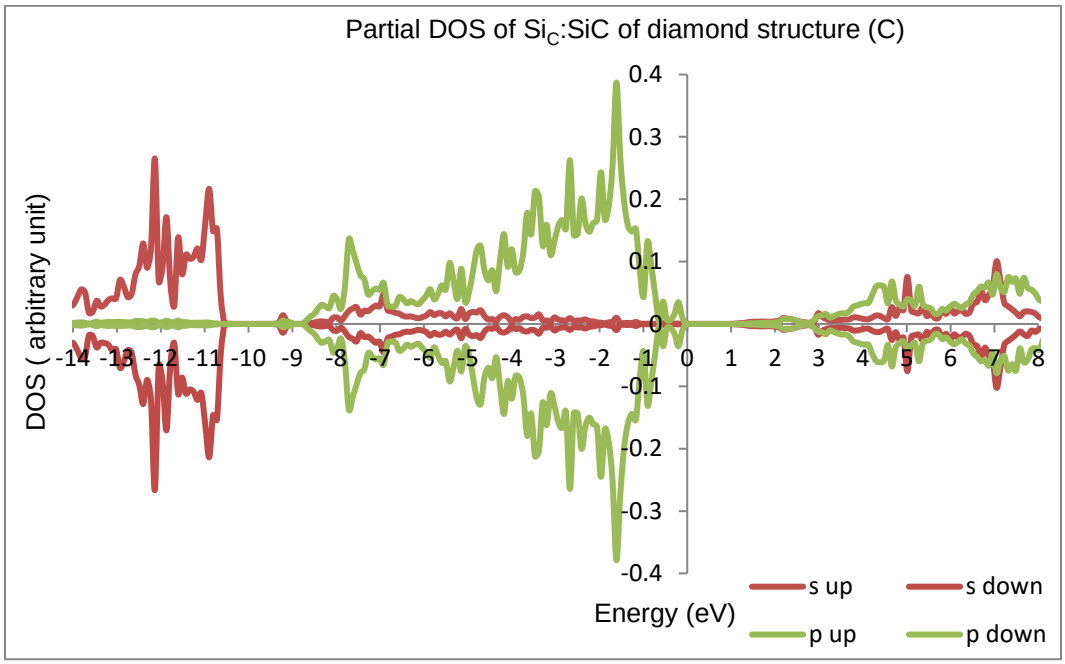

Figure A2 The partial DOS plot of diamond structure of Si_C:SiC (C)

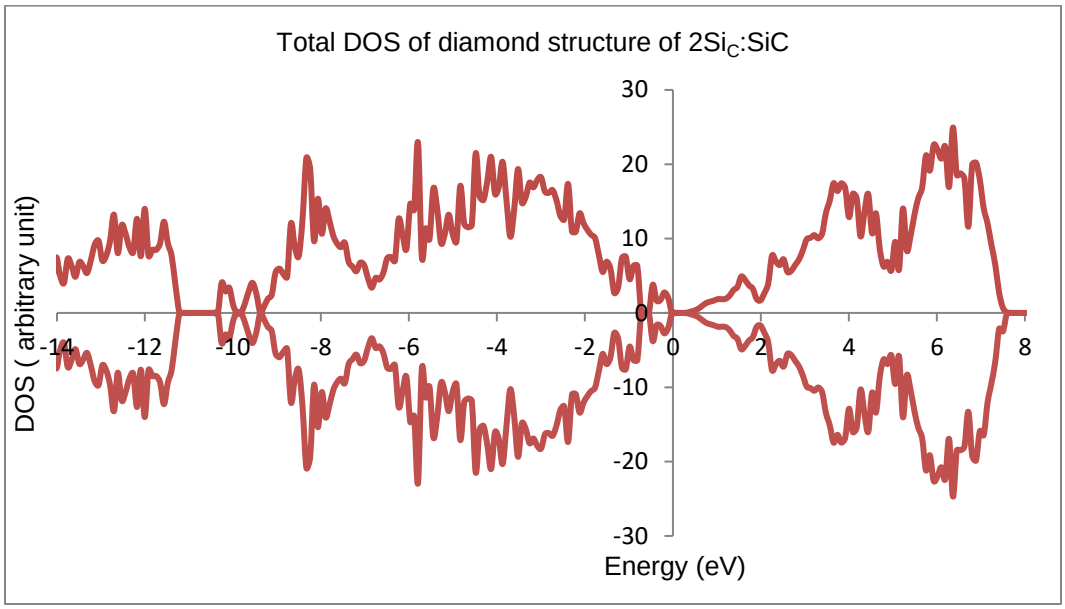

Figure A3 The total DOS plot of diamond structure of 2Si$_C$:SiC

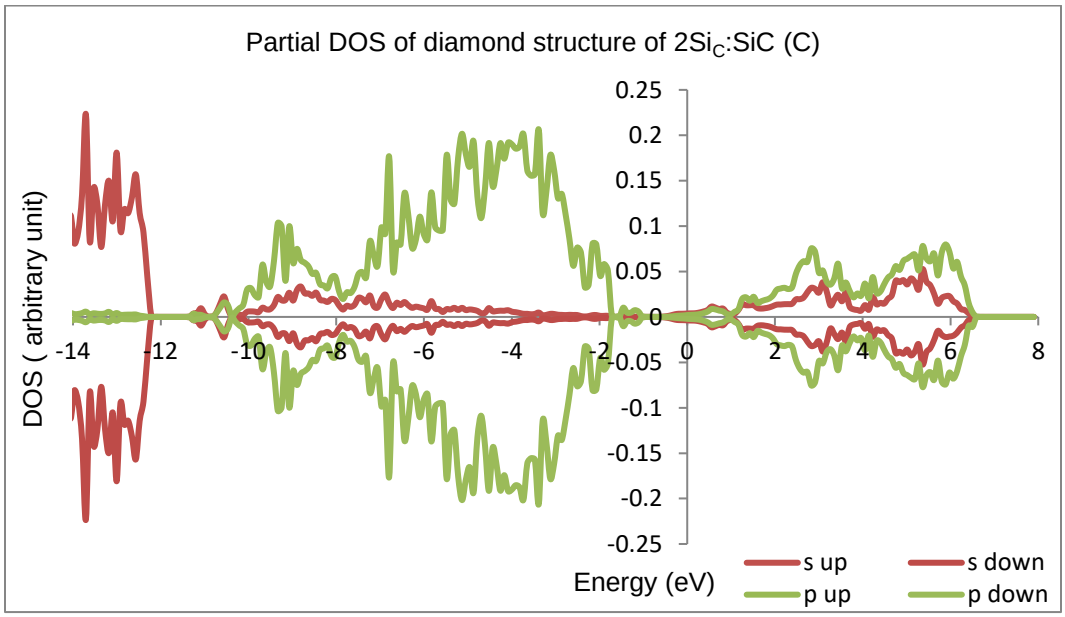

Figure A4 The partial DOS plot of diamond structure of 2Si$_C$:SiC (C)

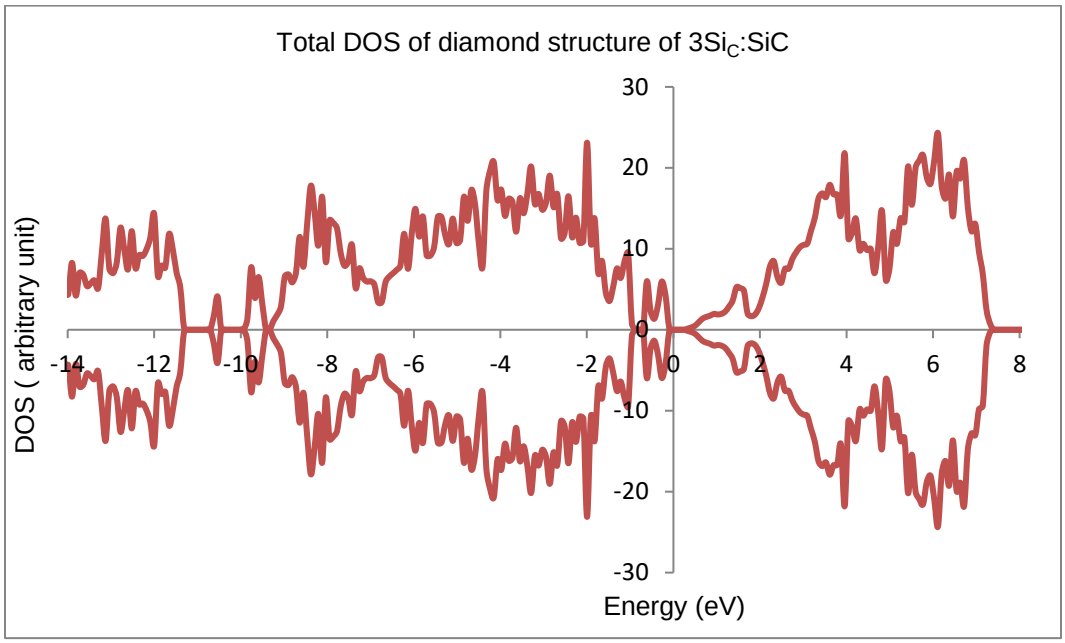

Figure A5 The total DOS plot of diamond structure of 3Si$_C$:SiC

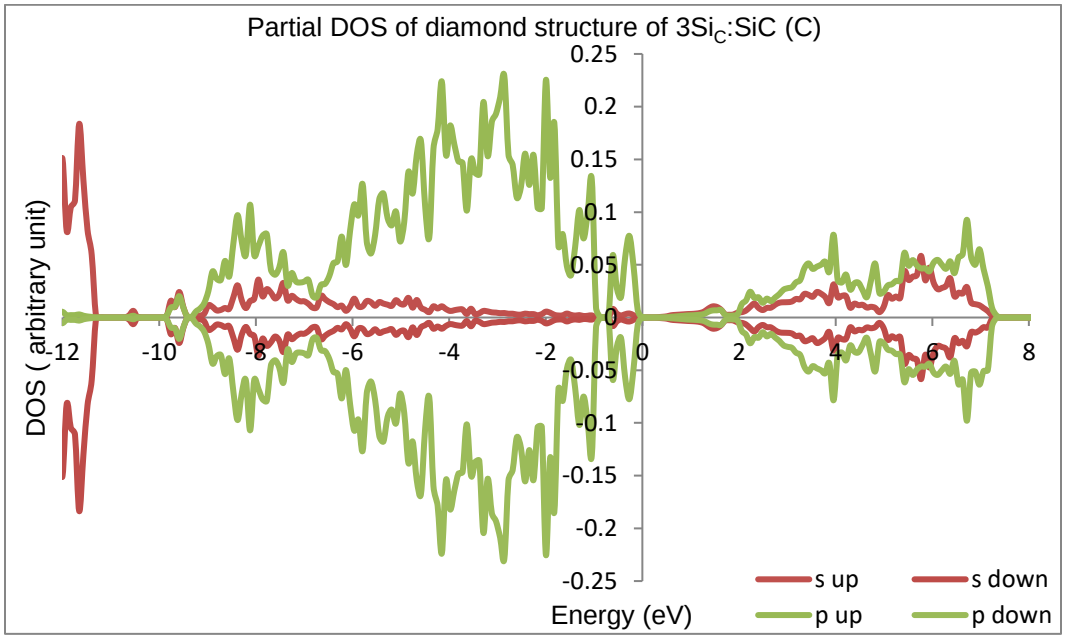

Figure A6 The partial DOS plot of diamond structure of 3Si$_C$:SiC (C)

Appendix B

DOS Plot of wurtzite Structures of Silicon Rich Silicon Carbide

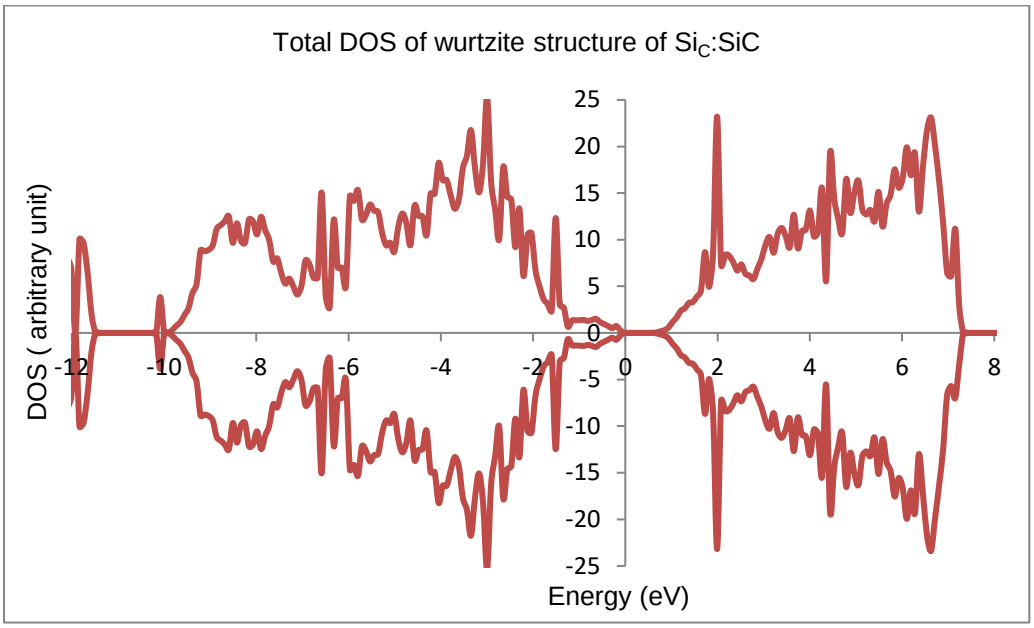

Figure B1 The total DOS plot of wurtzite structure of Si_C:SiC

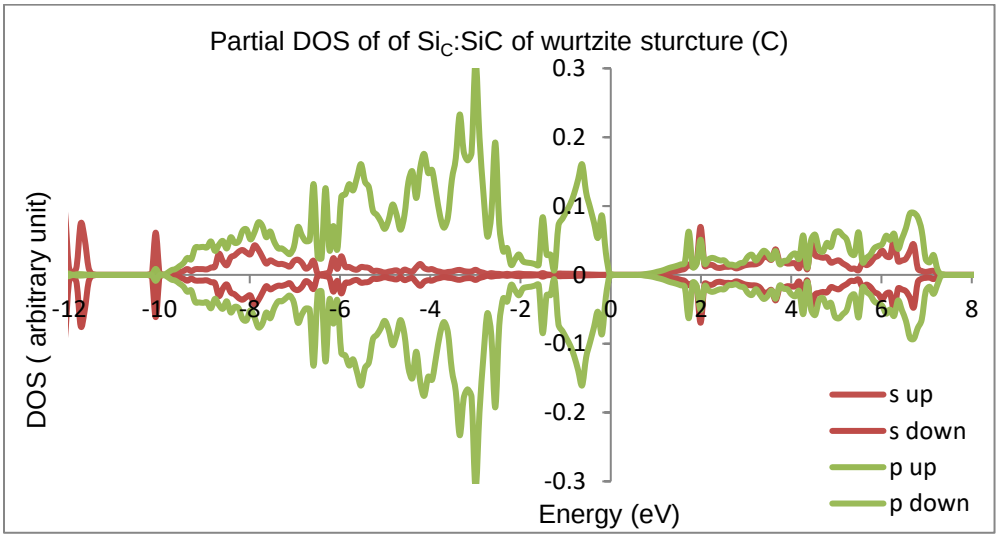

Figure B2 The partial DOS plot of wurtzite structure of Si_C:SiC (C)

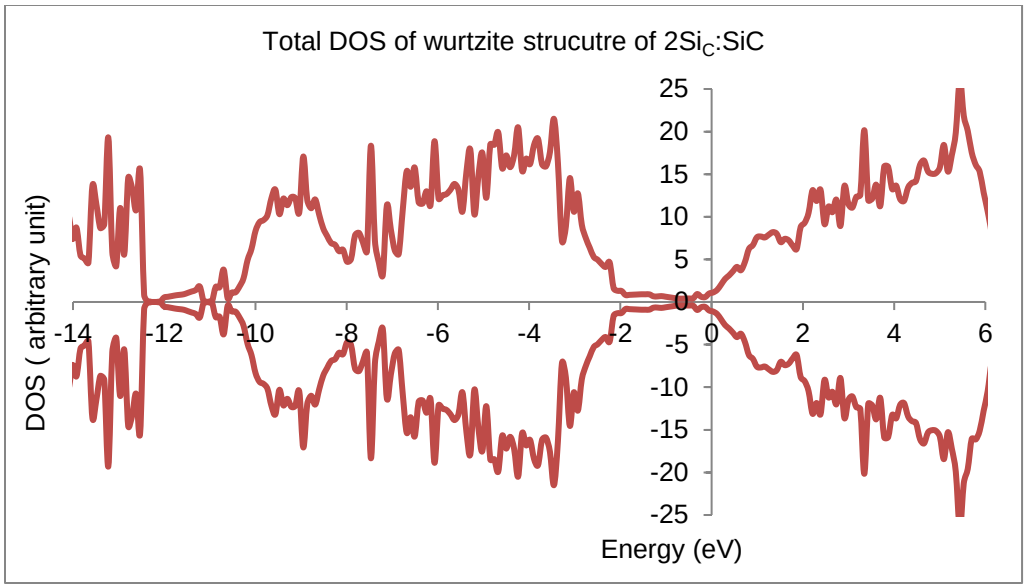

Figure B3 The total DOS plot of wurtzite structure of 2Si$_C$:SiC

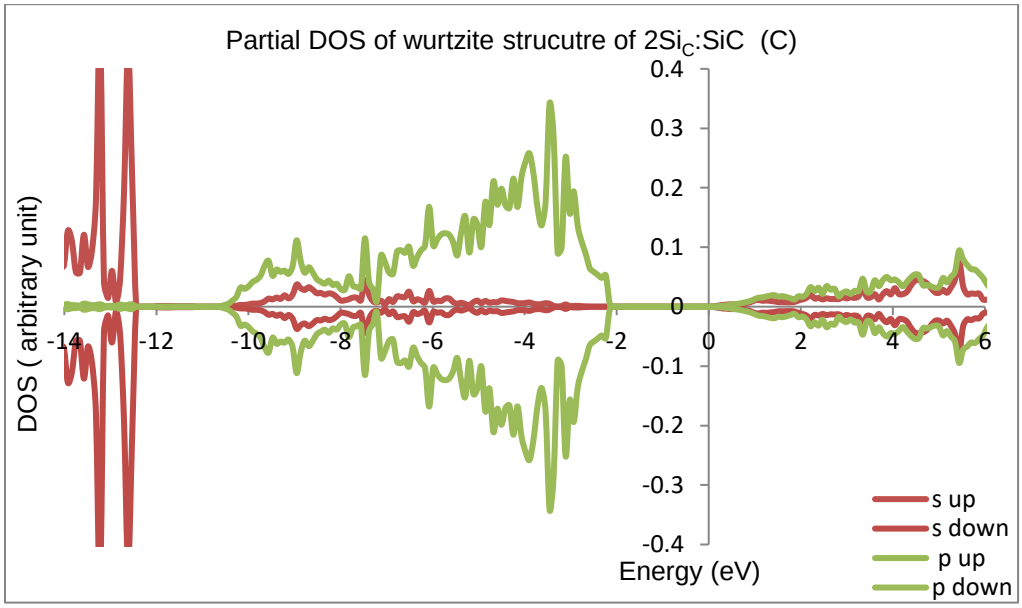

Figure B4 The partial DOS plot of wurtzite structure of 2Si$_C$:SiC (C)

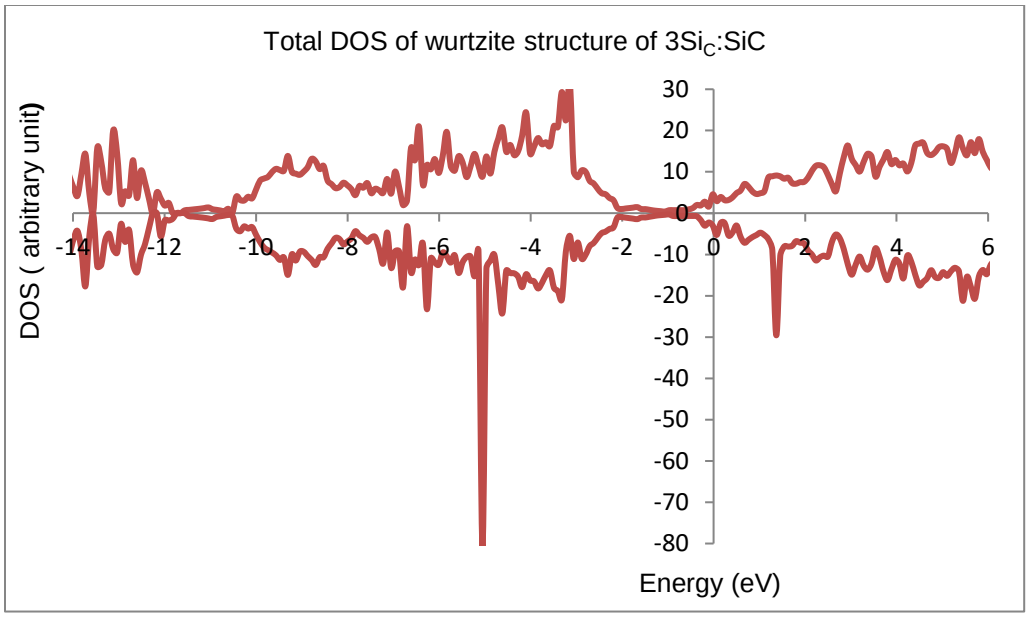

Figure B5 The total DOS plot of wurtzite structure of 3Si$_C$:SiC

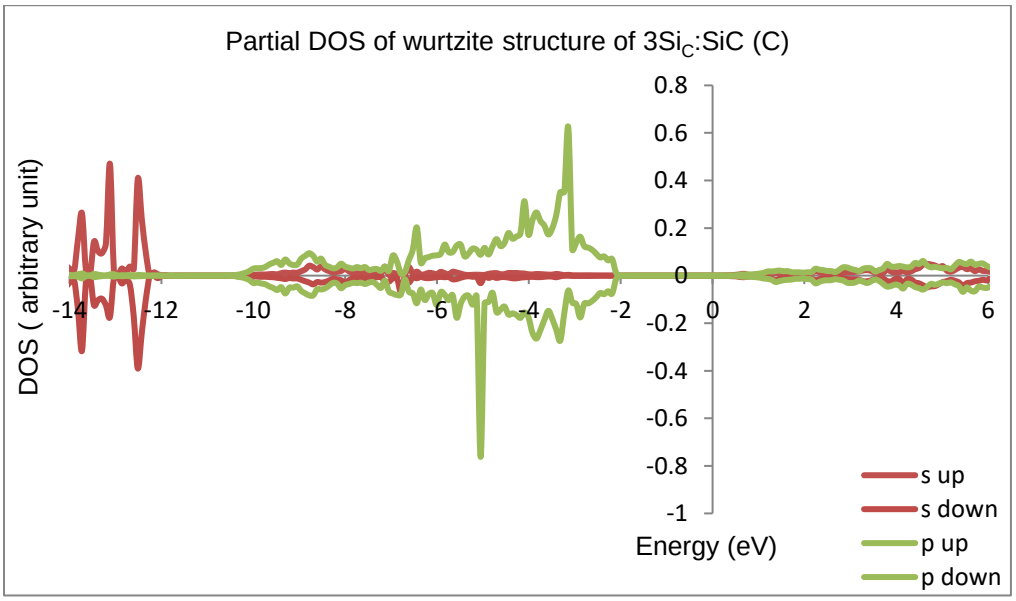

Figure B6 The partial DOS plot of wurtzite structure of 3Si$_C$:SiC (C)

Appendix C

DOS plot of FeSi Structures of Silicon Rich Silicon Carbide

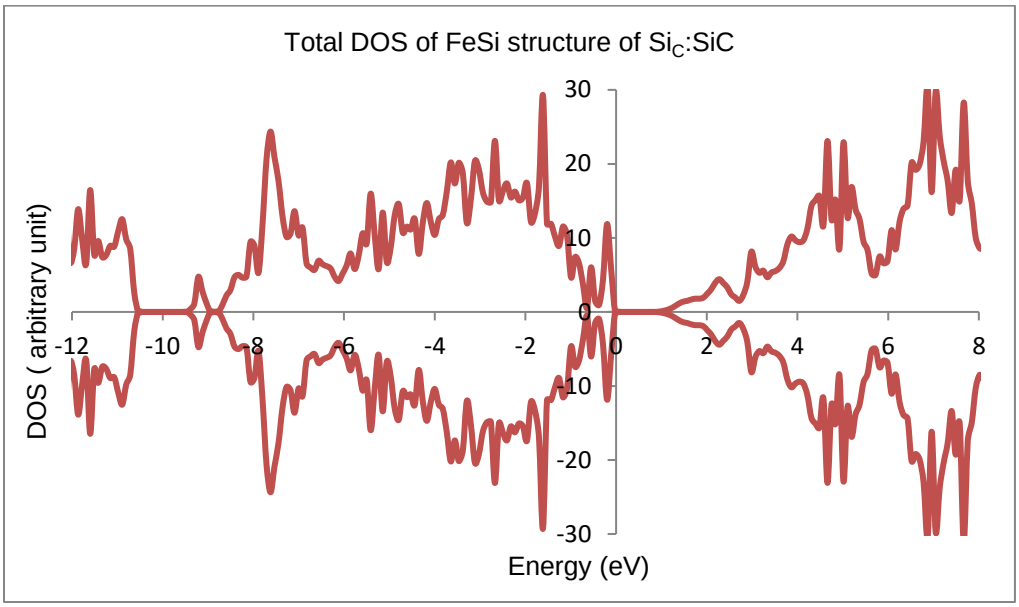

Figure C1 The total DOS plot of FeSi structure of Si$_C$:SiC

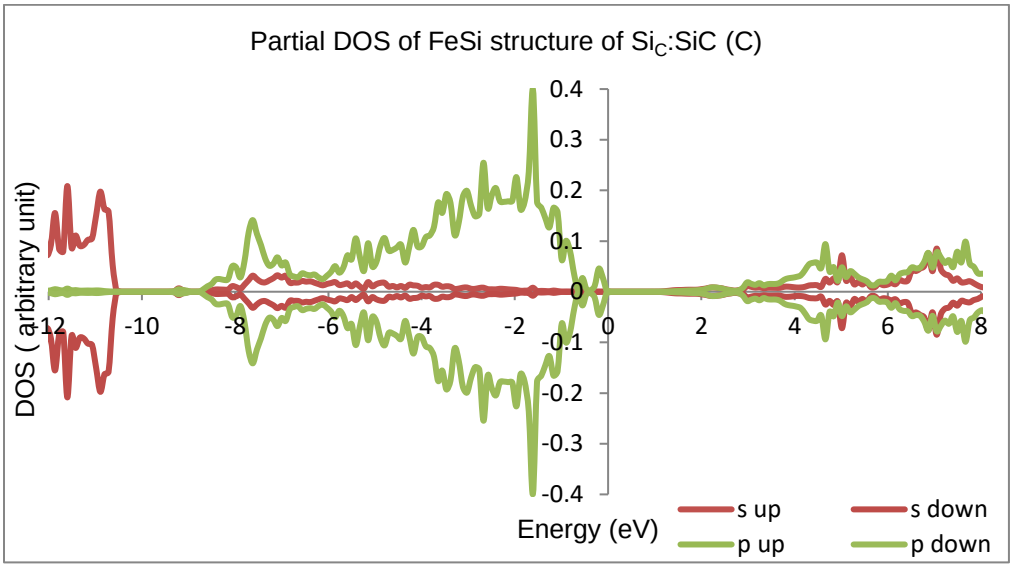

Figure C2 The partial DOS plot of FeSi structure of Si$_C$:SiC (C)

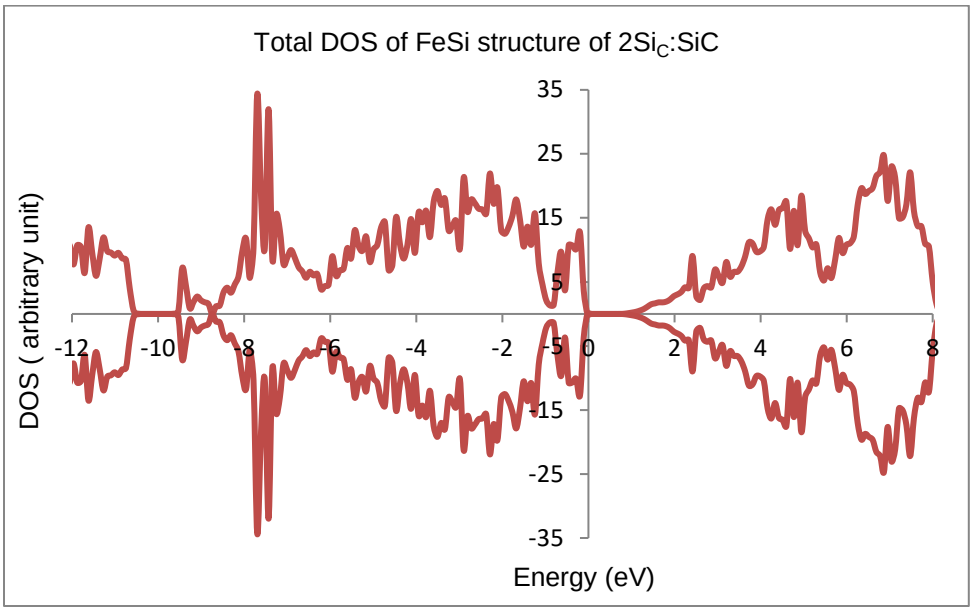

Figure C3 The total DOS plot of FeSi structure of 2Si$_C$:SiC

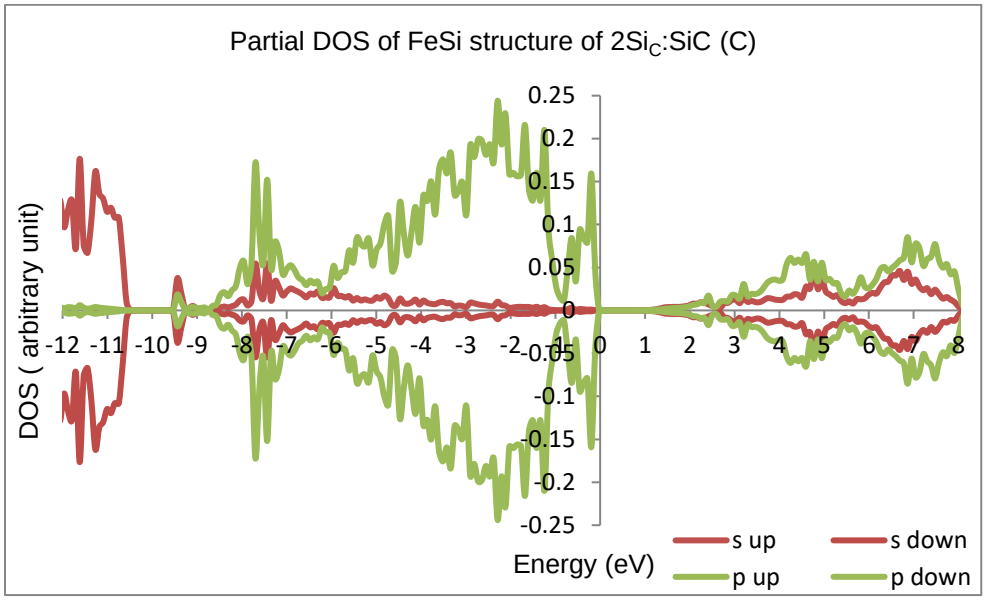

Figure C4 The partial DOS plot of FeSi structure of 2Si$_C$:SiC (C)

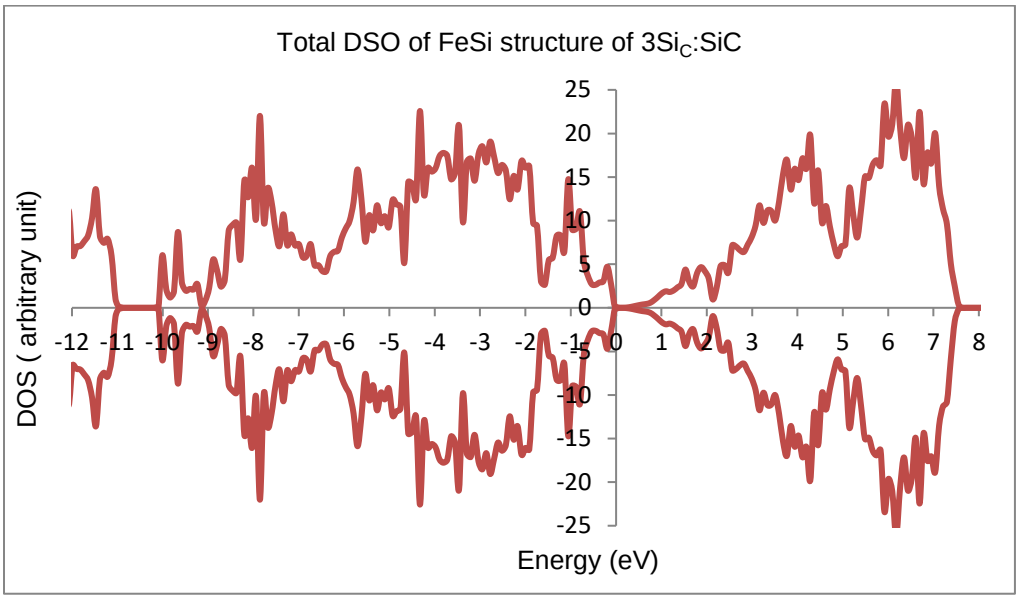

Figure C5 The total DOS plot of FeSi structure of 3Si$_C$:SiC

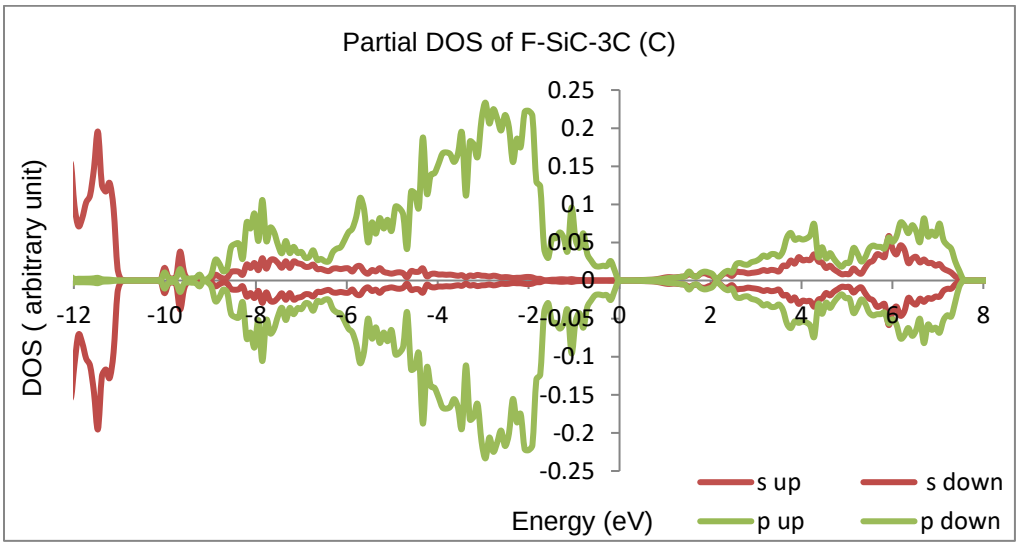

Figure C6 The partial DOS plot of FeSi structure of 3Si$_C$:SiC (C)

Appendix D

DOS Plot of 6H Structures of Silicon Rich Silicon Carbide

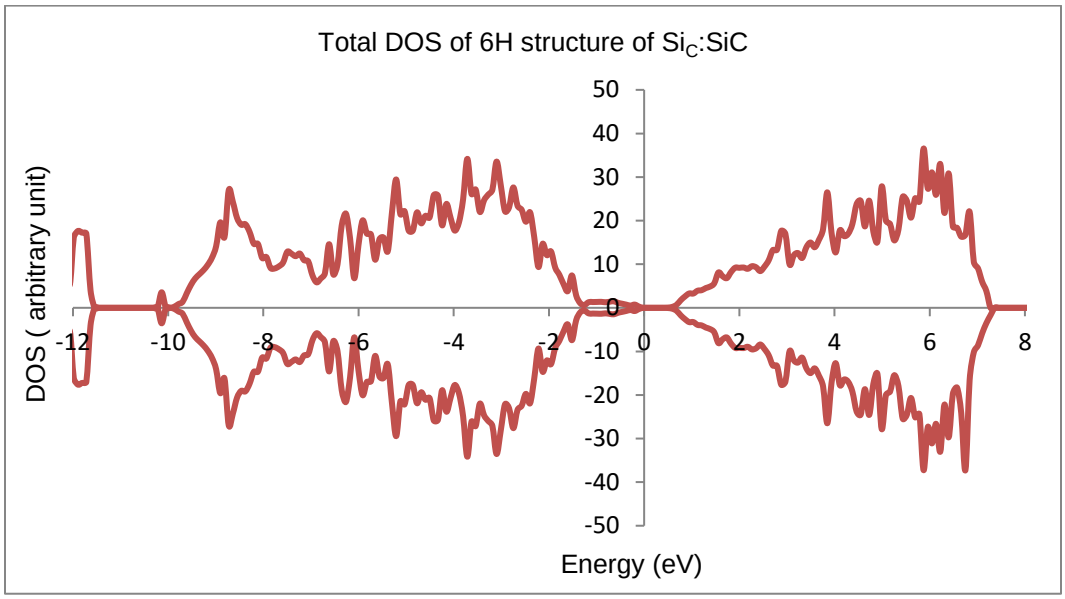

Figure D1 The total DOS plot 6H structure of Si_C:SiC

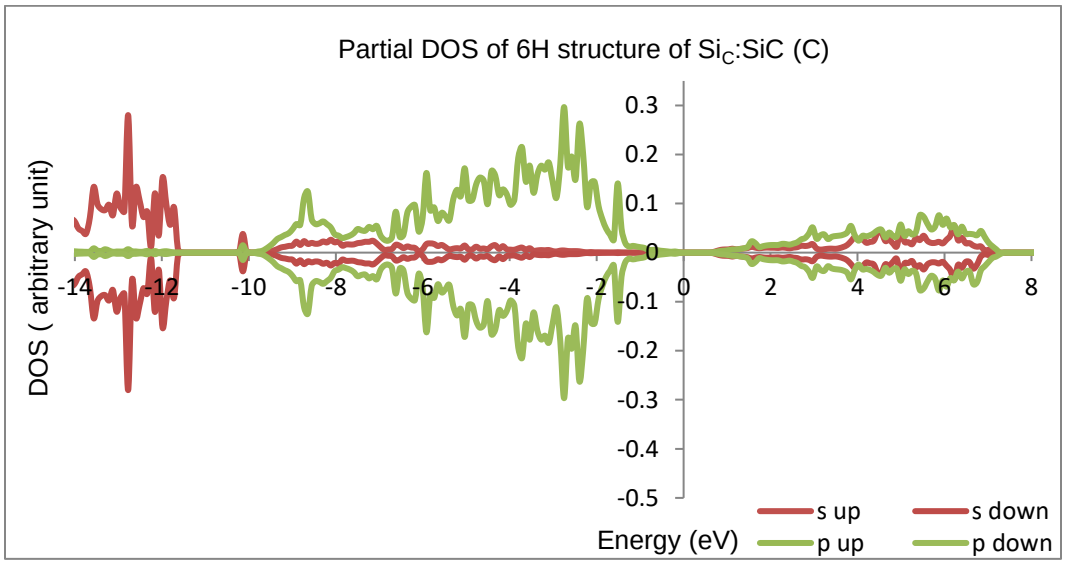

Figure D2 The partial DOS plot of 6H structure of Si_C:SiC (C)

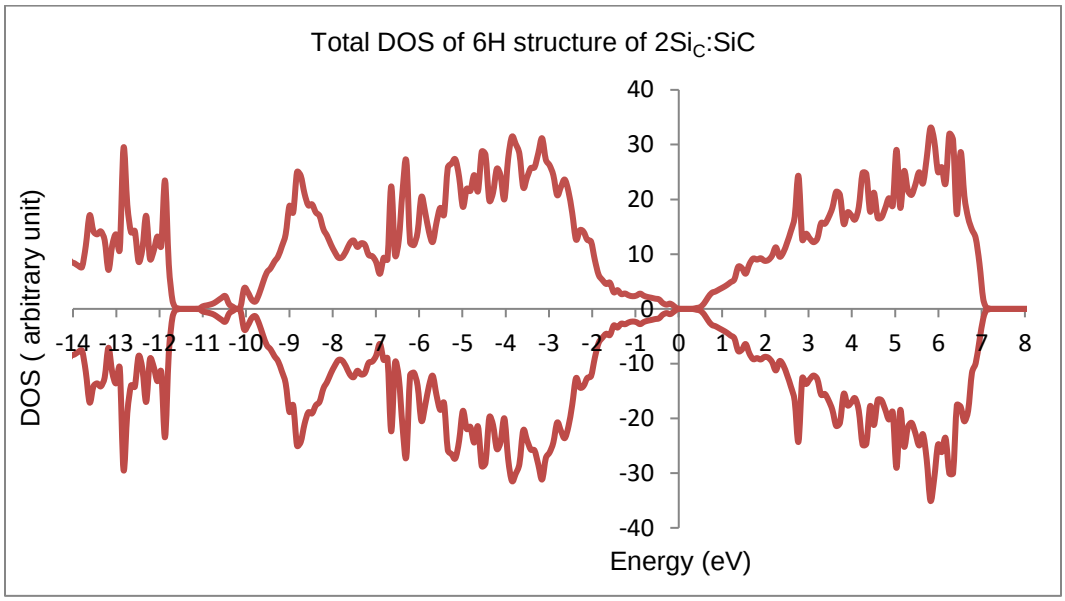

Figure D3 The total DOS plot of 6H structure of 2Si$_C$:SiC

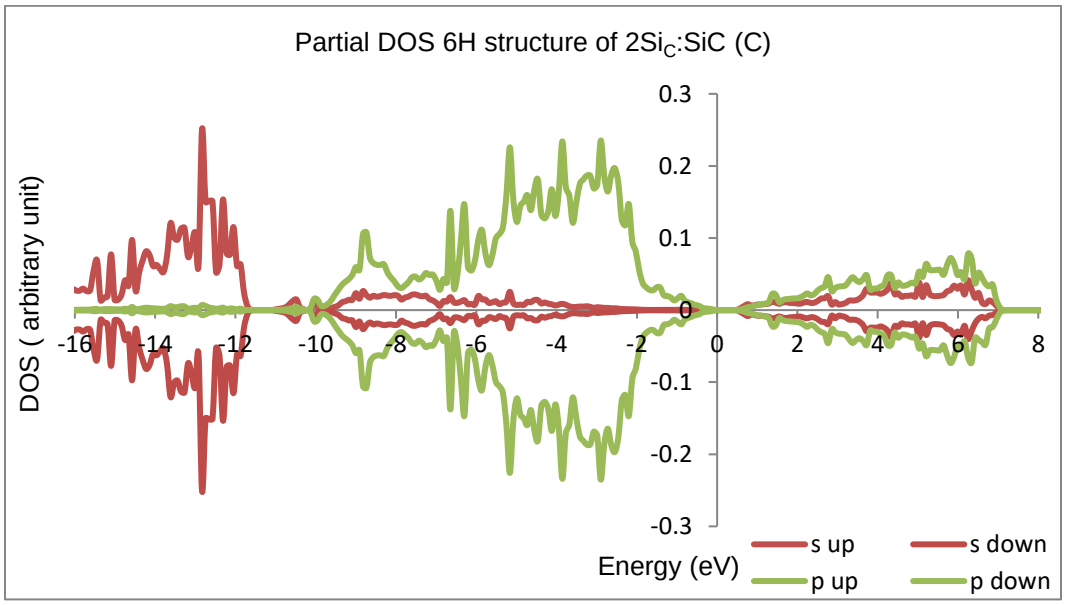

Figure D4 The partial DOS plot of 6H structure of 2Si$_C$:SiC (C)

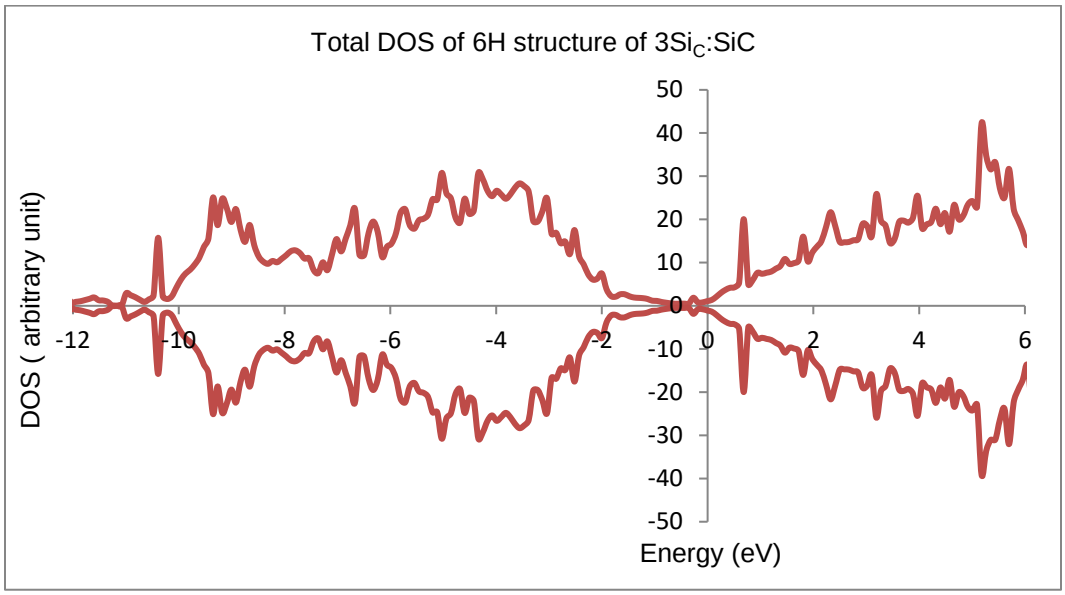

Figure D5 The total DOS plot of 6H structure of 3Si$_C$:SiC

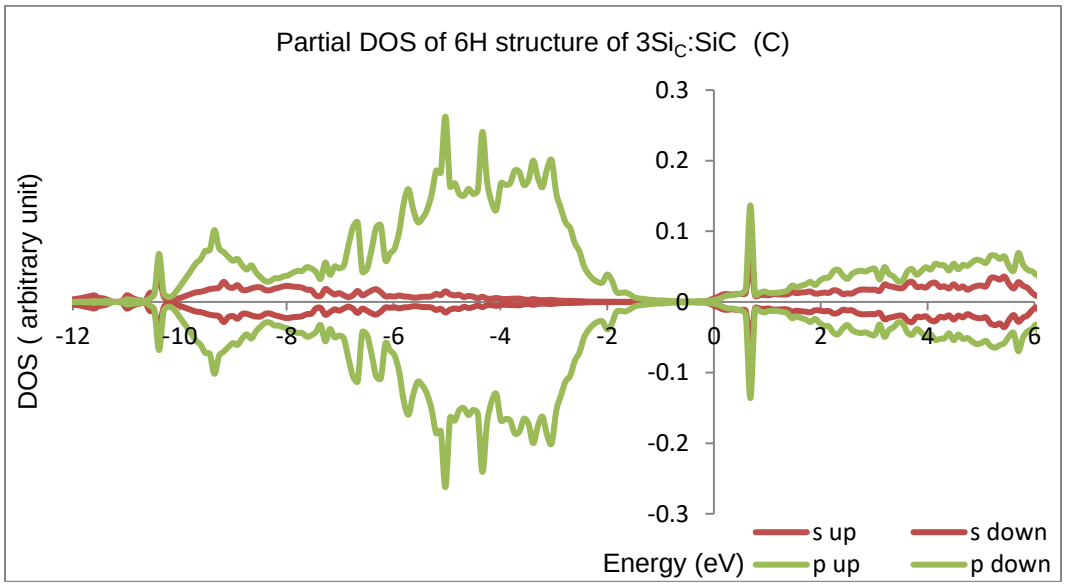

Figure D6 The partial DOS plot of 6H structure of 3Si$_C$:SiC (C)

References

[1] M. Willander, M. Friesel, Q. U. Wahab, and B. Straumal, J. Mater. Sci. Mater. Electron. **17**, 1 (2006).

[2] M. W. Huang, N. Goldsman, C. H. Chang, I. Mayergoyz, J. M. McGarrity, and D. Woolard, J. Appl. Phys. **84**, 2065 (1998).

[3] A. W. Weimar., J. Eur. Ceram. Soc. **18**, 735 (1998).

[4] L. N. Satapathy, P. D. Ramesh, D. Agrawal, and R. Roy, Mater. Res. Bull. **40**, 1871 (2005).

[5] Z. Li and R. C. Bradt, J. Appl. Phys. **60**, (1986).

[6] S. W. Lee, S. D. Park, S. Kang, I. C. Bang, and J. H. Kim, Int. J. Heat Mass Transf. **54**, 433 (2011).

[7] W. Kim, D. Kim, and J. I. Y. Park, Nucl. Eng. Technol. **45**, 565 (2013).

[8] R. A. Andrievski, Rev. Adv. Mater. Sci. **22**, 1 (2009).

[9] F. Wang, D. Xiang, Y. Wang, and J. Li, Ceram. Int. **43**, 4970 (2017).

[10] X. Li, G. Zhang, R. Tronstad, and O. Ostrovski, Ceram. Int. **42**, 5668 (2016).

[11] A. Kohyama, J. Park, and H. Jung, J. Nucl. Mater. **417**, 340 (2011).

[12] S. Kondo, T. Hinoki, M. Nonaka, and K. Ozawa, Acta Mater. **83**, 1 (2015).

[13] X. Luo, P. Guo, Y. Yang, N. Jin, S. Liu, Z. Kou, and S. Wu, Mater. Sci. Eng. A **647**, 265 (2015).

[14] H. Liu, H. Cheng, J. Wang, and G. Tang, J. Alloys Compd. **491**, 248 (2010).

[15] B. Huang, Y. Q. Yang, M. H. Li, Y. X. Chen, X. Luo, M. S. Fu, Y. Chen, B. Huang, Y. Q. Yang, M. H. Li, Y. X. Chen, X. Luo, M. S. Fu, and Y. Chen, Mater. Sci. Technol. **30**, 1751 (2017).

[16] A. Weber, R. Remfort, N. Woehrl, W. Assenmacher, and S. Schulz, Thin Solid

Films **593**, 44 (2015).

[17] B. W. G. Zhang and K. J. Hüttinger, Chem. Vap. Depos. **7**, 167 (2001).

[18] P. Drieux, G. Chollon, S. Jacques, G. Couégnat, S. Jouannigot, and P. Weisbecker, J. Eur. Ceram. Soc. **36**, 1873 (2016).

[19] B. A. Henry, J. Hassan, J. P. Bergman, C. Hallin, and E. Janzén, Chem. Vap. Depos. **12**, 475 (2006).

[20] L. Tsai, C. Lee, Y. Lin, and G. Lin, IEEE 1232 (2011).

[21] K. L. Choy, Prog. Mater. Sci. **48**, 57 (2003).

[22] M. A. Ouadfel, A. Keffous, A. Brighet, N. Gabouze, T. Hadjersi, A. Cheriet, M. Kechouane, A. Boukezzata, Y. Boukennous, Y. Belkacem, and H. Menari, Appl. Surf. Sci. **265**, 94 (2013).

[23] K. Chirakawikul, T. Sujaridchai, B. Ratwises, and D. Kruangam, J. Non-Crystalline Solids 227–230 **227**–**230**, 1156 (1998).

[24] R. Gharbi, M. Fathallah, C. F. Pirri, E. Tresso, G. Crovini, and F. Giorgis, Can. J. Phys. **77**, 699 (1999).

[25] G.-R. Lin, T.-C. Lo, L.-H. Tsai, Y.-H. Pai, C.-H. Cheng, C.-I. Wu, and P.-S. Wang, J. Electrochem. Soc. **159**, K35 (2012).

[26] K. Sugita, M. Itoh, A. Masuda, and H. Matsumura, Thin Solid Films **430**, 170 (2003).

[27] L. Wang, J. Lu, G. Luo, W. Song, L. Lai, M. Jing, R. Qin, J. Zhou, Z. Gao, and W. N. Mei, J. Phys. Chem. C **111**, 18864 (2007).

[28] Y. Tawada, K. Tsuge, M. Kondo, H. Okamoto, and Y. Hamakawa, J. Appl. Phys. **53**, 5273 (1982).

[29] C.-T. Lee, L.-H. Tsai, Y.-H. Lin, and G.-R. Lin, ECS J. Solid State Sci. Technol. **1**, Q144 (2012).

[30] D. Song, E. C. Cho, G. Conibeer, C. Flynn, Y. Huang, and M. A. Green, Sol. Energy Mater. Sol. Cells **92**, 474 (2008).

[31] M. Perani, D. Cavalcoli, M. Canino, M. Allegrezza, M. Bellettato, and C. Summonte, Sol. Energy Mater. Sol. Cells **135**, 29 (2015).

[32] G. Conibeer, M. Green, R. Corkish, Y. Cho, E. C. Cho, C. W. Jiang, T. Fangsuwannarak, E. Pink, Y. Huang, T. Puzzer, T. Trupke, B. Richards, A. Shalav, and K. lung Lin, Thin Solid Films **511**–**512**, 654 (2006).

[33] G. Conibeer, M. Green, E. C. Cho, Y. H. Cho, T. Fangsuwannarak, G. Scardera, E. Pink, Y. Huang, T. Puzzer, S. Huang, D. Song, C. Flynn, S. Park, X. Hao, and D. Mansfield, Thin Solid Films **516**, 6748 (2008).

[34] M. A. Green, Mater. Sci. Eng. B Solid-State Mater. Adv. Technol. **74**, 118 (2000).

[35] Z. Wan, S. Huang, M. A. Green, and G. Conibeer, Nanoscale Res. Lett. **6**, 1 (2011).

[36] H.-Y. Tai, C.-H. Cheng, P.-S. Wang, C.-I. Wu, and G.-R. Lin, RSC Adv. **5**, 105239 (2015).

[37] M. A. Green, Elsevier Sci. B.V. PII **14**, 11 (2002).

[38] Grätzel Michael, Nature **414**, 338 (2001).

[39] H. Ehrenreich and J. H. Martin, Phys. Today **41**, 52 (1979).

[40] G. K. Singh, Energy **53**, 1 (2013).

[41] F. Diner, Renew. Sustain. Energy Rev. **15**, 713 (2011).

[42] L. Wilson, J. Ting, M. B. Heyman, E. H. Yen, D. Usatin, M. Ahuja, H. Davis, and A. Uc, Gastroenterology **146**, S (2014).

[43] J. Huang, S. Varlamov, J. Dore, J. S. Yun, and M. A. Green, Sol. Energy Mater. Sol. Cells **132**, 282 (2015).

[44] G. Beaucarne, Adv. Optoelectron. **2007**, (2007).

[45] R. O. Jones, Rev. Mod. Phys. **87**, (2015).

[46] K. Burke and L. O. Wagner, Int. J. Quantum Chem. **113**, 96 (2013).

[47] X. Y. Pan and V. Sahni, Phys. Rev. A - At. Mol. Opt. Phys. **86**, 1 (2012).

[48] A. Görling, Phys. Rev. A **59**, 3359 (1999).

[49] R. G. Parr and W. Yang, *Density-Functional Theory of Atoms and Molecules* (1989).

[50] S. Kümmel and J. P. Perdew, Phys. Rev. Lett. **90**, 43004 (2003).

[51] G. Kresse and J. Furthmüller, Phys. Rev. B **54**, 11169 (1996).

[52] G. Kresse and J. Furthmüller, Comput. Mater. Sci. **6**, 15 (1996).

[53] P. E. Blöchl, Phys. Rev. B **50**, 17953 (1994).

[54] J. P. Perdew, K. Burke, and M. Ernzerhof, Phys. Rev. Lett. **77**, 3865 (1996).

[55] J. Paier, R. Hirschl, M. Marsman, and G. Kresse, J. Chem. Phys. **122**, (2005).

[56] K. Berland, V. R. Cooper, K. Lee, E. Schröder, T. Thonhauser, P. Hyldgaard, and B. I. Lundqvist, Reports Prog. Phys. **78**, 41 (2015).

[57] F. RozpŁoch, J. Patyk, and J. Stankowski, Acta Phys. Pol. A **112**, 557 (2007).

[58] K. Momma and F. Izumi, J. Appl. Crystallogr. **41**, 653 (2008).

[59] R. T. Downs and M. Hall-Wallace, Am. Mineral. **88**, 247 (2003).

[60] N. Shi, W. Bai, G. Li, M. Xiong, J. Yang, Z. Ma, and H. Rong, Acta Geol. Sin. **86**, 533 (2012).

[61] G. L. Harris, Properties of Silicon Carbide Ceramics International **93** (1995).

Biographical Information

Noura was born and raised in Saudi Arabia. She holds bachelor's degree in physics from University of Dammam in Saudi Arabia. She has been in USA since 2013 to master the English language in order to get the master degree in physics in USA. She obtained a certificate of completing all levels successfully from English Language Institution at University of Texas at Arlington. She joined the Department of Physics at UTA and started her graduate study in 2015, and received her master degree in physics, in May 2017. Her research focuses on condensed matter theory with applications in photovoltaic materials. Prior to coming to UTA, Ms. Alkhaldi worked as an instructor in University of Hafar Al-Batin, Saudi Arabia, who is sponsoring her graduate studies.